

AD-758 515

AN ENVIRONMENTAL HEAT TRANSFER STUDY OF  
A ROCKET MOTOR STORAGE CONTAINER SYSTEM

Allen H. Wirzburg:

Naval Postgraduate School  
Monterey, California

December 1972

DISTRIBUTED BY:

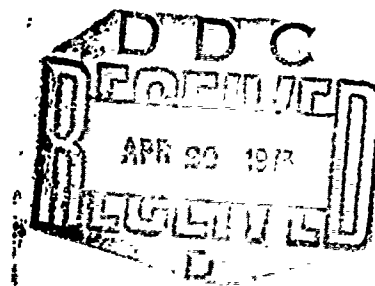
**NTIS**

National Technical Information Service  
U. S. DEPARTMENT OF COMMERCE  
5285 Port Royal Road, Springfield Va. 22151

AD 758515

# NAVAL POSTGRADUATE SCHOOL

## Monterey, California



# THESIS

AN ENVIRONMENTAL HEAT TRANSFER STUDY  
OF  
A ROCKET MOTOR STORAGE CONTAINER SYSTEM

by

Allen Henry Wirzburger

Thesis Advisor:

T. E. Cooper

December 1972

Reproduced by  
NATIONAL TECHNICAL  
INFORMATION SERVICE  
U S Department of Commerce  
Springfield VA 22151

Approved for public release; distribution unlimited.

168

## DOCUMENT CONTROL DATA - R &amp; D

(Security classification of title, body of abstract and indexing annotation must be entered when the overall report is classified)

1. ORIGINATING ACTIVITY (Corporate author) Naval Postgraduate School Monterey, California 93940		2a. REPORT SECURITY CLASSIFICATION Unclassified	
		2b. GROUP	
3. REPORT TITLE An Environmental Heat Transfer Study of a Rocket Motor Storage Container System			
4. DESCRIPTIVE NOTES (Type of report and, inclusive dates) Master's Thesis; December 1972			
5. AUTHOR(S) (First name, middle initial, last name) Allen H. Wirzburger			
6. REPORT DATE December 1972	7a. TOTAL NO. OF PAGES 168	7b. NO. OF REFS 16	
8a. CONTRACT OR GRANT NO.	9a. ORIGINATOR'S REPORT NUMBER(S)		
8. PROJECT NO.			
c.	9b. OTHER REPORT NO(S) (Any other numbers that may be assigned this report)		
d.			
10. DISTRIBUTION STATEMENT Approved for public release; distribution unlimited.			
11. SUPPLEMENTARY NOTES		12. SPONSORING MILITARY ACTIVITY Naval Postgraduate School Monterey, California 93940	
13. ABSTRACT <p>The heat transfer characteristics of a rocket motor storage container system have been investigated using analytical and experimental techniques. Analytically, both closed form and numerical solutions have been developed. These solutions may be used to determine maximum temperatures and temperature gradients within the rocket motor. Comparison between theoretical and experimental values of temperature are within the estimated experimental uncertainties of <math>\pm 3^\circ\text{F}</math>. It is proposed that the theoretical solutions can be used to thermally optimize container design.</p> <p>A secondary investigation was carried out to determine the feasibility of using cholesteric liquid crystals, a temperature sensitive material, to thermally map the surface of the container. The crystals appear to remain stable under desert type conditions and produce brilliantly colored displays of the temperature field.</p>			

14.

## KEY WORDS

## LINK A

## LINK B

## LINK C

ROLE

WT

ROLE

WT

ROLE

WT

heat transfer

conduction

radiation

convection

concentric cylinders

TRUMP

liquid crystals

dump storage

environmental effects

An Environmental Heat Transfer Study  
of  
A Rocket Motor Storage Container System

by

Allen Henry Wirzburger  
Lieutenant, United States Navy  
S.B., Massachusetts Institute of Technology, 1964

Submitted in partial fulfillment of the  
requirements for the degree of

MASTER OF SCIENCE IN MECHANICAL ENGINEERING

from the  
NAVAL POSTGRADUATE SCHOOL  
December 1972

COLOR ILLUSTRATIONS REPRODUCED  
IN BLACK AND WHITE

Author

Allen H. Wirzburger

Approved by:

Thomas E. Cooper

Thesis Advisor

Robert H. Mum  
Chairman, Department of Mechanical Engineering

Milton H. Chesser

Academic Dean

## TABLE OF CONTENTS

I.	INTRODUCTION -----	11
II.	BACKGROUND -----	14
III.	EXPERIMENTAL PROCEDURE -----	17
IV.	THEORETICAL ANALYSIS -----	28
	A. ONE DIMENSIONAL ANALYTICAL MODEL -----	28
	B. TRUMP MODEL -----	36
V.	RESULTS -----	43
	A. ANALYTICAL MODEL -----	43
	B. TRUMP MODEL -----	47
	1. One Dimensional -----	47
	2. Two Dimensional -----	52
	C. GENERAL -----	55
	D. LIQUID CRYSTALS -----	58
VI.	CONCLUSIONS -----	62
VII.	RECOMMENDATIONS -----	64
	APPENDIX A: INTRODUCTION TO LIQUID CRYSTALS. -----	66
	APPENDIX B: ANALYTICAL SOLUTION -----	72
	APPENDIX C: TRUMP SOLUTION -----	99
	APPENDIX D: EXPERIMENTAL DATA -----	151
	APPENDIX E: UNCERTAINTY ANALYSIS -----	161
	LIST OF REFERENCES -----	164
	INITIAL DISTRIBUTION LIST -----	166
	FORM DD 1473 -----	167

## LIST OF TABLES

I. Calibration of Liquid Crystals -----	25
II. Thermal Properties of Materials -----	100
III. Matrix Form of Energy Balance Equations -----	110
IV. Radiosities at Nodes -----	111
V. Change in Parameters Due to Changes in Thermal Properties -----	161

## LIST OF ILLUSTRATIONS

### Figure

1.	Simulated Storage Dump at China Lake -----	15
2.	Thermocouple Locations on Experimental System -----	18
3.	Top View of Rocket Motor Storage Container System -----	19
4.	Stevenson Shelter -----	20
5.	Rocket Motor Mounted in Storage Container -----	22
6.	Experimental System at Dump Storage Site -----	26
7.	Comparison of Sinusoidal Temperature Variation to Bulk Temperature -----	29
8.	Variation in Time Delay with Change in Biot Modulus -----	33
9.	Variation in Relative Amplitude with Change in Biot Modulus -----	34
10.	Analytical Prediction of Temperature Variation with Time -----	38
11.	Comparison of Bulk Temperature to Two TRUMP Approximations -----	39
12.	Comparison of Analytical and Experimental Temperatures at Surface of Rocket Motor -----	44
13.	Comparison of Analytical and Experimental Temperatures at Center of Rocket Motor -----	45
14.	Comparison of 1-D TRUMP and Experimental Temperatures at Surface of Rocket Motor -----	48
15.	Comparison of 1-D TRUMP and Experimental Temperatures at Center of Rocket Motor -----	49
16.	Comparison of Temperatures from Four TRUMP Variations at Surface of Rocket Motor -----	50
17.	Comparison of Temperatures from Four TRUMP Variations at Center of Rocket Motor -----	51



18.	Comparison of 2-D TRUMP and Experimental Temperatures at Surface of Rocket Motor -----	53
19.	Comparison of 2-D TRUMP and Experimental Temperatures at Center of Rocket Motor -----	54
20.	Temperature Distribution at Surface of Storage Container at Maximum Bulk Temperature -----	56
21.	Temperature Distribution at Surface of the Rocket Motor at Maximum Bulk Temperature -----	57
22.	Thermal Mapping with Liquid Crystals -----	59
23.	Liquid Crystals Feasible Under Hostile Environment -----	60
24.	Molecular Structure of Cholesteric Ester -----	67
25.	Light Reflection from Liquid Crystals -----	67
26.	Analytical Model of Experimental System -----	73
27.	Location of Nodes for One Dimensional TRUMP Model -----	101
28.	Location of Nodes for Two Dimensional TRUMP Model -----	104
29.	Graphical Construction for Crossed- Strings Method -----	105
30.	Radiation Network -----	108
31.	Equivalent Radiation Network -----	112
32.	Thermocouple Locations for Experimental Data -----	152

# TABLE OF SYMBOLS

$a$	$= \sqrt{\frac{\omega r_o^2}{\alpha}}$ = conduction parameter
$A_n$	= area of surface $n$ $\frac{\text{sq in}}{\text{in}}$
$B$	$= \frac{1}{T}$ = volume coefficient of expansion $\frac{1}{^\circ R}$
$c$	= specific heat $\frac{\text{BTU}}{\text{lbm } ^\circ F}$
$D_n$	$= D_n' + D_n''$ = length of minimum length line, $n$ in.
$D_n'$	= length of tangential segment of minimum length line, $n$ in.
$D_n''$	= length of radial segment of minimum length line, $n$ in.
$E$	$= \frac{\epsilon}{1-\epsilon}$ = emissivity parameter
$F_{m-n}$	= view factor, fraction of isotropic radiation from $A_m$ intercepted directly by $A_n$
$F_{m-n}$	= radiation exchange factor, fraction of radiation passing from $A_m$ to $A_n$ directly and indirectly
$g$	= acceleration of gravity $\frac{\text{ft}}{\text{sec}^2}$
$h_{\text{CON}}$	= convection heat transfer coefficient $\frac{\text{BTU}}{\text{hr-ft}^2 \cdot ^\circ F}$
$h_{\text{RAD}}$	= radiation heat transfer coefficient $\frac{\text{BTU}}{\text{hr-ft}^2 \cdot ^\circ F}$
$\bar{h}$	$= h_{\text{CON}} + h_{\text{RAD}}$ = effective heat transfer coefficient $\frac{\text{BTU}}{\text{hr-ft}^2 \cdot ^\circ F}$
$i$	$= \sqrt{-1}$
$J_n$	= radiosity of node $n$ $\frac{\text{BTU}}{\text{hr-ft}^2}$
$k$	= thermal conductivity $\frac{\text{BTU}}{\text{hr ft } ^\circ F}$

- $k_c$  = effective thermal conductivity  $\frac{\text{BTU}}{\text{hr ft}^\circ\text{F}}$   
 $r_n$  = radial distance from center of rocket motor to point n in  
 $r_o$  = inner radius of rocket motor in  
 $S_n$  = length of surface n in  
 $t$  = time min  
 $T$  = temperature of position r at time t  $^\circ\text{R}$   
 $T_\infty$  = storage container temperature  $^\circ\text{R}$   
 $T_M$  = maximum temperature of storage container  $^\circ\text{R}$   
 $T_A$  = average temperature of storage container  $^\circ\text{R}$   
 $Z = \sqrt{\frac{i\omega r_o^2}{\alpha}} \xi$  = dimensionless distance parameter  
 $\alpha$  = thermal diffusivity  $\frac{\text{ft}^2}{\text{hr}}$   
 $\beta = \frac{\bar{h}r_o}{k}$  = Biot modulus  
 $\delta$  = width of air gap in  
 $\epsilon$  = emissivity  
 $\xi = \frac{r}{r_o}$  = dimensionless distance  
 $\theta = \frac{T - T_A}{T_M - T_A}$  = dimensionless temperature  
 $\theta^*$  = dimensionless temperature for supplementary problem  
 $\theta_a$  = construction angle for crossed-strings method radians  
 $\theta_r$  = relative amplitude of maximum temperature at point of interest to the maximum temperature of the storage container  
 $\mu$  = dynamic viscosity  $\frac{\text{lbm}}{\text{ft-hr}}$

- $\rho$  = density  $\frac{\text{lbm}}{\text{ft}^3}$   
 $\sigma$  = Stefan-Boltzman constant  $0.171 \times 10^{-8} \frac{\text{BTU}}{\text{hr ft}^2 \text{ } ^\circ\text{R}^4}$   
 $\tau$  =  $\tau(t)$  = solution of  $\psi$  ;  
                     =  $e^{im\omega t}$  for large values of time  
 $\phi$  =  $\phi(r)$  = solution of  $\psi$   
 $\psi$  = complex temperature =  $\theta^*(r,t) + i\theta(r,t)$   
 $\omega$  = frequency of sinusoidal variation  $\frac{2\pi}{24 \text{ hours}}$   
 $\omega_T$  = resulting uncertainty in calculated temperature  $^\circ\text{R}$   
 $\omega_C$  = uncertainty in calculated temperature due to variation in volumetric heat capacity  $^\circ\text{R}$   
 $\omega_K$  = uncertainty in calculated temperature due to variation in conductivity  $^\circ\text{R}$   
 $\omega_\epsilon$  = uncertainty in calculated temperature due to variation in emissivity  $^\circ\text{R}$   
 $Gr$  =  $\frac{\rho^2 g B (\Delta T) \delta^3}{\mu^2}$  = Grashof Number  
 $Pr$  =  $\frac{c\mu}{k}$  = Prandtl Number

#### Bessel Functions

$I_0$  ,  $J_0$  ,  $K_0$  ,  $BER$  ,  $BEi$

$$X_R = BER_0(a) + \frac{a}{\sqrt{2}\beta} BER_1(a) + \frac{a}{\sqrt{2}\beta} BEi_1(a)$$

$$X_i = BEi_0(a) + \frac{a}{\sqrt{2}\beta} BEi_1(a) - \frac{a}{\sqrt{2}\beta} BER_1(a)$$

$$\delta^* = \tan^{-1} \frac{BEi_0(a\xi)X_R - BER_0(a\xi)X_i}{BER_0(a\xi)X_R + BEi_0(a\xi)X_i} = \text{time delay} \quad \text{radians}$$

## ACKNOWLEDGEMENTS

I wish to express my sincere appreciation to my advisor, Professor Thomas E. Cooper, for his invaluable assistance in the preparation of this thesis. A special thanks is also due Mr. Howard C. Schafer of the Naval Weapons Center, China Lake for the use of his facilities for the experimental part of this thesis.

I would also like to express my thanks to the Naval Post-graduate School Computer Facility Staff for their guidance in the computer work.

## I. INTRODUCTION

The purpose of this investigation was to develop a heat transfer model that will allow prediction of the temperature distribution in a container stored rocket motor placed in a hostile thermal environment such as the desert. It is proposed that such a model would be a useful tool for thermally optimizing future container designs. As extreme variations in the rocket motor temperature may lead to large thermal stresses in the propellant which could result in fracture, or otherwise degrade the performance of the motor, a major objective of this study was to design a model that could reliably predict the thermal gradient in the motor. The predictions would be based on the surface temperature distribution, the thermal properties and the geometrical details of the system. The model may also be used to predict a critical temperature range over which the propellant must be chemically stable when in a storage situation. The upper limit of this temperature range is referred to as the design temperature of the system. As the design temperature for most weapon development projects is derived from dump storage conditions, a dump storage situation was used to obtain the experimental data for this project.

Several approaches were taken to predict the rocket motor temperature distribution from a knowledge of only the surface temperature distribution of the storage container and the thermal properties and geometrical details of the

experimental model. The experimental model used in this test was a once-fired Navy antisubmarine rocket (ASROC) motor, filled with dry desert blow sand to simulate the propellant, and placed in its storage container. This container system was placed in a dump storage site at the Naval Weapons Center, China Lake, California to simulate a desert environment.

The method of complex temperatures [Ref. 1] was used to develop an analytical prediction of the transient temperature field that exists in a container stored rocket motor. The analytical model assumes that heat is transferred only in the radial direction and that the container surface temperature variation is sinusoidal with time. Comparison between theory and experiment is within experimental uncertainty when temperature is interpreted as "bulk" temperature. The analytical model is especially useful for studying geometrical and thermal physical property effects on rocket motor temperature. Such parameter studies have been carried out and the results are presented in a form that will be useful from a container design point of view.

TRUMP [Refs. 2 and 3], a computer program for transient and steady-state temperature distributions in multidimensional systems, was used to obtain detailed information about the thermal state of the rocket motor. TRUMP allows actual container surface temperature distributions to be used as well as sinusoidal variations. In addition, both one dimensional (radial) and two dimensional (radial and circumferential)

heat transfer were modeled with TRUMP, using both the sinusoidal and actual temperature distributions. The actual temperature distributions were obtained from the experimental data of the motor container system.

Comparisons between the experimental values and those predicted by the models were in good agreement, with those predicted by TRUMP using the actual temperature distribution as the boundary condition being the closest. However, the sinusoidal variations used in both the analytical model and the TRUMP model are also suitable for design purposes.

Another aspect of this project was to obtain the storage container surface temperature distribution using cholesteric liquid crystals, a material that undergoes brilliant changes in color over known, well defined temperature ranges. Color slides and movies were taken of the liquid crystals demonstrating the feasibility of using them for on site temperature measurements.



## II. BACKGROUND

In 1959 the Naval Weapons Center, China Lake recognized the need for a concerted attack on the problem of thermal criteria assignment for new weapon systems. In 1963 a task force was established to study the complete environmental criteria determination problem. The key to this problem seemed to be the thermal area in the storage and transportation events of any item. It was realized that transportation was a short term situation compared to the storage situation. Therefore, the major portion of the life of an item must be in storage. There are three types of storage; covered, igloo and dump. The dump storage situation leads to the more extreme thermal exposure situations which then leads to the design temperature.

As data was not available for the dump storage situation, instrumented storage dumps were created at representative places on a worldwide basis so that statistical data could be derived on a variety of ordnance. The first site was at China Lake, California, in the middle of the Mojave Desert. This site now has the capability to return about 250 channels of information on a continuous time-temperature basis (Figure 1). Other arctic and tropical sites were set up to study extreme conditions.

The dump storage situation was reproduced to study the extreme situation. The ordnance was exposed singly, directly situated on the ground, with the long axis aligned in the



Figure 1. Simulated Storage Site at China Lake.

north-south direction to allow maximum normal exposure of the container surface to the sun's rays. In actual practice, ordnance is usually stacked and oriented in other than a north-south direction, thereby avoiding the extreme situation. Ordnance sitting on the ground receives reflected radiation from the ground, cannot quickly give off heat by conduction to the soil, and is not as apt to be cooled by the prevailing breeze; therefore, extreme temperatures result.

The most important source of heat to the ordnance is the direct radiation from the sun, with reflected radiation of secondary importance. For extreme conditions to occur the wind must be calm (less than 5 knots), the sky clear, and the outside air temperature high. After sunrise, the ordnance skin temperature rises much more rapidly than the ambient air temperature; therefore, the surrounding air cools the ordnance, rather than heats it.

The rocket motors used for the tests were military surplus. Even though the material had served its intended in-Fleet purpose, it was still representative of new hardware, when viewed in a thermodynamic context. When inert rocket motors were available, they were used intact; however, in most cases, once-fired hardware was used. Thoroughly dried desert blown sand, being similar in thermal properties to most propellants, was used to backfill empty rocket motors. It was assumed that the thermal response of the sand filled motors was essentially the same as actual propellant filled motors.

### III. EXPERIMENTAL PROCEDURE

Although Naval Weapons Center, China Lake had accumulated vast amounts of data in the past, it was decided to instrument a rocket motor storage container system especially for this project. This would allow base data to be taken exactly where it was required. It also allowed variations in the system without interfering with one of China Lake's ongoing projects. An ASROC system was chosen for this study. The outer storage container was 75 inches long with an inner diameter of 18 inches and a wall thickness of 1/16 inch. The rocket motor was 57 inches long with an outside diameter of 12 inches and a wall thickness of 1/4 inch. Both the container and motor were made of steel.

The rocket motor storage container system was instrumented with 20 gage copper-constantan insulated thermocouple wire which has an ISA Calibration of  $\pm 1\text{-}1/2^{\circ}\text{F}$  over the range  $-75$  to  $+200^{\circ}\text{F}$ . Twenty-one thermocouples were originally placed on the system with positions indicated in Figures 2 and 3. The ambient air temperature was measured with thermocouple number 19 which was located in a Stevenson shelter about 60 feet away from the system (Figure 4). The thermocouples were mounted intrinsically on the motor and storage container. Two small holes were drilled approximately 1/8 inch apart in the metal and the individual wires were inserted in the holes. The metal was then hammered around the wires until a snug fit was obtained. Bead thermocouples were mounted at the

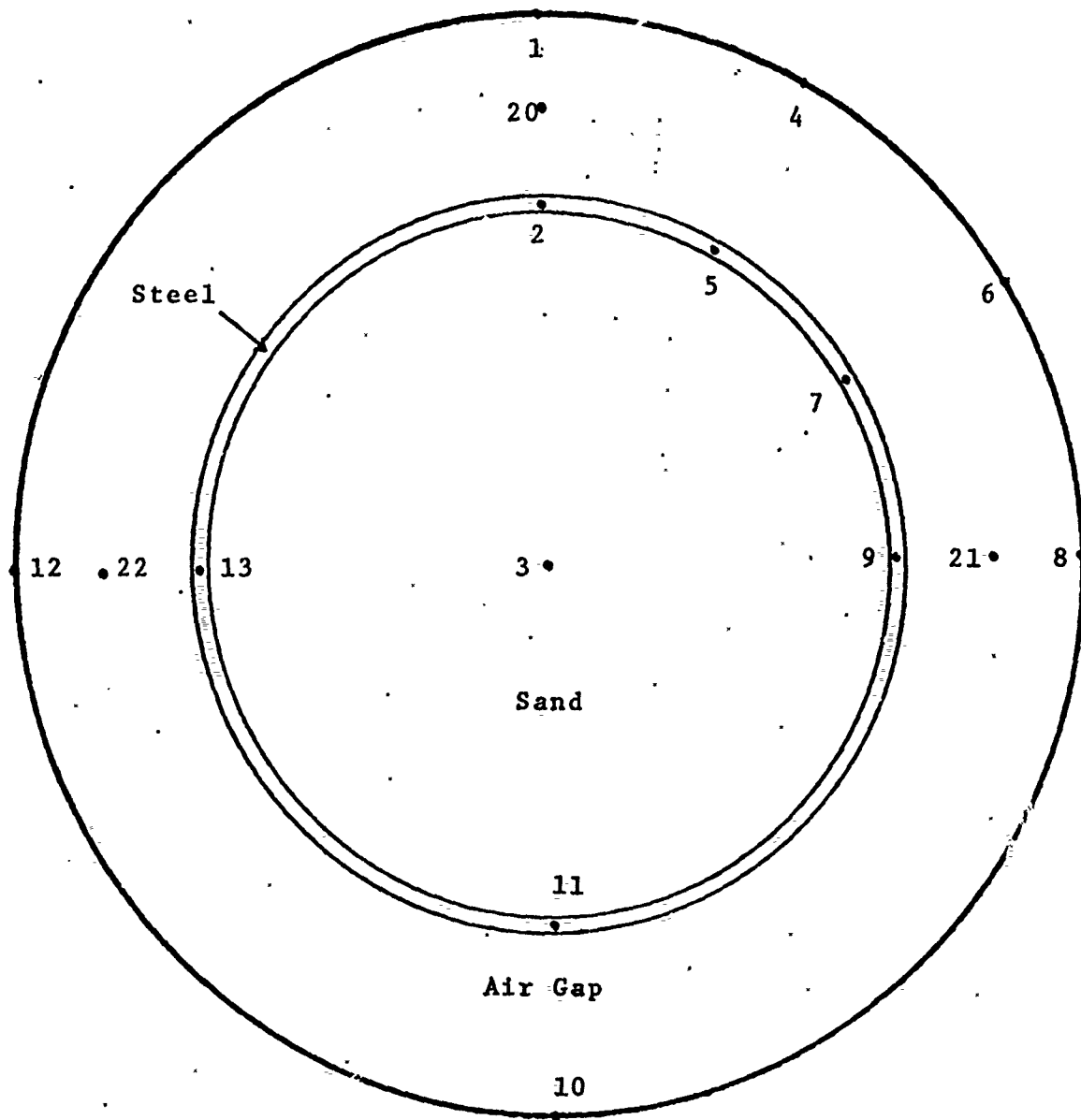


Figure 2. Thermocouple Locations on Experimental System.

Five thermocouples were located under the section painted with the liquid crystals. Their locations corresponding to the ones shown above are: #14= #1, #15= #2, #16= #8, #17= #9, and #18= #3 (See Figure 3).

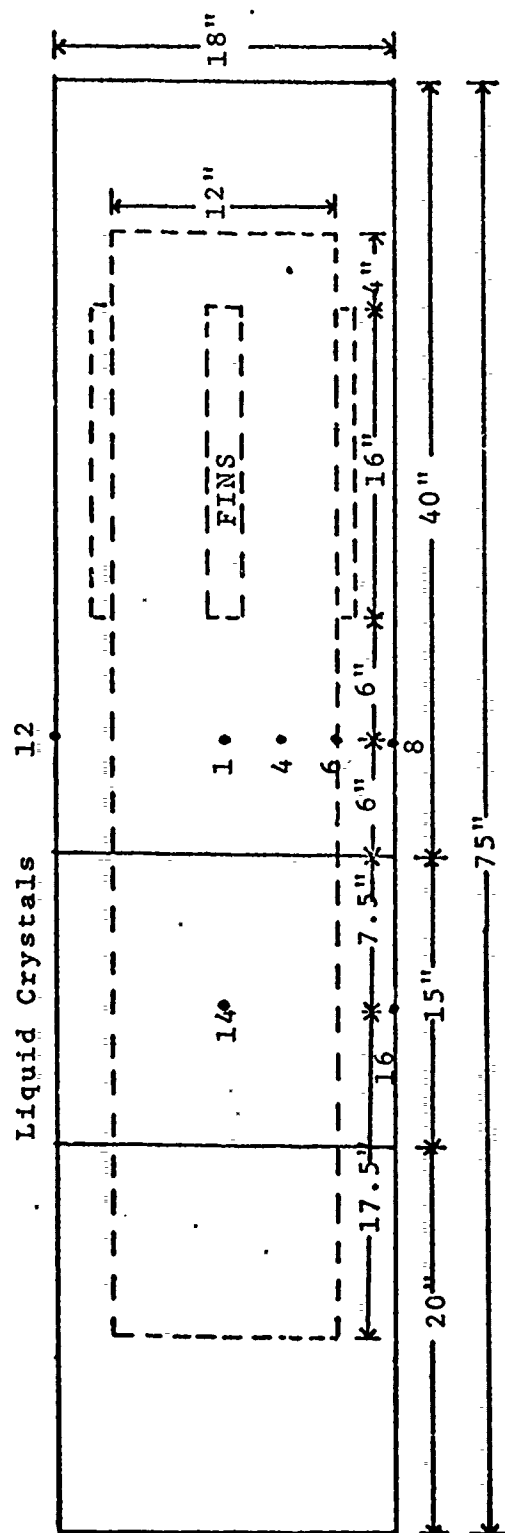


Figure 3. Top View of Rocket Motor Storage Container System.

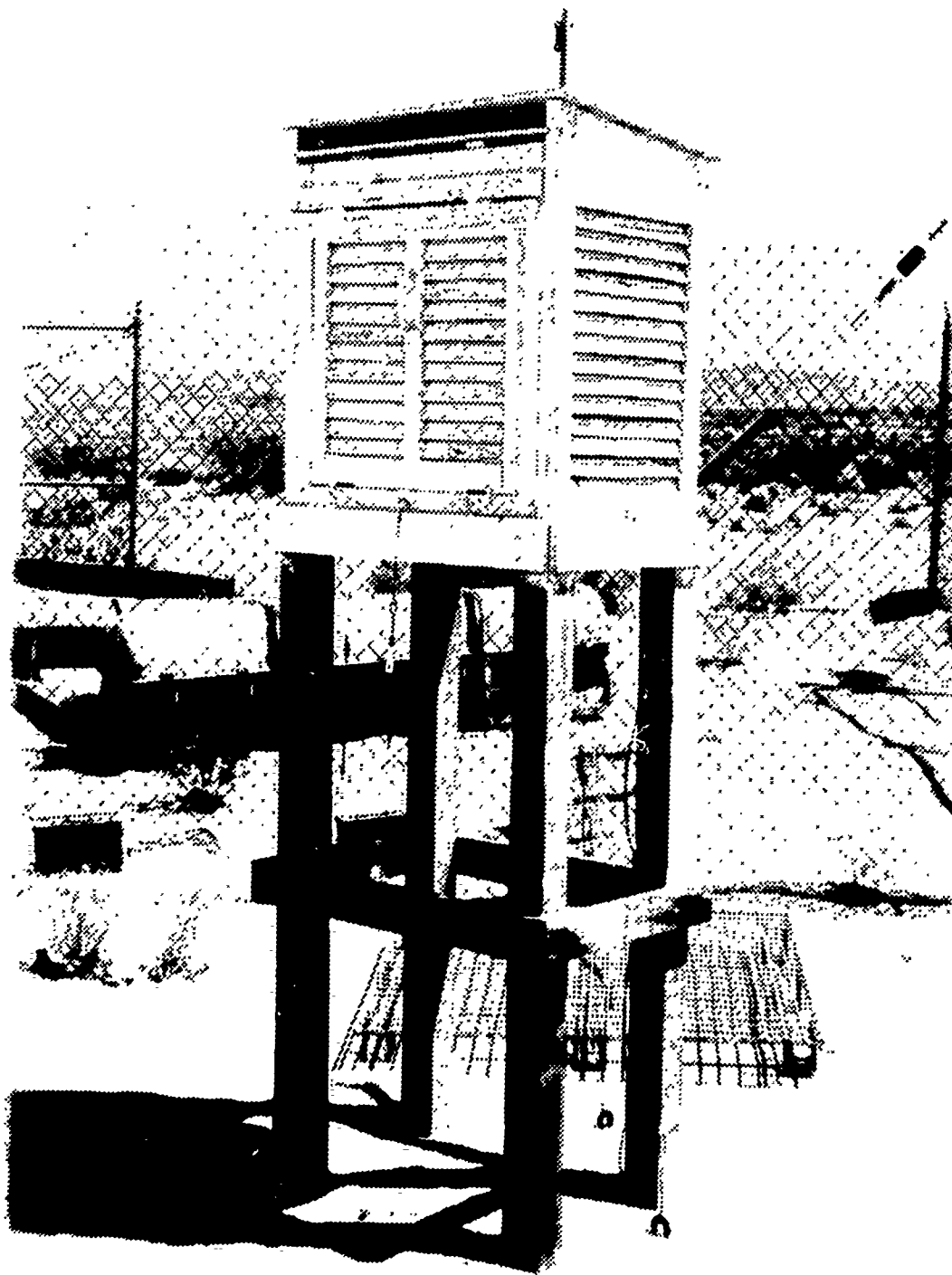


Figure 4. Stevenson Shelter.

center of the motor and in the air gap. The thermocouples located at the center of the motor were supported by small pieces of wood several inches from the head. The use of these supports was necessary to keep the thermocouples in position when the motor was being filled with sand. After all the thermocouples on the rocket motor were in place, the rocket motor was filled with dry desert blown sand. The wires from the two thermocouples located in the center of the motor were led out a hole in the end cap. To avoid settling of the sand after the motor was in place on the site, with a resulting air gap being formed between the sand and the motor skin, the sand was compacted by striking the sides of the motor with small sledge hammers and then adding additional sand through the hole in the end cap. This was continued until the sand was tightly packed. The hole in the end cap was then sealed. The rocket motor was carefully placed in its storage container (Figure 5) which had previously been instrumented with thermocouples. The thermocouples in the air gap were mounted by affixing the lead wire to the rocket motor at the desired position and then putting a 90 degree bend in the wire so that it placed the bead of the thermocouple approximately 1.5 inches into the air gap. Neither the thermocouples in the center of the motor nor those in the air gap could be considered accurately positioned; however, every effort was made to minimize positioning errors. All thermocouple wires were located inside the storage container and were led through a



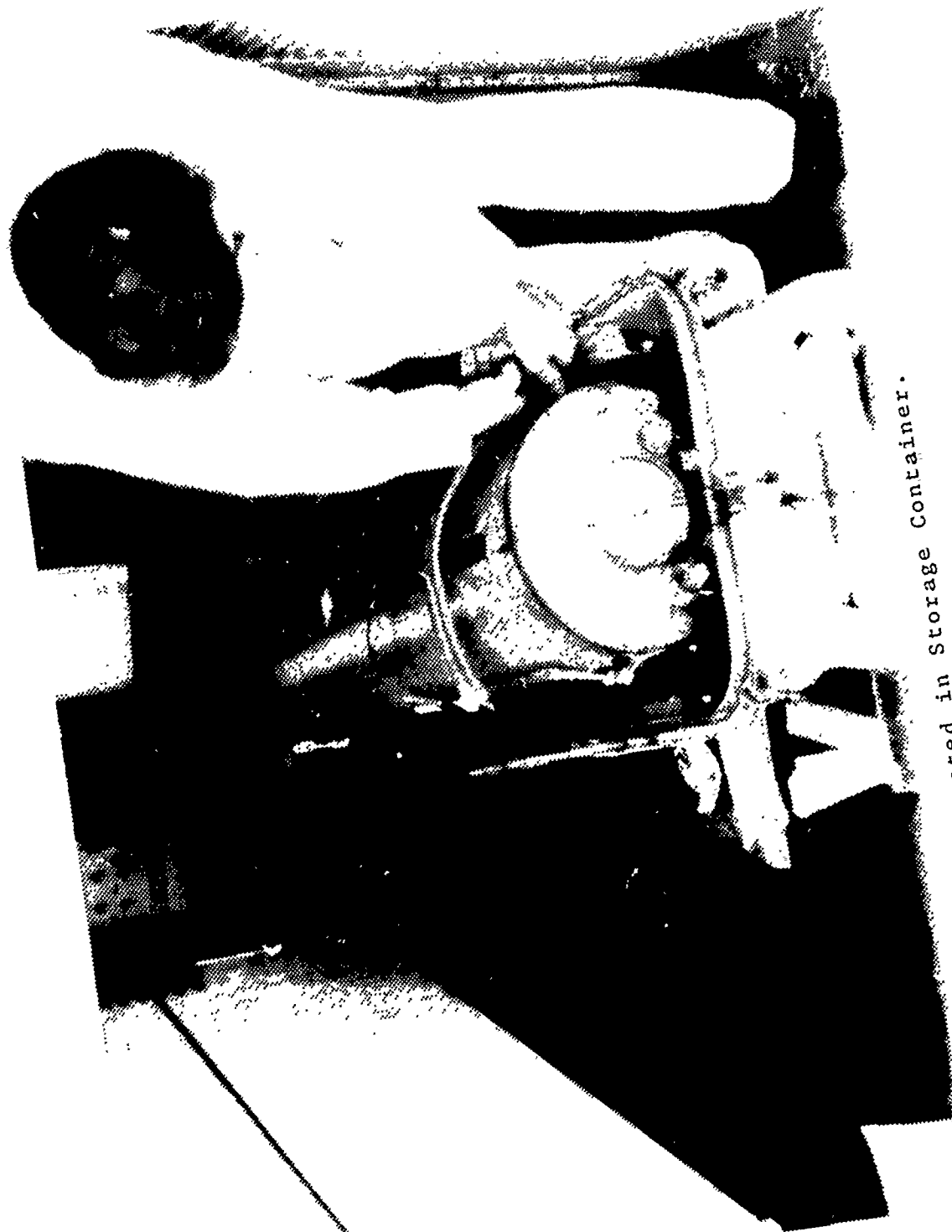


Figure 5. Rocket Motor Mounted in Storage Container.

Reproduced from  
best available copy.



hole in one end. This hole was then sealed. The two halves of the storage container were then bolted shut.

The outer surface of the rocket motor and the inner and outer surfaces of the storage container were all painted various shades of haze gray. Weathering had caused the painted surfaces to appear fairly rough. This is typical of the conditions of a storage dump. From the condition of the surfaces, it was estimated that the emissivity was approximately 0.9.

Prior to loading the rocket motor into the storage container, it was decided to apply liquid crystals (See Appendix A) to part of the storage container surface in order to obtain a thermal mapping of the surface temperature at any instant of time. Liquid crystals are temperature sensitive materials that produce immediate thermal images in a pattern of colors which respond rapidly to minute changes in substrate surface temperatures. A second reason for applying the crystals to the container surface was to determine the feasibility of using the crystals under adverse environmental conditions (desert atmosphere). Prior to applying the crystals, a 15 inch strip of the storage container, 20 inches from one end, was sprayed with two coats of Testors Spray Pla Enamel No. 1249, Flat Black as a background for the crystals. A one inch strip of 11 different ranges of crystal, with approximately 1/2 inch of black paint between them, was applied over the black paint. Two coats of each crystal were applied, using a small paint brush. The first coat was allowed to dry completely before the second coat

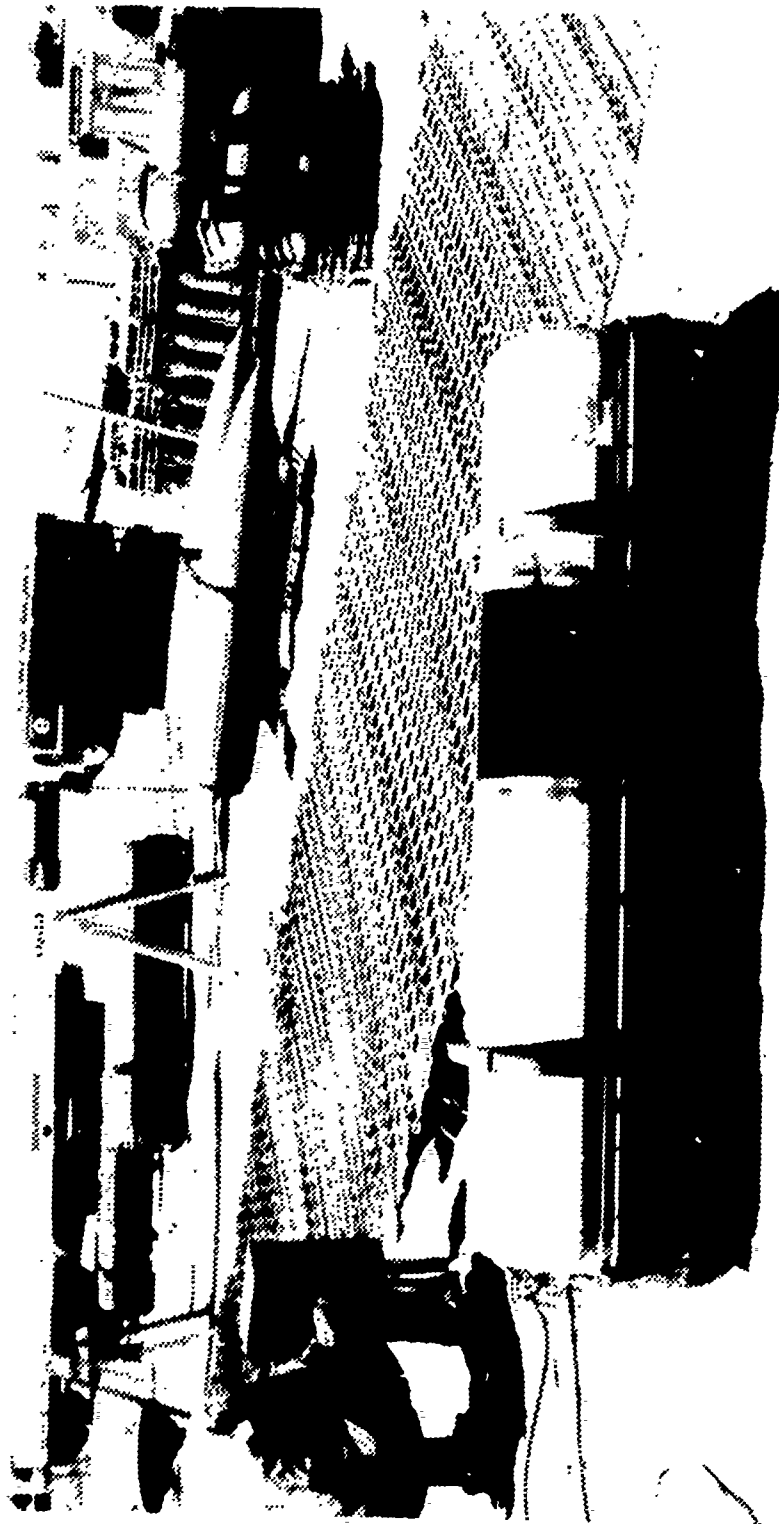
was applied. After the crystals were dry, two coats of Rez polyurethane (gloss clear plastic coating, interior-exterior 77-5) coating were applied by brush completely covering the crystals and black painted area. The polyurethane coating was applied to protect the crystals from wind blown sand and from the ultraviolet rays of the sun. Ten of the eleven crystals had been previously calibrated [Ref. 4]. Using the constant temperature bath procedure recommended in Ref. 4, R-27 was calibrated and the complete calibration results are shown in Table I.

The rocket motor storage container system was then moved to the China Lake dump storage site. The system was aligned in a north-south direction, well away from the influence of other ordnance (Figure 6). The thermocouple leads were connected through a junction box and underground cable to a Honeywell Electronik 25 Recorder which had been calibrated to read the thermocouple output directly in degrees Fahrenheit to an accuracy of  $\pm 1^{\circ}\text{F}$ . The recorder was located in an air-conditioned building about 60 feet from the system.

Initial data indicated that the number 7 thermocouple was not responding properly and therefore this data was neglected. Initial color photographs were taken of the liquid crystals and it was immediately apparent that good thermal mappings could be obtained if the crystals were stable under the adverse desert environment. The brilliance of the colors exhibited by the crystals under the bright desert sun was much better than had been expected. The

TABLE I  
Calibration of Liquid Crystals

NCR Desig.	Color Change	Manufacturer's	Calibration Bath
		Responses	2 Coats Liquid Crystals
		°C	°C
R-27	Red	27.0	25.6 $\pm$ .5
	Green	28.6	28.0 $\pm$ .5
	Blue	30.0	28.7 $\pm$ .5
R-33	Red	33.0	32.7 $\pm$ .5
	Green	34.6	33.3 $\pm$ .5
	Blue	36.0	34.2 $\pm$ .5
R-37	Red	37.0	36.2 $\pm$ .5
	Green	38.6	37.1 $\pm$ .5
	Blue	40.0	38.0 $\pm$ .5
R-41	Red	41.0	40.3 $\pm$ .5
	Green	42.6	41.0 $\pm$ .5
	Blue	44.0	42.0 $\pm$ .5
R-45	Red	45.0	42.8 $\pm$ .5
	Green	46.6	43.6 $\pm$ .5
	Blue	48.0	44.3 $\pm$ .5
R-49	Red	49.0	46.7 $\pm$ .5
	Green	50.6	47.1 $\pm$ .5
	Blue	52.0	48.4 $\pm$ .5
R-53	Red	53.0	50.5 $\pm$ .5
	Green	54.6	52.1 $\pm$ .5
	Blue	56.0	53.3 $\pm$ .5
R-56	Red	56.0	53.8 $\pm$ .5
	Green	57.6	56.0 $\pm$ .5
	Blue	59.0	56.5 $\pm$ .5
R-59	Red	59.0	56.9 $\pm$ .5
	Green	60.6	57.5 $\pm$ .5
	Blue	62.0	58.9 $\pm$ .5
S-62	Red	62.0	60.1 $\pm$ .5
	Green	62.6	60.4 $\pm$ .5
	Blue	63.0	60.9 $\pm$ .5
S-64	Red	64.0	60.9 $\pm$ .5
	Green	64.6	61.4 $\pm$ .5
	Blue	65.0	62.7 $\pm$ .5



Reproduced from  
best available copy.

Figure 6. Experimental System at Dump Storage Site.

system was allowed two weeks to reach a periodic steady state before additional photographic data was obtained. . .

Extensive photographic data was collected on 27 and 28 July 1972 after two weeks of exposure to the desert environment. Both super 8 mm and 16 mm color movies and 35 mm color slides were taken of the liquid crystals. No colored filters were used on any of the cameras, although standard haze filters were used to take the super 8 mm movies and most of the 35 mm slides.

At this time, a second storage container, this one without a rocket motor inside, was instrumented with intrinsic thermocouples in the same manner as the previous container. As only three data channels remained open on the recorder, only three thermocouples were applied to this new container. The three thermocouples were applied at the 0300, 0900, and 1200 positions at the midpoint of the container. This container was set end to end with the system that was already in place at the site. The purpose of this study was to determine if the inclusion of the rocket motor in the container had a significant effect on the surface temperature of the container. Thermocouple #7 was connected at the 0900 position, #23 at the 1200 position, and #24 at the 0300 position. It was immediately apparent that thermocouple #7 was continuing to give unreliable readings and therefore the data taken on channel #7 was neglected.

#### IV. THEORETICAL ANALYSIS

##### A. ONE-DIMENSIONAL ANALYTICAL MODEL

The first step was to try to devise an analytical model that would simulate the actual rocket motor storage container experimental system. The first simplifying assumption was that the storage container temperature could be modeled by a sine wave which had a period of 24 hours. A comparison of the sinusoidal variation to the average (bulk) storage container temperature [obtained by averaging the four thermocouple readings on the surface of the container (1, 8, 10, and 12) as shown in Appendix D] is given in Figure 7.

The method of complex temperature as presented by Arpaci [Ref. 1] was used to find the steady periodic solution of a body experiencing a periodic sinusoidal disturbance. A complete analytical derivation is given in Appendix B. The general heat conduction equation in cylindrical coordinates was the basis for this derivation. It was assumed that there was one dimensional radial heat flow with no conduction in the axial or circumferential directions, that no heat sources existed in the model, that the rocket motor storage container system was infinitely long, and that the sinusoidally varying surface temperature was spatially uniform over the entire container surface. The storage container temperature is assumed to vary as

$$T_{\infty} = (T_M - T_A) \sin \omega t + T_A$$

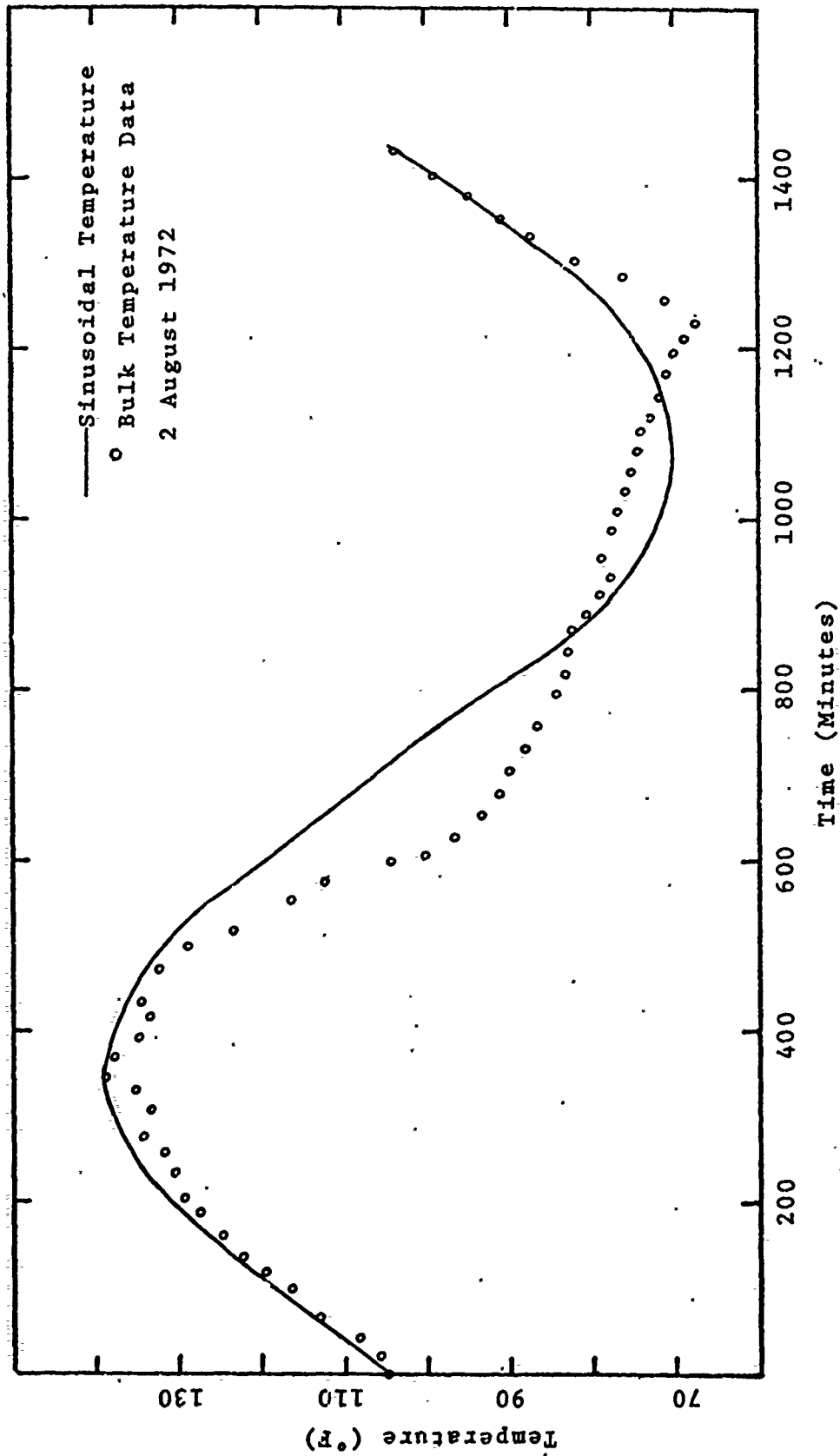


Figure 7. Comparison of Sinusoidal Temperature Variation to Bulk Temperature.



where  $T_M$  = maximum bulk temperature of the storage container  
 $T_A$  = average bulk temperature of the storage container  
 $\omega$  = frequency of the sinusoidal variation  
 $(2\pi/24 \text{ hours})$   
 $t$  = time (hours)

It was assumed that all the thermal properties remained constant over the temperature range of the problem. The effective heat transfer coefficient,  $\bar{h}$ , across the air gap between the storage container and the rocket motor combines the heat transfer effects of radiation, convection, and conduction into one coefficient. The radiation coefficient was linearized by assuming constant representative temperatures in the equation

$$h_{\text{RAD}} = \mathcal{F}_{1-2} \sigma (T_1 + T_2)(T_1^2 + T_2^2)$$

where  $\sigma$  is the Stefan-Boltzmann constant and  $\mathcal{F}_{1-2}$  is the radiation exchange factor. The convection coefficient is the effective conductivity of air, obtained from the Beckmann correlations [Ref. 5], divided by the width of the air gap. In the analytical model, the effective conductivity was assumed to equal the conductivity, thereby treating it as pure conduction and giving the equation

$$\bar{h} = h_{\text{RAD}} + h_{\text{CON}}$$

An initial condition was not specified in this derivation as the only concern was the steady-state, periodic behavior. The steady-state solution is (Appendix B)

$$\theta(r,t) = \frac{T(r,t) - T_A}{T_M - T_A} = \frac{\sqrt{\text{BER}_o^2(a\xi) + \text{BEi}_o^2(a\xi)}}{\sqrt{X_R^2 + X_1^2}} \sin(\omega t + \delta^*)$$

$$\theta(r,t) = \theta_r \sin(\omega t + \delta^*)$$

where  $T(r,t)$  = the temperature of a point  $r$  in the rocket motor at time  $t$

$$a = \sqrt{\frac{\omega r_o^2}{\alpha}} = \text{conduction parameter}$$

$$\xi = \frac{r}{r_o} = \text{dimensionless distance from the center of the rocket motor}$$

$$r_o = \text{inner radius of the rocket motor}$$

$$r = \text{distance from the center of the rocket motor}$$

$$\alpha = \frac{k}{\rho c} = \text{thermal diffusivity}$$

$$\rho = \text{density}$$

$$k = \text{thermal conductivity}$$

$$c = \text{specific heat}$$

$$\text{BER} = \text{real Bessel Function}$$

$$\text{BEi} = \text{imaginary Bessel Function}$$

$$X_R = \text{BER}_0(a) + \frac{a}{\sqrt{2}\beta} \text{BER}_1(a) + \frac{a}{\sqrt{2}\beta} \text{BEi}_1(a)$$

$$X_i = \text{BEi}_0(a) + \frac{a}{\sqrt{2}\beta} \text{BEi}_1(a) - \frac{a}{\sqrt{2}\beta} \text{BER}_1(a)$$

$$\beta = \frac{\bar{h}r_o}{k} = \text{Biot modulus}$$

$$\delta^* = \tan^{-1} \frac{\text{BEi}_0(a\xi)X_R - \text{BER}_0(a\xi)X_i}{\text{BER}_0(a\xi)X_R + \text{BEi}_0(a\xi)X_i}$$

Two computer studies were done based on the steady state solution. The first study was a completely dimensionless situation which served as a parameter study of the effects of varying  $a$  and  $\beta$  on the temperature and the time lag of the temperature at various positions in the model.

$$a = \sqrt{\frac{\omega r_o^2}{\alpha}} = \text{conduction parameter}$$

and

$$\beta = \frac{\bar{h}r_o}{k} = \text{Biot modulus}$$

Parameter  $a$  was varied from 1.0 to 5.0 and  $\beta$  was varied from 0.1 to 100. These were the only values studied, as

only values within this range are of interest in this type problem. The computer program and its output are given at the end of Appendix B. The output lists the following values:

- 1)  $a$ , the conduction parameter
- 2)  $\beta$ , the Biot modulus
- 3)  $\xi$ , the non-dimensional distance from the center of the motor
- 4)  $\delta^*$ , the time delay between the maximum storage container temperature and the maximum temperature reached at the point of interest in the motor
- 5)  $\theta_r$ , the relative amplitude of the maximum temperature at the point of interest compared to the maximum temperature of the storage container

The time delay is given in radians, where  $2\pi$  radians equals one complete cycle. A graph of the time delay versus  $\beta$  for a constant value of " $a$ " is given in Figure 8 at three different positions within the motor. A graph of the relative amplitudes of the temperatures versus  $\beta$  for a constant value of " $a$ " is given in Figure 9. It was noted that for a constant value of " $a$ ", the time delay decreased as  $\beta$  became larger. As the point of interest approaches the center of the rocket motor, the time delay increases. The relative amplitude of the temperatures also becomes larger as  $\beta$  is increased when the value of " $a$ " is held constant. If  $\beta$  is held constant and " $a$ " is varied, the time delay increases and the relative amplitude decreases as " $a$ " increases.

The second study was obtaining the analytical solution to the particular rocket motor storage container system

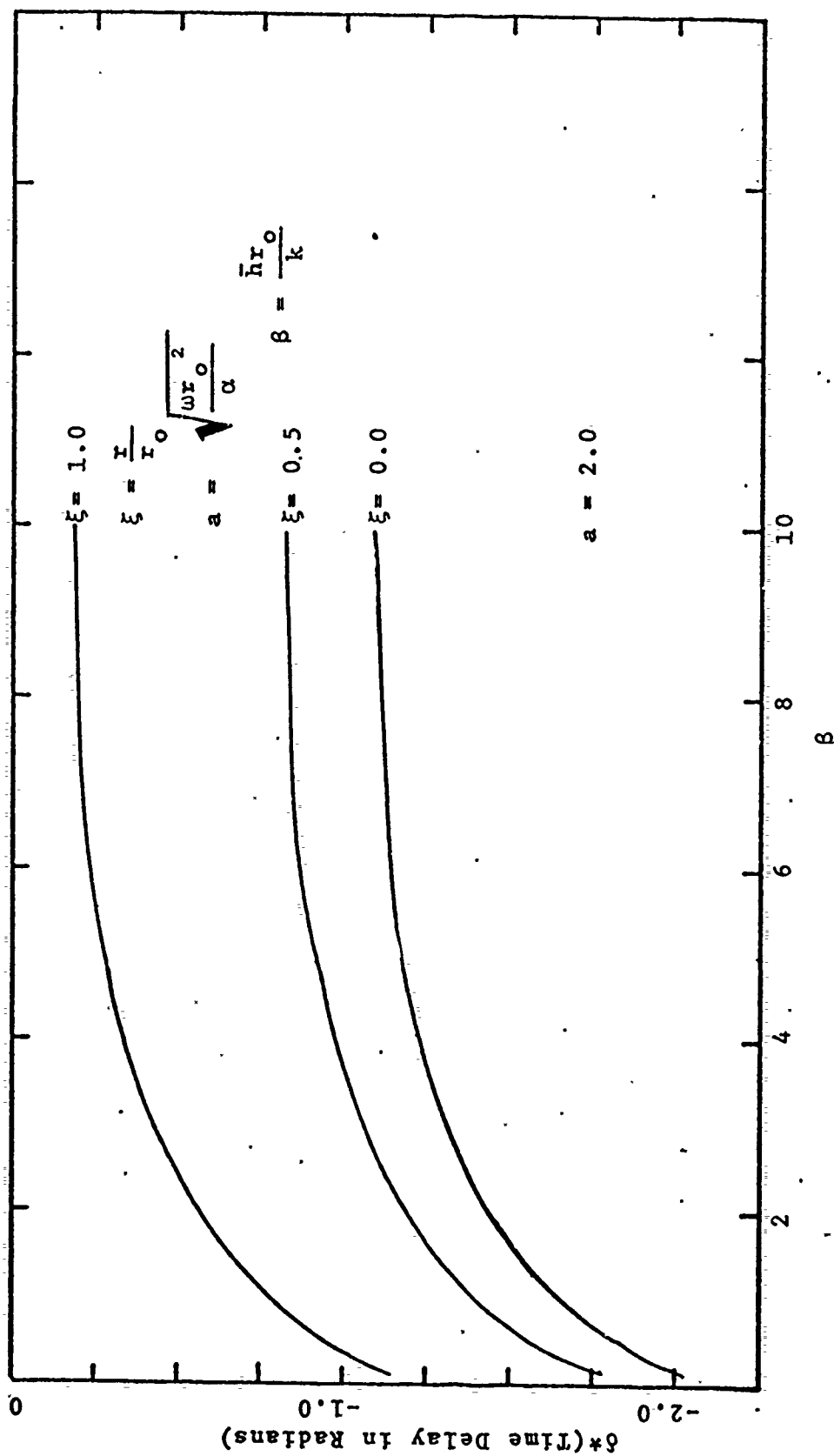


Figure 8. Variation in Time Delay with Change in Biot Modulus

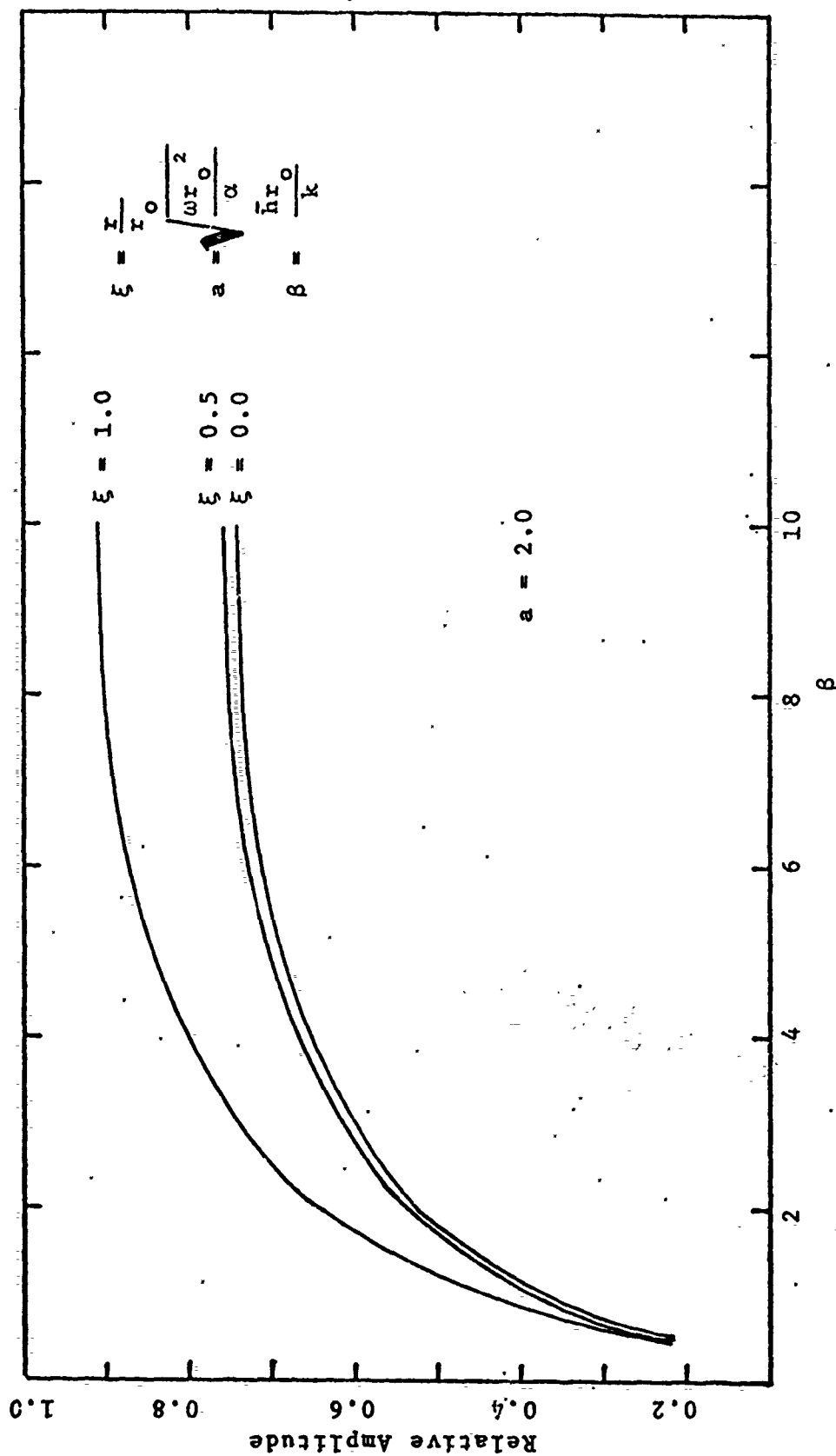


Figure 9: Variation in Relative Amplitude with Change in Biot Modulus.

studied at China Lake. The thermodynamic properties of dry sand were obtained from Ref. 6 as

$$\begin{aligned}\rho &= 94.8 \text{ lbm/ft}^3 \\ k &= 0.188 \text{ BTU/hr ft } ^\circ\text{F} \\ c &= 0.195 \text{ BTU/lbm } ^\circ\text{F}\end{aligned}$$

Substituting these values and using 1440 minutes (24 hours) as a complete cycle, the parameters  $a$  and  $\beta$  were calculated for this model as

$$a = \sqrt{\frac{\omega r_o^2}{\alpha}} = 2.43$$

where  $r_o = 5.75$  inches, the inner radius of the rocket motor.

$$\beta = \frac{\bar{h} r_o}{k} = 2.90$$

where  $\bar{h} = h_{\text{CON}} + h_{\text{RAD}}$

$$\text{and } h_{\text{CON}} = \frac{k_{\text{AIR}}}{\Delta r} = 6.48 \times 10^{-2} \frac{\text{BTU}}{\text{hr-ft}^2 \cdot ^\circ\text{F}}$$

where  $\Delta r = 2.94$  inches, the distance across the air gap

$$\text{and } k_{\text{AIR}} = 1.62 \times 10^{-2} \frac{\text{BTU}}{\text{hr ft}^2 \cdot ^\circ\text{F}}$$

$$h_{\text{RAD}} = \mathcal{F}_{1-2} \sigma (T_1 + T_2) (T_1^2 + T_2^2) = 1.09 \frac{\text{BTU}}{\text{hr ft}^2 \cdot ^\circ\text{F}}$$

where  $\sigma$  is the Stefan-Boltzmann constant,  $\mathcal{F}_{1-2}$  is the radiation exchange factor which for this geometry is

$$\mathcal{F}_{1-2} = \frac{1}{\frac{1}{\epsilon_1} + \frac{r_1}{r_2} \left( \frac{1}{\epsilon_2} - 1 \right)} = 0.84$$

when  $\epsilon_1 = \epsilon_2 = .9$ ,  $r_1 = 6.0$ ,  $r_2 = 8.94$

therefore  $\bar{h} = 1.15 \text{ BTU/hr ft}^2 \cdot ^\circ\text{F}$

The average surface temperature of the storage container was found to be  $104^\circ\text{F}$  for a particular day at China Lake,

with a maximum temperature of 138°F. These values were obtained by averaging the readings of thermocouples 1, 8, 10, and 12 as shown in Appendix D which give the bulk temperature.

The temperatures of seven positions within the rocket motor were calculated and the results are printed at 30 minute intervals for one complete cycle in Appendix B. A graph of temperature versus time was plotted by the computer showing the relationship between the surface temperature of the storage container (TINF), the temperature on the outer skin of the rocket motor (TEDG), and the temperature at the center of the motor (TCEN). This graph is Figure 10.

#### B. TRUMP MODEL

The rocket motor storage container system at China Lake was modeled on TRUMP, a numerical conduction code, (See Appendix C for a description of the TRUMP program) to predict the temperature at any point in the system from a knowledge of the storage container surface temperature variation, the thermal properties and the geometrical details of the system. Two models were used to simulate the rocket motor storage container system and several variations of each model were investigated.

The first model assumed one dimensional heat transfer (radial). The system was modeled as two infinitely long concentric steel cylinders, the inner of which was filled with dry sand. A 2.94 inch air gap separated the cylinders. The model was subdivided into concentric volumetric elements

with representative nodal points as given in Figure 27, Appendix C. It was assumed that the storage container surface temperature was spacially uniform. From the data given in Appendix D and the observation of the liquid crystals' thermal mapping, it was obvious that the temperature distribution on the storage container was not spacially uniform. In order to simulate a spacially uniform condition, the readings of the thermocouples located at the 1200, 0300, 0600, and 0900 positions (#1, 8, 10, and 12) were averaged and this average value of the surface temperature (referred to as the bulk temperature) was used as the spacially uniform temperature distribution. Two methods were used to describe the container temperature. The first method used the maximum bulk temperature (138°F) and the average bulk temperature (104°F) of the storage container to generate a sine wave with a period of 24 hours (1440 minutes). The second method took the bulk temperature readings at two hour intervals and fed this data into the TRUMP program in a tabular (temperature versus time) form. The version of TRUMP used in this problem was limited to a table length of 12 tabular values. TRUMP interpolated between the tabular points. Figure 11 compares the actual bulk data with the sinusoidal approximation and the interpolated tabular values.

Several assumptions were made to simplify the solution of this problem. As the thermocouple data from the storage container gave an average value of the temperature across the 1/16 inch steel wall, node 12 was modeled as a zero



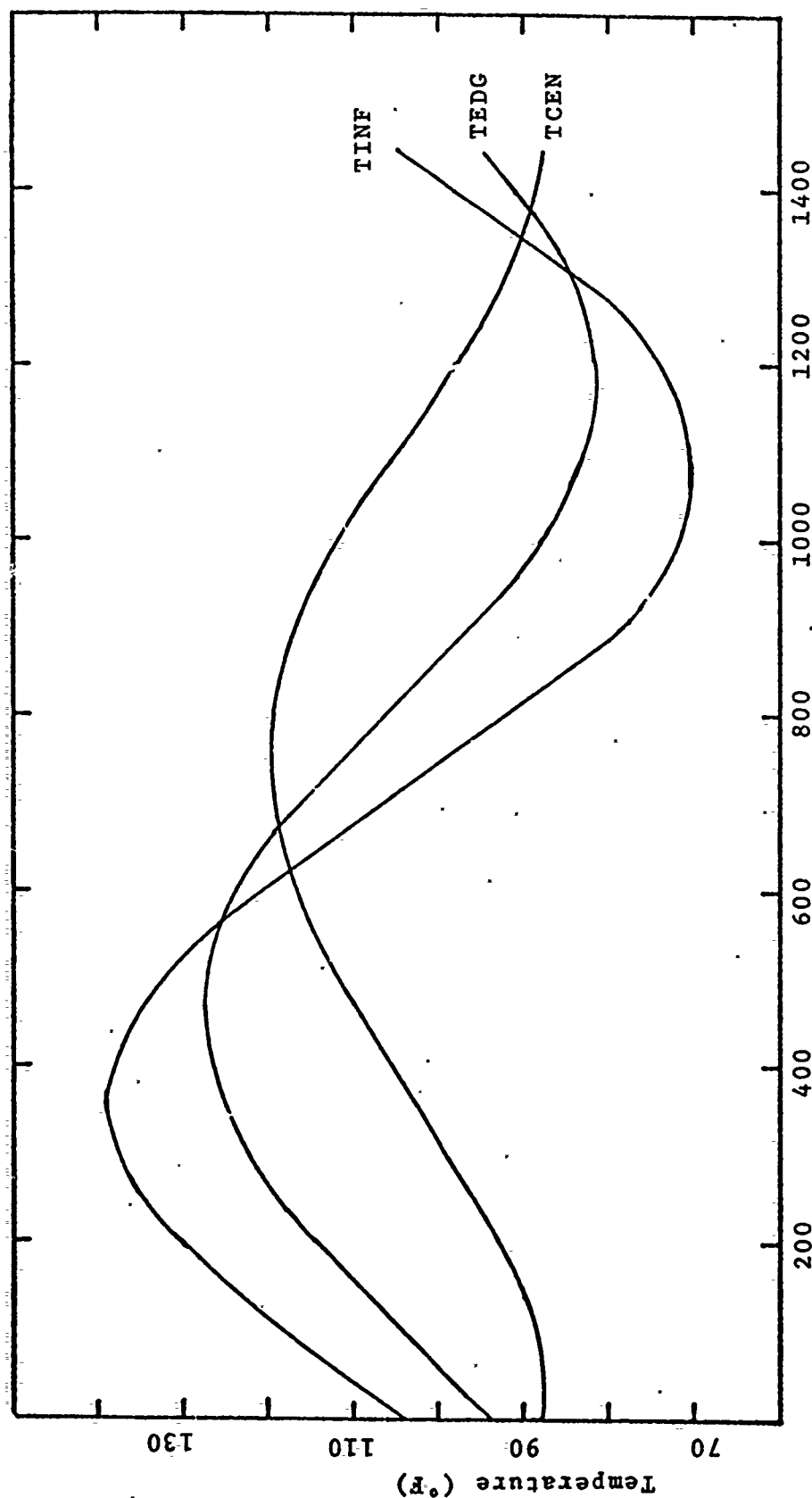


Figure 10: Analytical Prediction of Temperature Variation with Time, where TINF is the surface temperature of the storage container, TEDG is the surface temperature of the rocket motor, and TCEN is the temperature at the center of the motor.

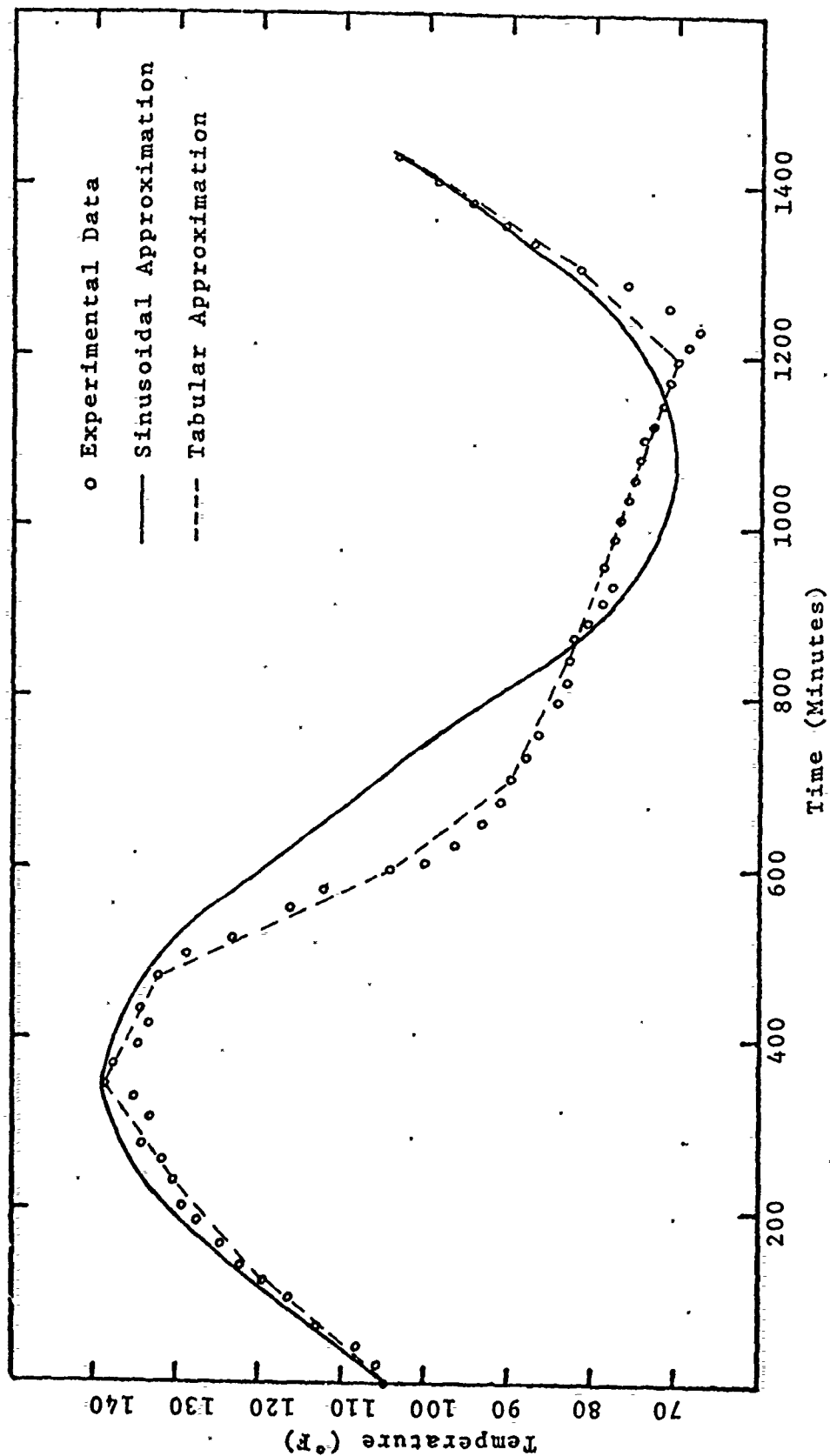


Figure 11: Comparison of Bulk Temperature to Two TRUMP Approximations.

volume boundary node with a known temperature impressed upon it. It was also assumed that heat transfer across the air gap occurred by radiation and conduction alone. Free convection effects were initially neglected. This assumption was later modified to investigate the free convection effects. All surfaces of the storage container and the outside surface of the rocket motor were painted various shades of haze gray and it was estimated that the emissivity of these surfaces was 0.9. The radiation exchange factor,  $F_{1-2}$ , for this model was the same as that for the analytical solution ( $F_{1-2} = 0.84$ ). It was also assumed that there was perfect thermal contact between the rocket motor and the sand that filled it. This neglects the possibility that the sand might slightly settle after being on the site for a long period of time.

The second model assumed two dimensional heat transfer (radial and circumferential). The same physical model was used as in the one dimensional case with the sole exception that 48 nodes were used instead of 12. The representative nodal points and an example of the thermal connections from one of the nodal points are shown in Figure 28 in Appendix C. The four nodes on the surface of the storage container were modeled as zero volume boundary nodes. The sinusoidal and tabular representations were used to describe the surface temperature of the storage container at each boundary node. Actual data taken at each position, rather than bulk data, were used as the input data for these representations.

The same assumptions made in the one dimensional case were also applicable to the two dimensional model. A complete discussion of the calculation of the radiation exchange factors in the two dimensional case is given in Appendix C.

The effect of natural convection was studied in both the one and two dimensional models. References 5 and 7 give correlations between the Grashof number based on the gap width and the effective thermal conductivity. The Grashof number was calculated from the equation

$$Gr = \frac{\rho^2 g B (\Delta T) \delta^3}{\mu^2}$$

where  $\delta$  = width of the air gap

$\Delta T$  = maximum temperature difference at any instant of time in the air gap

$B = \frac{1}{T}$  where  $T = 565^\circ R$

At  $T = 565^\circ R$ , air has the following properties

$$\rho = 0.07 \text{ lbm/ft}^3$$

$$\mu = 0.046 \text{ lbm/hr-ft}$$

The maximum Grashof number for this experiment was calculated to be  $1.25 \times 10^6$ . The diameter ratio was approximately 1.5 and the  $\log Gr = 6.1$ . From the Beckmann correlation [Ref. 5], the effective thermal conductivity ratio  $\left(\frac{k_c}{k}\right)$  was approximately 3.2. Using the Liu correlation [Ref. 7]

$$\frac{k_c}{k} = 0.135 \left( \frac{Pr^2 Gr \delta}{1.36 + Pr} \right)^{0.278} = 4.5$$

where the Prandtl Number = 0.707. An effective thermal conductivity of 4.0 was assumed as the average value of these

two correlations and it was used to study the effects of free convection. This change was placed into the TRUMP program by increasing the value of the thermal conductivity of air by a factor of 4 in each of the TRUMP runs.

## V. RESULTS

### A. ANALYTICAL MODEL

Using the sinusoidal temperature distribution as an approximation to the actual average experimental data as shown in Figure 7, comparisons were made between predicted temperatures and actual temperatures for two radial locations in the rocket motor. Figure 12 compares the results on the surface of the rocket motor and Figure 13 does the comparison at the center of the rocket motor. An uncertainty analysis is given in Appendix E which establishes the uncertainty bounds for both the predicted and the actual temperatures. These uncertainty bounds are included in Figures 12 and 13.

It is readily seen from Figure 7 that a sine wave was not an ideal fit as an approximation to the experimental data, as it varies as much as 20°F during part of the cycle. However, it was also noted that the sine wave closely approximated the experimental data during the heating phase of the cycle and only during the cooling phase were there large variations. As the main purpose of this study was to design a model that would be useful in optimizing storage container design, the errors in the cooling phase are not critical as long as the temperatures reach the same minimum point before beginning another cycle. Figure 12 shows that the maximum surface temperature of the rocket motor predicted by the analytical model is a good approximation to the actual

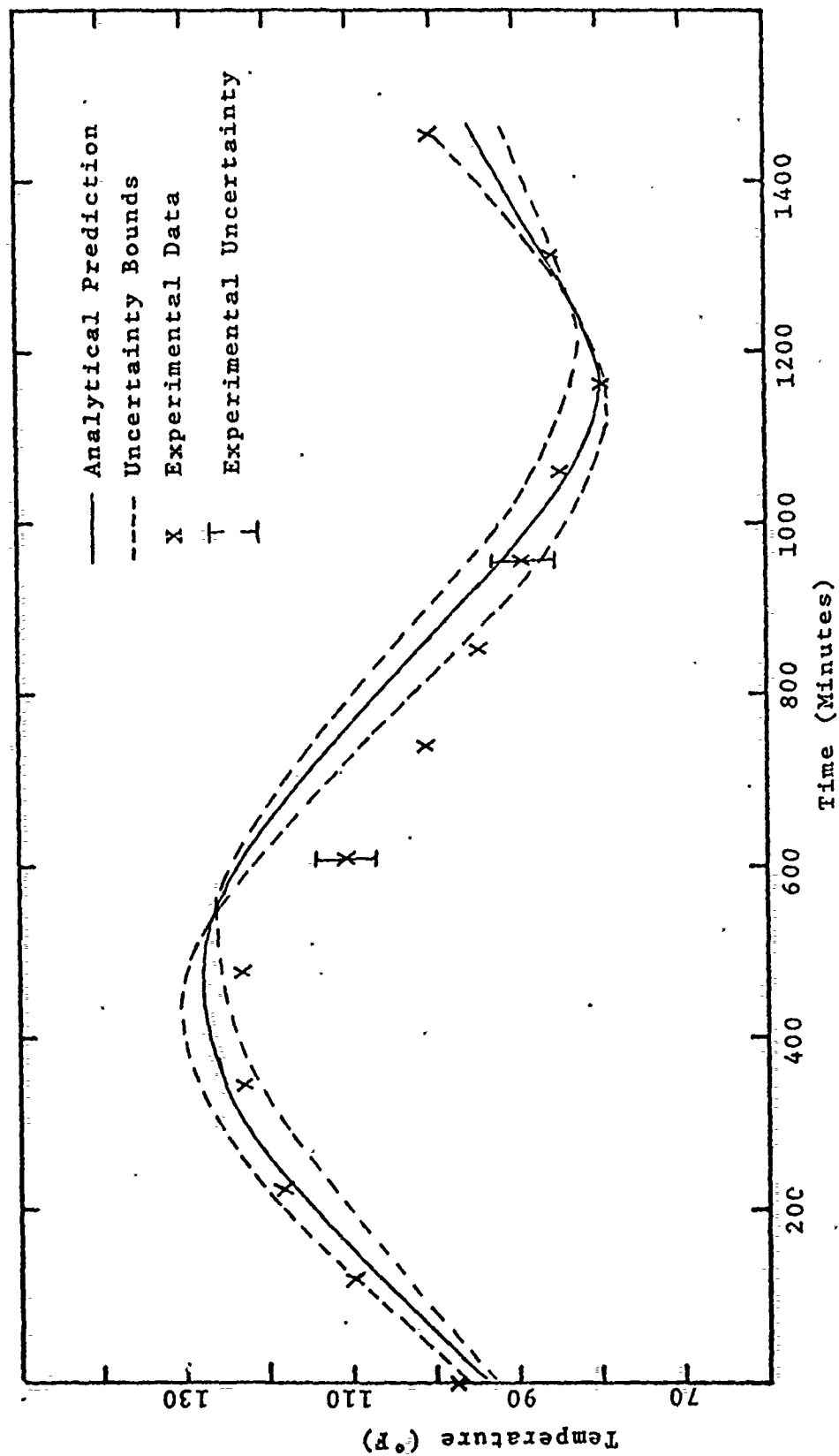


Figure 12: Comparison of Analytical and Experimental Temperatures at Surface of Rocket Motor.

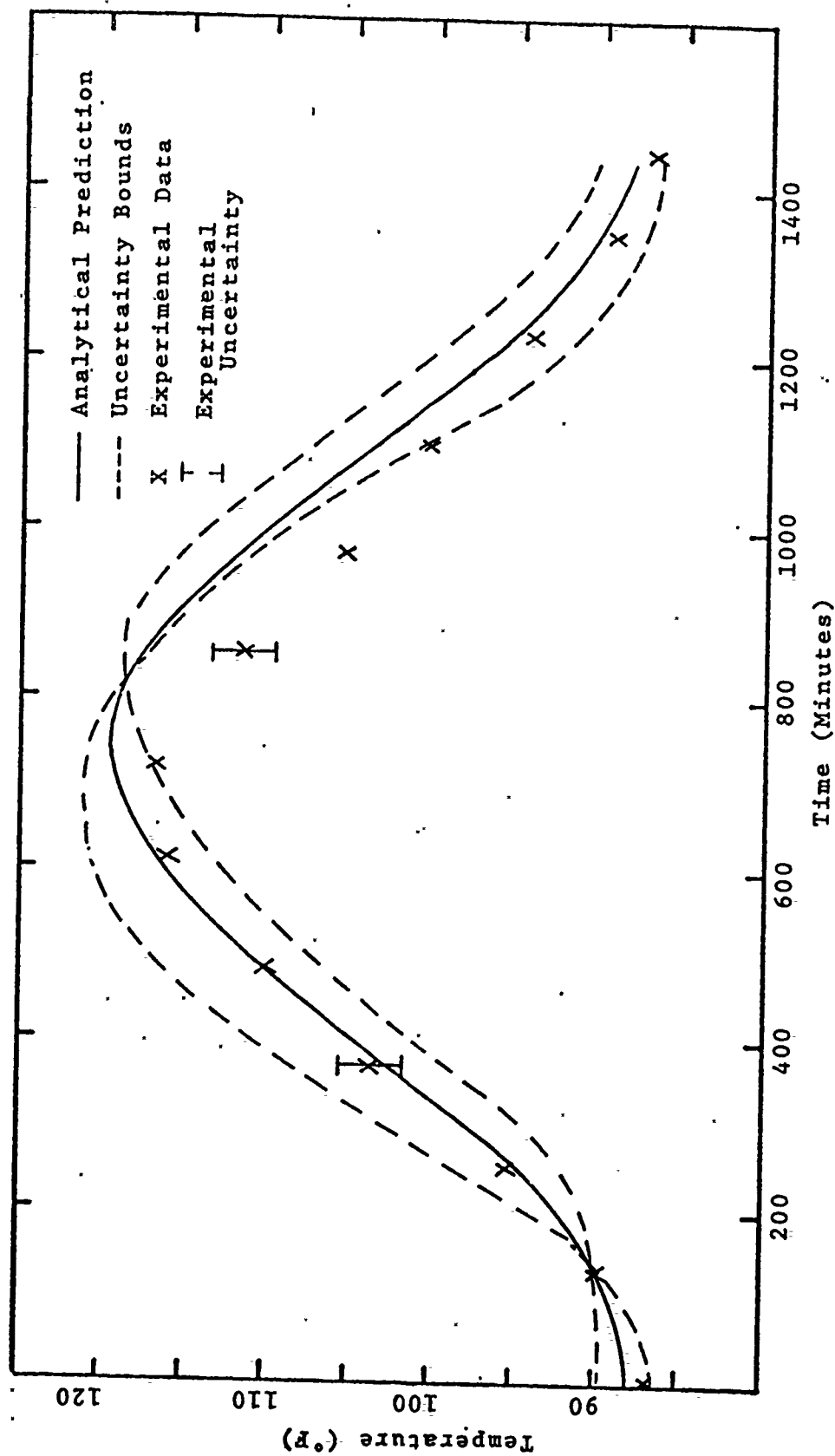


Figure 13: Comparison of Analytical and Experimental Temperature at Center of Rocket Motor.



experimental data. Again it is noted that, in actuality, the motor cools faster than the predicted value. The maximum difference in temperatures on the surface of the motor is  $15^{\circ}\text{F}$ . Figure 13 shows that the predicted value and the experimental value of the temperature at the center of the rocket motor were in close approximation except during the early stages of the cooling phase where a maximum temperature variation of about  $5^{\circ}\text{F}$  occurred.

One of the reasons the system cools faster than predicted could be the light breeze that is usually evident in the early afternoon hours at China Lake that is not present during the morning. No attempt was made to shield the system from the wind to study the effects of a light breeze on the surface temperature of the storage container.

Another point not taken into account by the analytical model is the fact that the time delay at any point in the system is not constant throughout the day as predicted in Figure 10, but varies as given by the data in Appendix D. Time delays between the peak temperature on the container surface and the peak temperature at the center of the rocket motor vary from about 250 to 400 minutes, whereas the low temperature on the surface of the container and the low temperature at the center of the rocket motor vary from about 150 to 250 minutes. The analytical model predicts a constant variation of 388 minutes at the center of the rocket motor and 159 minutes at the surface.

## B. TRUMP MODEL

### 1. One Dimensional

Four variations of the one dimensional TRUMP model were investigated and compared to the experimental data. Figures 14 and 15 compare the TRUMP predictions to the actual experimental data at the surface and the center of the rocket motor, respectively. The TRUMP variation used for this comparison modeled the storage container temperature with tabular data (See Figure 11) and assumed convection was present ( $\frac{k_c}{k} = 4.0$ ). The uncertainty analysis (Appendix E) established the uncertainty bounds for both the experimental and the analytical data in these Figures. The variation between the bulk temperature predicted by TRUMP and the experimental data closely matches with only two experimental points in Figure 14 falling outside the uncertainty bounds for this one dimensional model. Figure 11 shows that the tabular data that TRUMP interpolates is a good approximation to the averaged experimental data. At the center of the motor, as shown in Figure 15, all experimental points fall within the predicted error bounds. A comparison of the four one-dimensional TRUMP variations are given in Figures 16 and 17 at the surface and the center of the rocket motor respectively. It is clearly seen from these Figures that the convection assumption results in an increase of 2°F in the maximum temperature and a decrease of 2°F in the minimum temperature on the surface of the rocket motor. This temperature change drops to  $\pm 1.5^\circ\text{F}$  at the center of the

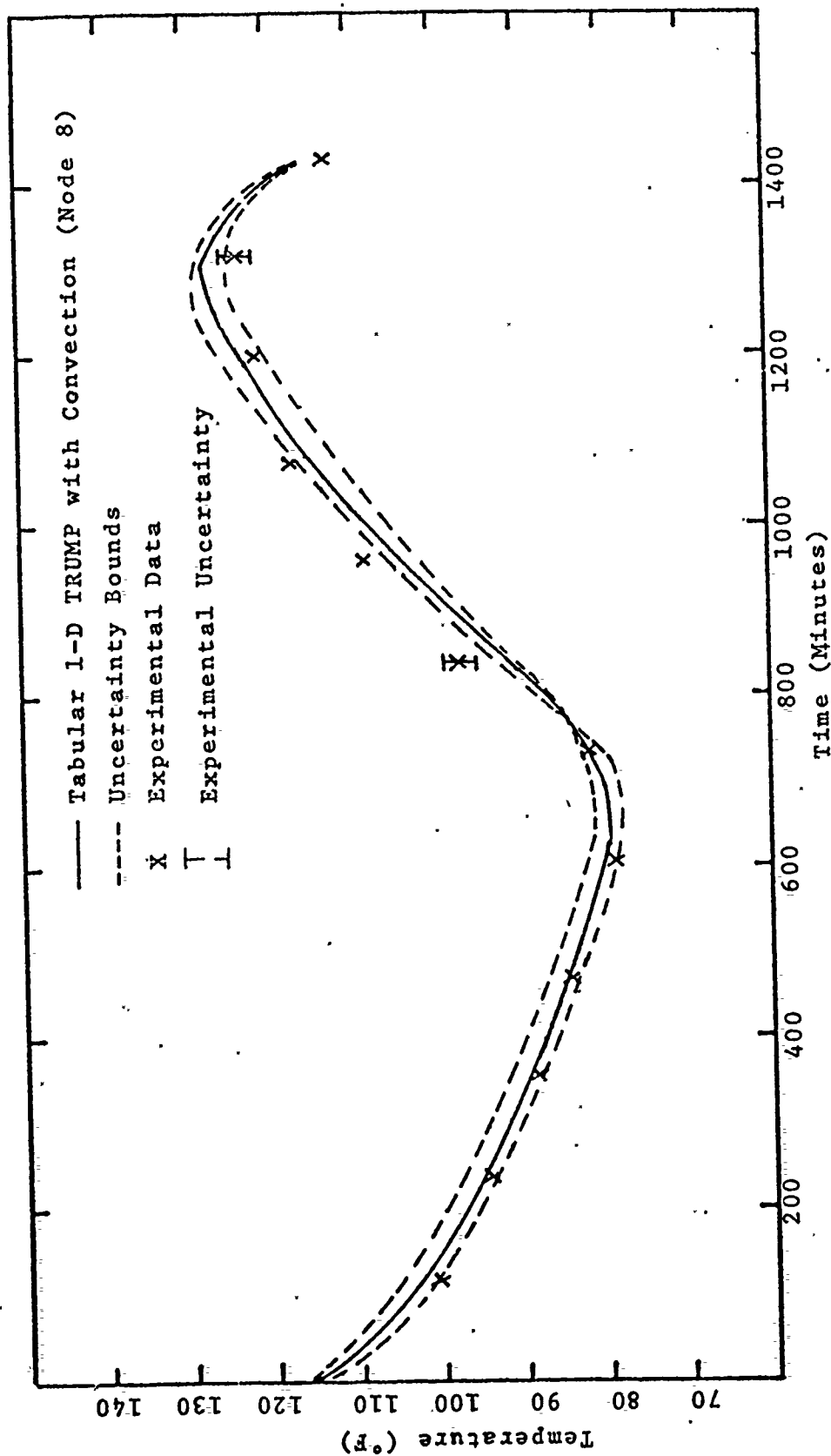


Figure 14: Comparison of 1-D TRUMP and Experimental Temperatures at Surface of the Rocket Motor.

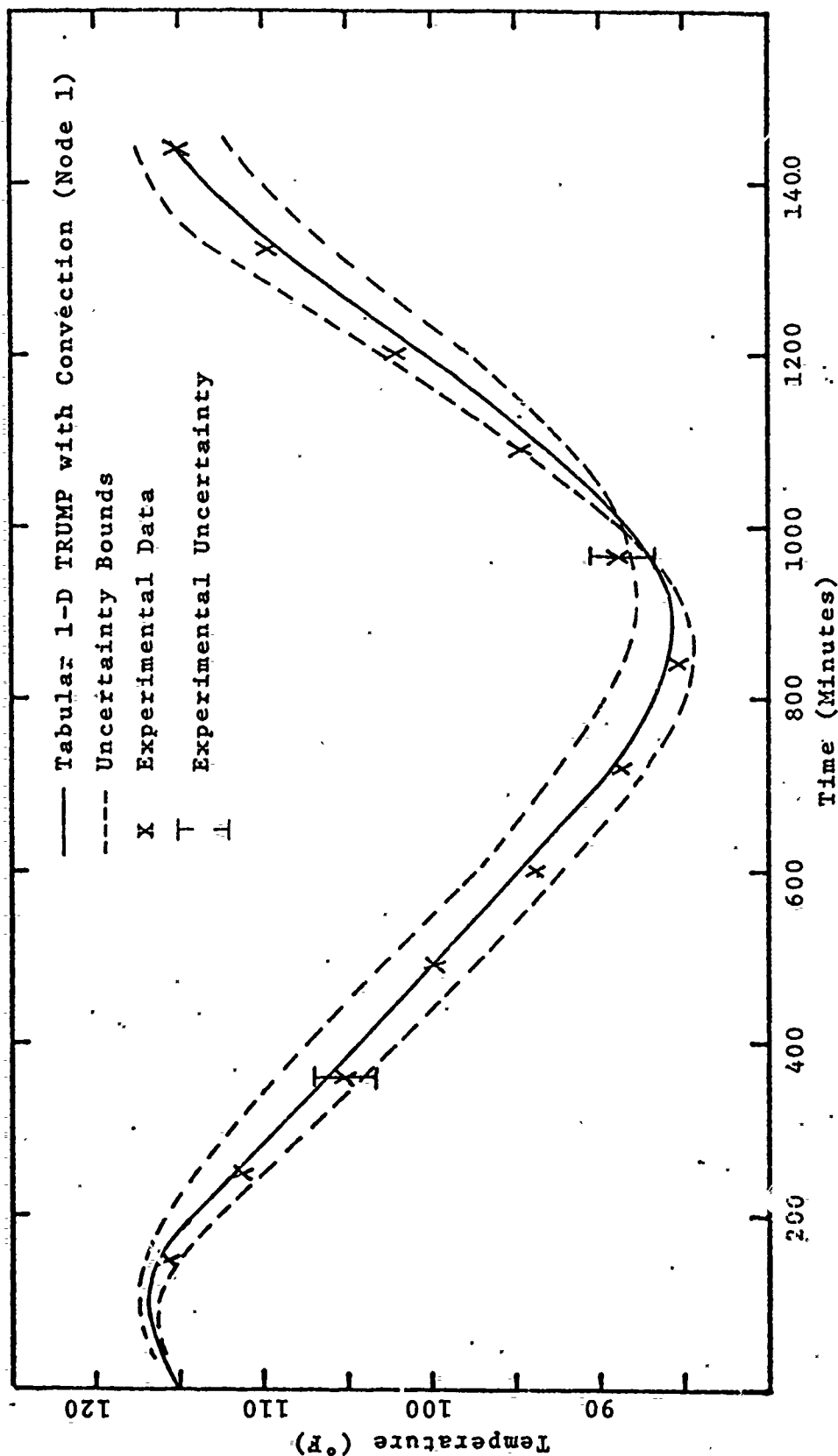


Figure 15: Comparison of 1-D TRUMP and Experimental Temperatures at Center of Rocket Motor.

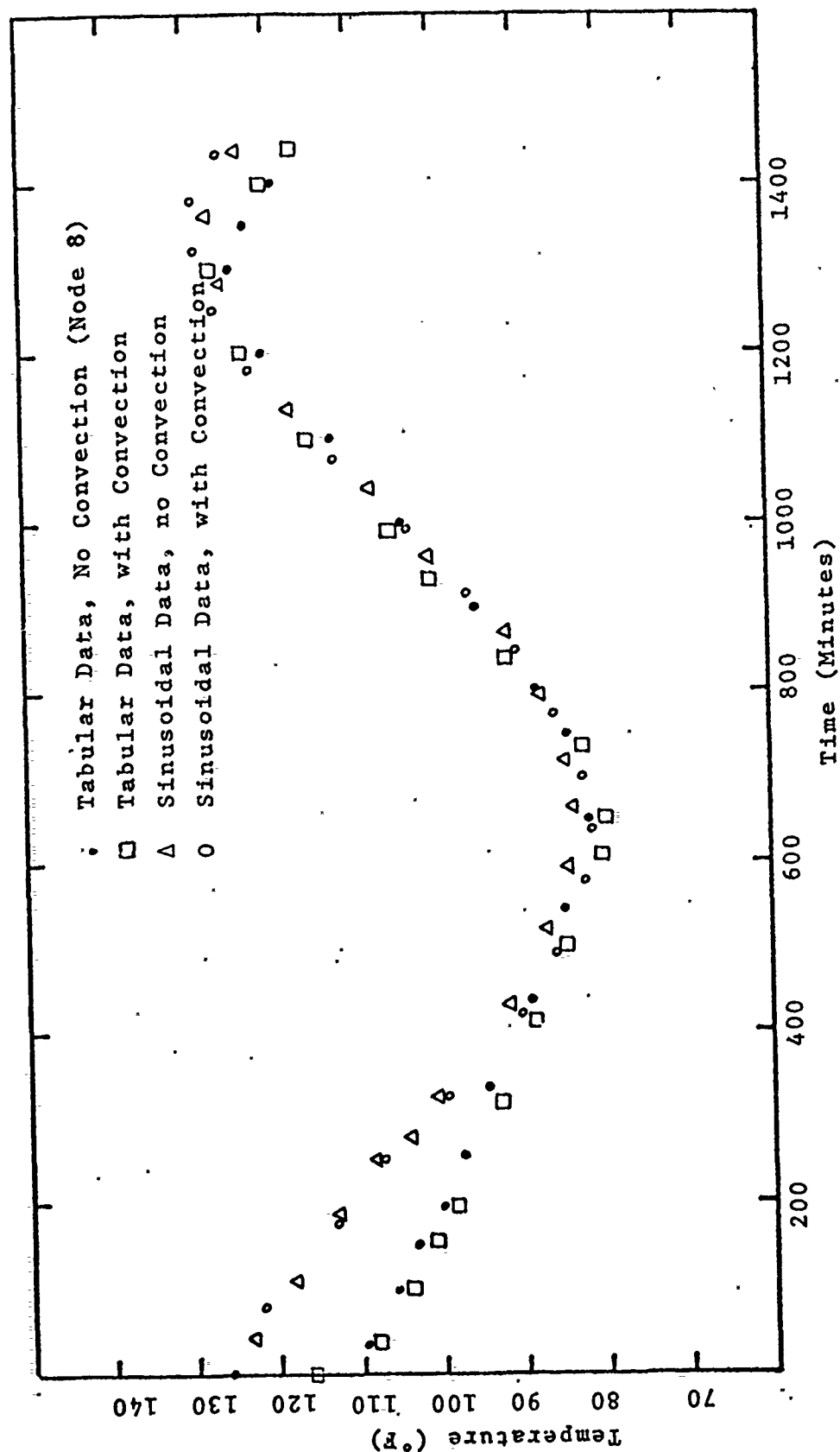


Figure 16: Comparison of Temperatures from Four 1-D TRUMP Variations at Surface of Rocket Motor.

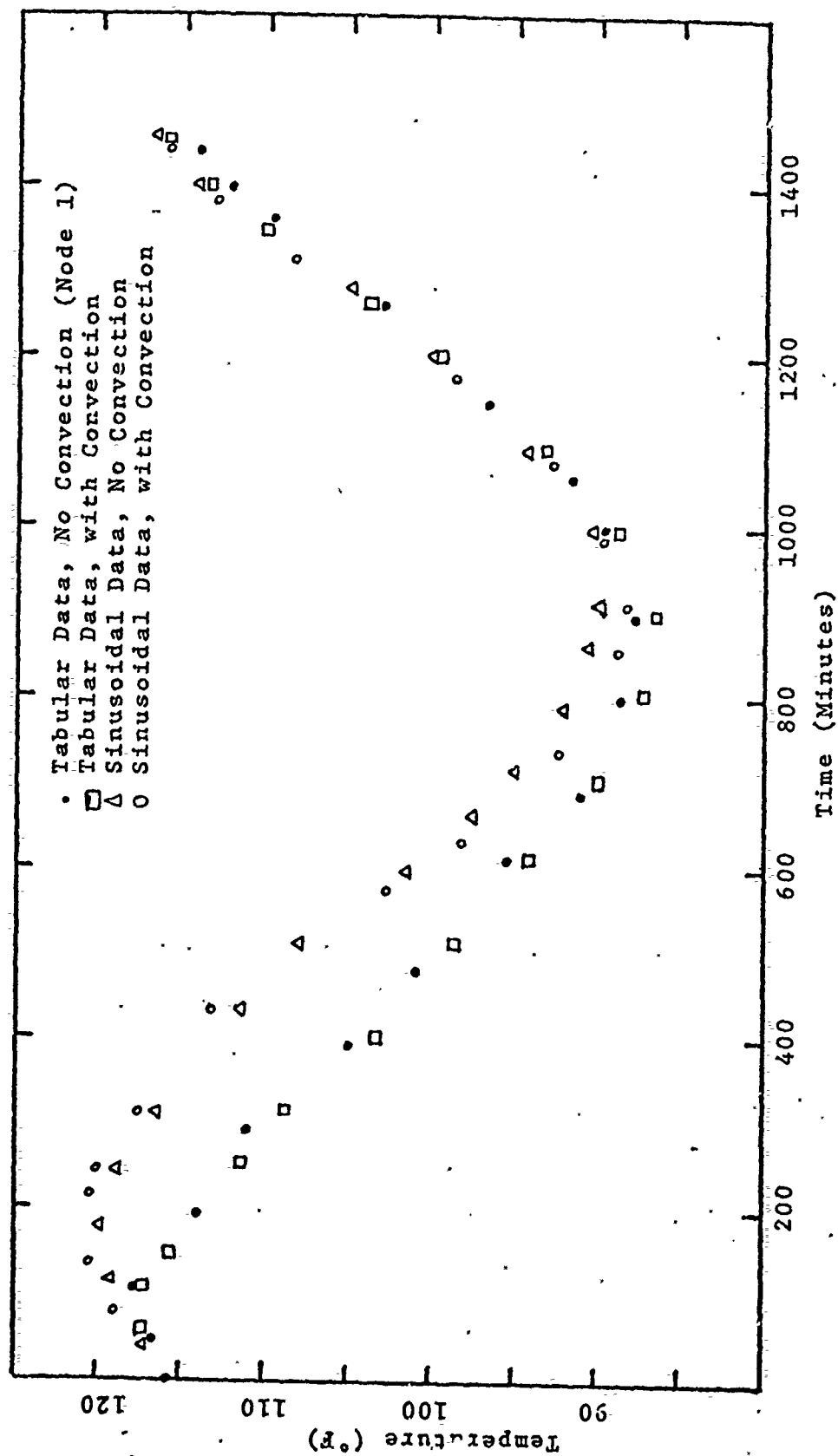


Figure 17: Comparison of Temperatures from Four 1-D TRUMP Variations at Center of Rocket Motor.

motor as shown in Figure 17. The differences between the sinusoidal approximation and the tabular approximation of the experimental data was clearly shown in Figure 11. The data in Figures 16 and 17 can be easily correlated to that in Figure 11, thereby explaining the differences in the predicted values.

## 2. Two Dimensional

Four variations of the two dimensional TRUMP model were investigated and compared to the experimental data. Comparisons of each TRUMP variation to the experimental data are given in Figures 18 and 19 for node 8 (located on the skin of the rocket motor at the 1200 position) and node 1 (at the center of the rocket motor) respectively. These Figures show that the TRUMP variations that used tabular data to model the surface temperature of the storage container predicted temperatures that more closely approximated the experimental values than were those predicted by TRUMP variations using sinusoidal data to model the surface temperature. Appendix D shows that all points on the surface of the storage container reach their minimum temperature at the same time; however, these points reach their maximum temperature as much as 200 minutes apart. Whereas, all the points on the surface of the storage container are in phase at the minimum temperature, they rapidly become out of phase as the container temperature rises. This varying phase shift makes it difficult to model the four boundary nodes with sinusoidal approximations which must have constant

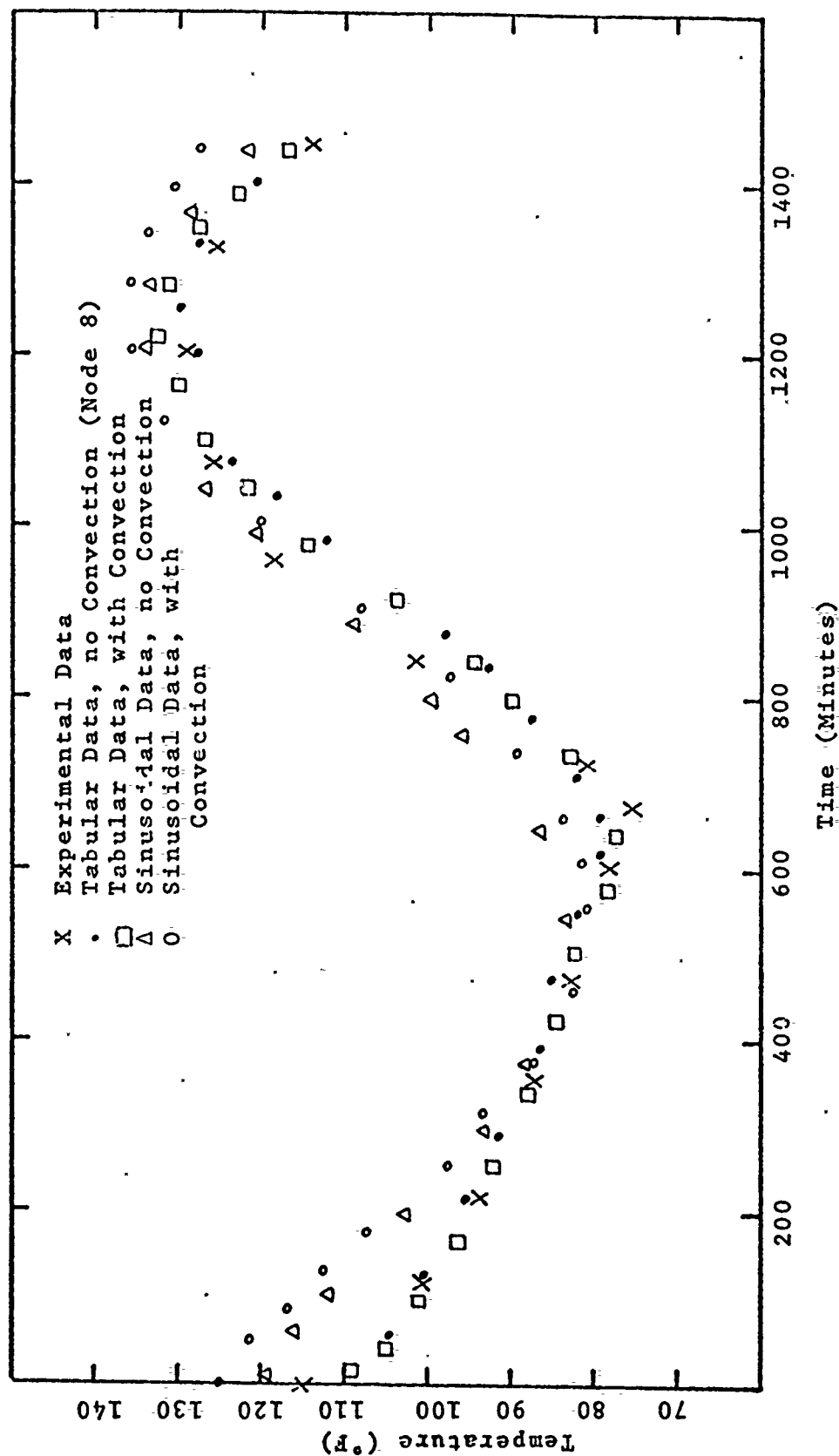


Figure 18: Comparison of 2-D TRUMP and Experimental Temperatures at Surface of Rocket Motor.



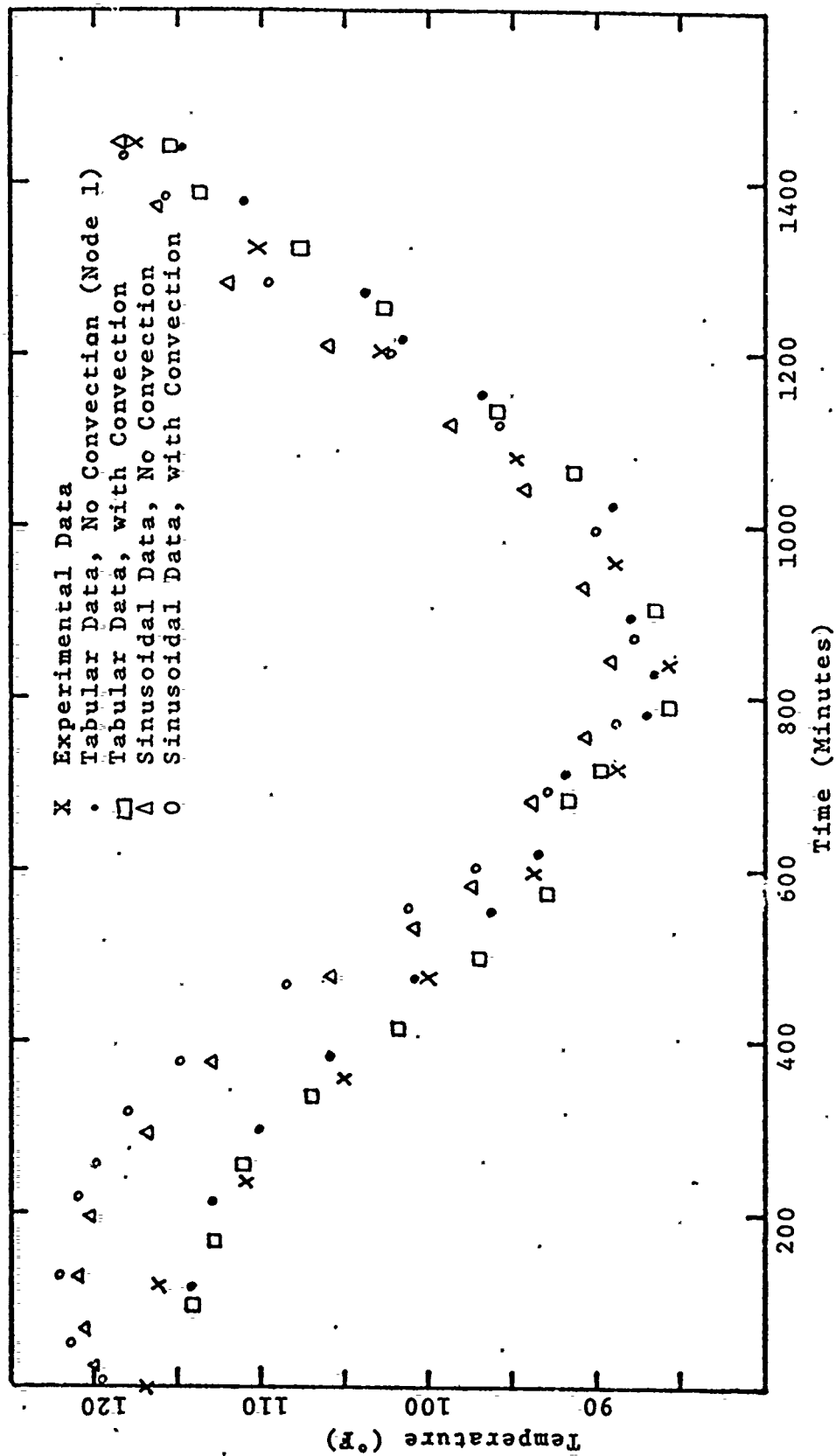


Figure 19: Comparison of 2-D TRUMP and Experimental Temperatures at Center of Rocket Motor.

phase shifts. Sizable errors in the input data during some parts of the cycle were caused by these varying phase shifts. These errors in the input data led to the variations in the predicted temperature values. As noted in the one dimensional section, the inclusion of convection effects does not produce large variations in the predicted temperatures.

Figures 20 and 21 show the actual temperature distributions on the surface of the storage container and on the surface of the rocket motor respectively at maximum bulk temperature compared to a two dimensional TRUMP program. The TRUMP variation used for this comparison assumed no free convection in the air gap and used tabular data to approximate the surface temperature of the storage container.

#### C. GENERAL

A comparison was made between surface temperatures on the storage container that contained the rocket motor and the storage container that was empty. The low temperature was about 4°F colder in the empty container, whereas the high temperature was about 4°F higher on the container that contained the rocket motor. The empty container had a faster response time than the one containing the motor. The differences in heat capacities, radiation effects, and natural convection all contribute to the changes in temperature noted.

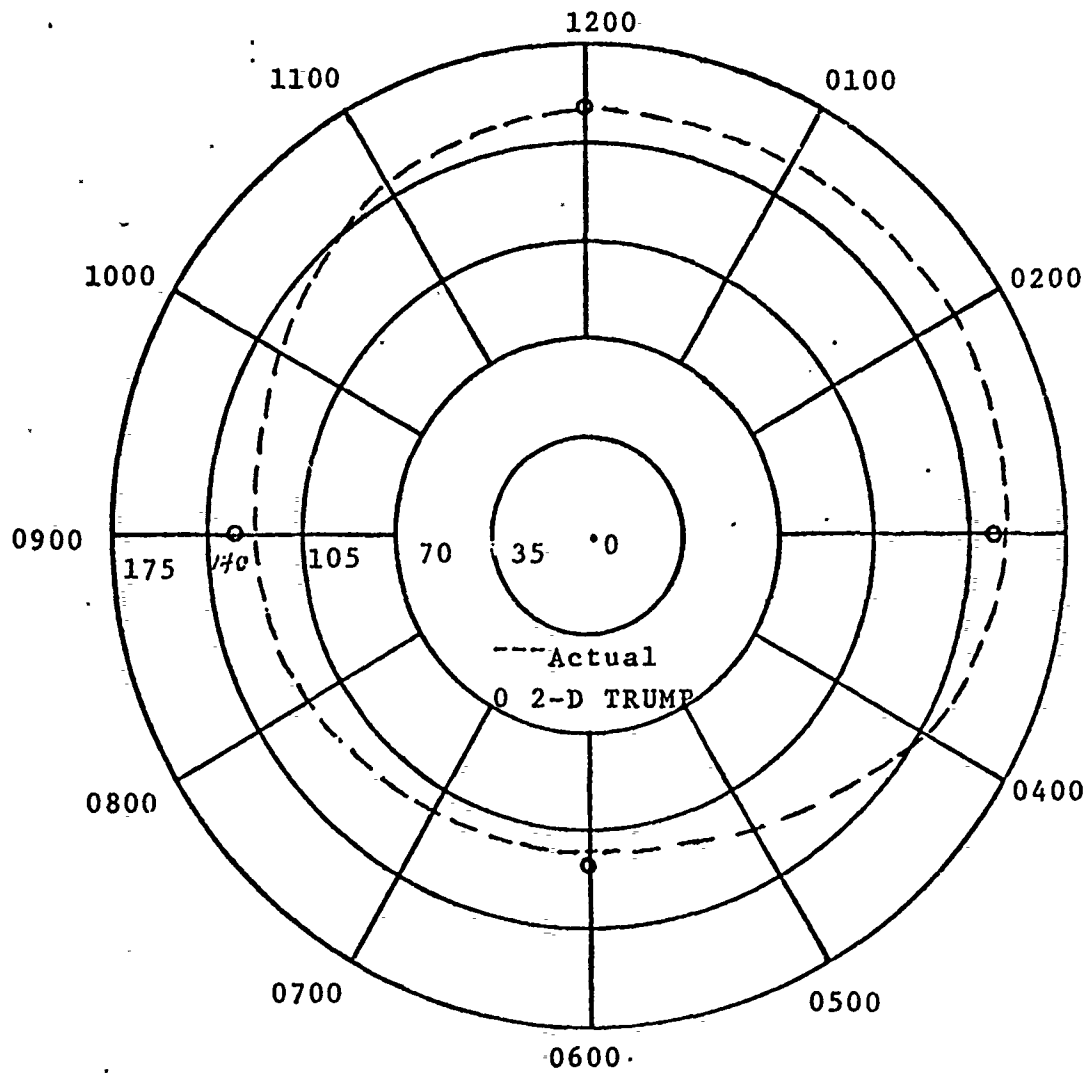


Figure 20: Temperature Distribution at Surface of Storage Container at Maximum Bulk Temperature at approximately 1500 on 2 August 1972.

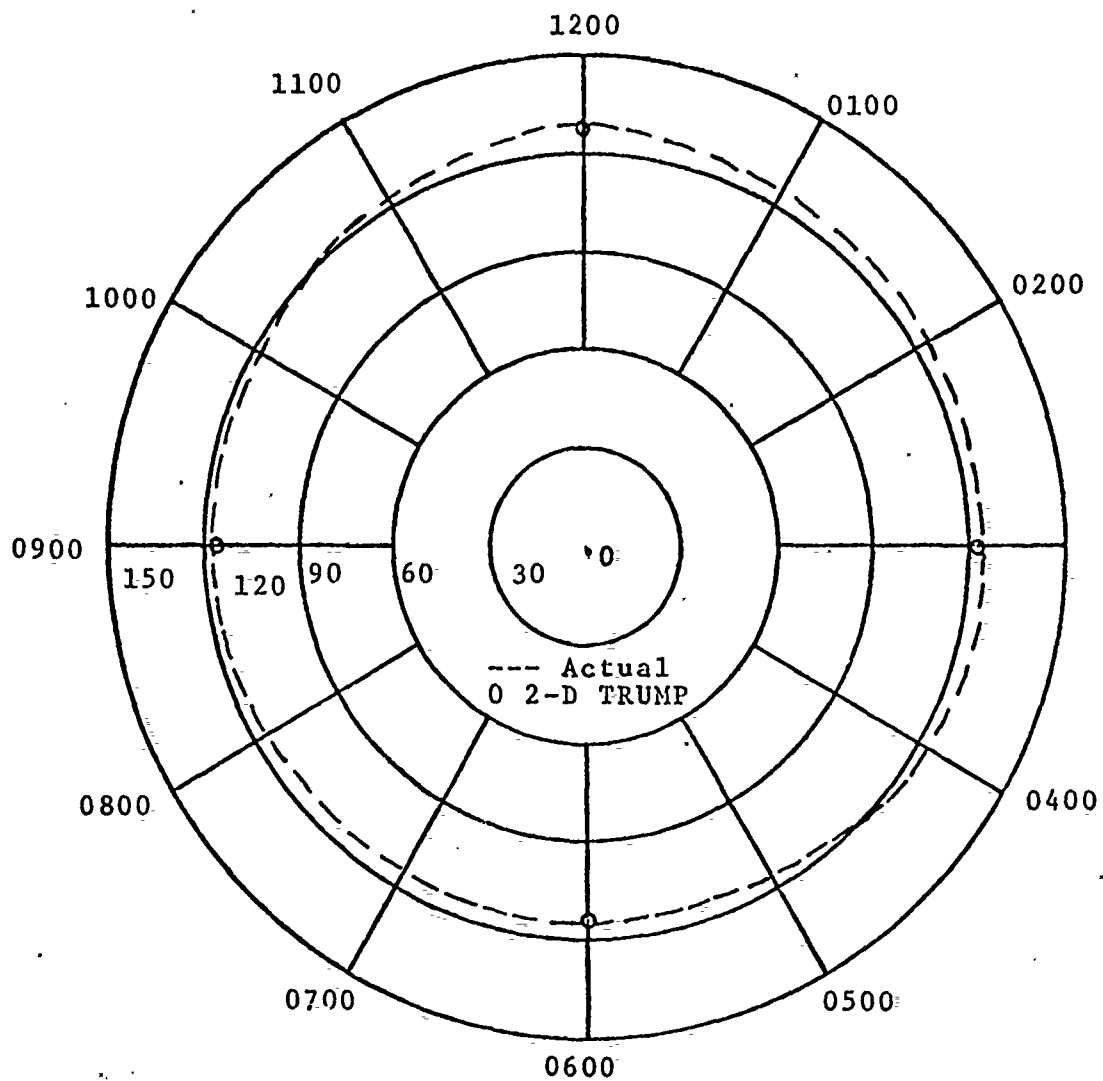


Figure 21: Temperature Distribution at Surface of the Rocket Motor at Maximum Bulk Temperature at approximately 1500 on 2 August 1972.

#### D. LIQUID CRYSTALS

The encapsulated cholesteric liquid crystals applied to the surface of the storage container gave brilliant colors under the intense desert sun. These colors were much clearer and brighter than the same crystals viewed under laboratory lighting conditions. The liquid crystals photographed well in both the color movies and the color slides. The movies showed by time lapse photography the rapidly changing surface temperature of the storage container. Two sample color prints made from the color slides are enclosed as Figures 22 and 23 to show the brilliance of the colors and the feasibility of obtaining data from color photos. The only photographic problem encountered was the intense reflection of the sunlight from the polyurethane film. This problem was partially overcome by taking the photographs from angles where the reflection was less intense. Qualitatively the liquid crystals were not adversely affected by the sun's rays after two weeks of desert exposure. No accurate quantitative determination was attempted; however, rough approximations were made at the site. These approximations were made by noting the color exhibited by a crystal at a certain time and then comparing the calibration of the crystal (Table 1) to the temperature recorded by the thermocouple located directly beneath the region of color change. The readings were within  $\pm 2^{\circ}\text{F}$ , which was very encouraging, especially considering the approximations made while taking these measurements. Although photos were taken only during



Figure 22. Thermal Mapping with Liquid Crystals.

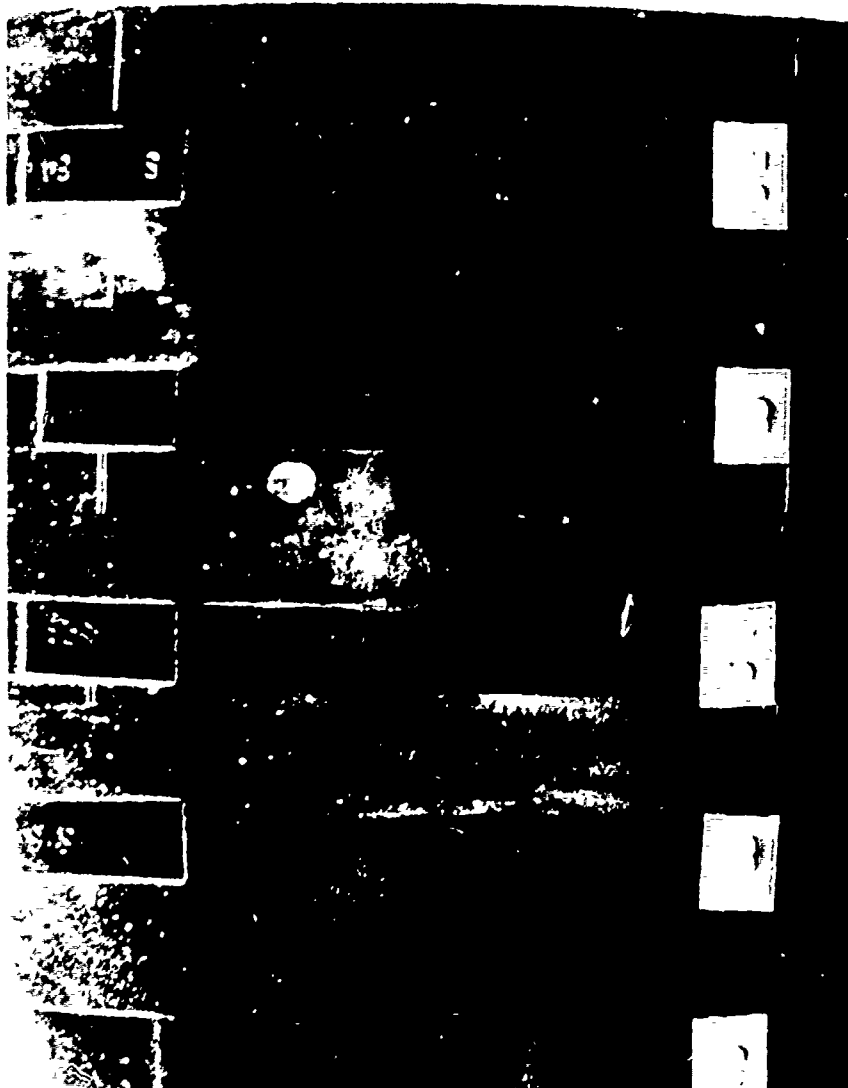


Figure 23. Liquid Crystals Feasible Under Hostile Environment.

the initial two weeks of the study, on site observations indicate that the crystals are still showing brilliant colors after 3-1/2 months. Preliminary evidence indicates that the polyurethane film did protect the crystals from decomposing from the sun's rays and from being worn away by the wind blown sand.

It was noted that the surface temperature of the storage container under the liquid crystals reached temperatures up to 15°F higher than a similar point not under the crystals. This 15°F difference was only evident when maximum temperatures were obtained. During sunlight hours the temperature under the liquid crystals was always somewhat higher; however, at night both temperatures were equal. The difference in the container surface temperatures led to a difference of 4°F on the surface of the rocket motor and 1°F at the center of the motor. It is believed that the difference in emissivities of the gray and black surfaces resulted in the difference in container surface temperature.



## VI. CONCLUSIONS

From the results of this investigation, the following conclusions were drawn:

1. Although a sine wave is not a perfect fit for the experimental data at all points, it is useful in predicting bulk temperatures in the rocket motor, especially if only the high and low bulk temperatures are of concern. This is especially true in the one dimensional case. In the two dimensional case, the problem of phase shift variations make the method of sinusoidal variation less desirable, although still useful.

2. The simulation of the actual data by a table of temperatures gave the most accurate predictions of the experimental data. This method should be used whenever tabulated data are available; however, this will generally not be the case for design work, in which case the sinusoidal approximations must be used.

3. The flexibility of both the analytical and computer simulations allow the changing of many parameters. The resulting effects of these changes on rocket motor temperature can be studied with the models.

4. The convection assumption for this system resulted in only small changes in temperature and can be neglected when predicting design temperatures. Either the Liu or Beckmann correlation should be used to determine if convection can be neglected in a particular system.

5. The use of an empty storage container to obtain surface temperature data is a good approximation to using one with a rocket motor inside.

6. It is feasible to use liquid crystals for thermal mapping under desert conditions. Color photography with standard equipment gives excellent results since brilliant colors were observed.

7. The liquid crystals appear to be stable for at least two weeks under the desert conditions when protected with a polyurethane coating.

8. The application of the liquid crystal system to the surface of the storage container resulted in large increases in the surface temperature of the container throughout the hottest part of the day. Care must be taken in applying and interpreting thermal readings from liquid crystals when exposed to radiant heating.

## VII. RECOMMENDATIONS

From the results of this basic study, the following recommendations for future work are offered:

1. To refine the results of this project, a second rocket motor storage container system should be instrumented with the following changes:

- a. Liquid crystals should not be applied to the system used as the experimental model. As steel is a good thermal conductor, axial conduction on the surface of the storage container may be significant. Heat flow from the area where the crystals are applied may lead to higher than normal temperatures at other points on the surface of the container.

- b. The rocket motor should be weighed before and after the loading of the dry sand so that an accurate determination of the density of the propellant simulant can be determined.

- c. Four additional thermocouples should be located on the surface of the storage container to better enable the averaging of data. At present, the #1 thermocouple which was used as the average temperature reading of the top quarter of the surface of the container, in actuality is its hottest point; likewise the #10 thermocouple was used as the average temperature of the bottom quarter of the surface, in actuality it's the coldest point. For averaging data, it is recommended that thermocouples be placed at 0130,

0430, 0730, and 1030 and the quarters of the system be divided at 0300, 0600, 0900, and 1200 to give a more realistic bulk temperature. Thermocouples at 1200 and 0600 will provide the maximum and minimum temperature of the system.

2. The TRUMP program should be rerun in both the one and two dimensional form, varying the mesh sizes to determine the optimum number of nodes.

3. A long term study of the effects of the desert environment on liquid crystals should be done. The crystals should be calibrated before being placed in the desert and then brought to a laboratory for recalibration at specific intervals.

4. Several modifications should be made to the TRUMP program to make it comparable to the version used at Lawrence Radiation Laboratory. The variable conductivity section (BLOCK 2) and the PLOT subroutine (BLOCK 11) need to be corrected. The TIMEP subroutine which allows the setting of the problem time interval between data output should be added to this version of TRUMP. It would also be advantageous to increase the amount of tabular data that could be read in as boundary temperatures.

5. From an academic standpoint, the effects of free convection in an air gap with varying boundary temperatures should be investigated.

## APPENDIX A

### Introduction to Liquid Crystals

Liquid crystals were first discovered in 1889 by Reinitzer [Ref. 8] and the investigations of Lehmann which continued to 1915. Liquid crystals were considered to be laboratory curiosities with no scientific or practical merit until the 1950's. They share some of the properties of both liquids and crystals; for example, a typical liquid crystal substance scatters light in symmetrical patterns and reflects different colors depending on the angle from which it is viewed. Studies in the last few years have helped to clarify the unusual molecular structure of liquid crystals. Many applications arise from their ability to detect minute fluctuations in temperature, mechanical stress, electromagnetic radiation and chemical environment by changes in their color.

Liquid crystals are divided into three classes; smectic, nematic, and cholesteric, depending on the degree of spatial arrangement of the molecules in the mass of the material and the type of the material [Ref. 9]. In this project only cholesteric liquid crystals were used and therefore only their properties will be mentioned. The molecular structure of cholesteric liquid crystals is characteristic of the esters of cholesterol (Figure 24). The molecular layers are very thin with the long axis of the molecules parallel to the plane of the layers. The individual molecules are

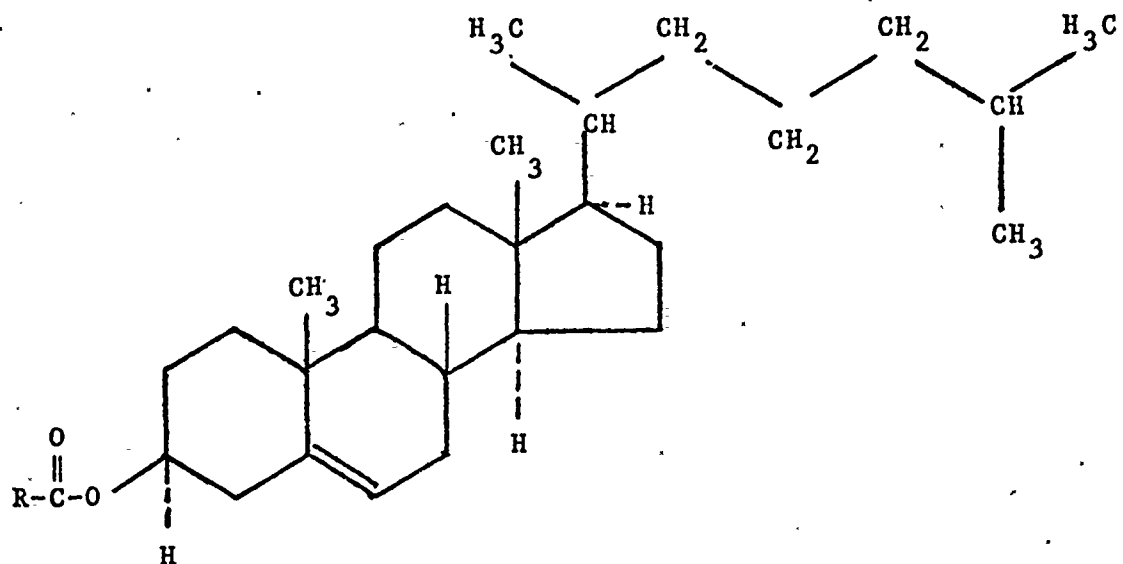


Figure 24: Molecular Structure of Cholesteric Ester

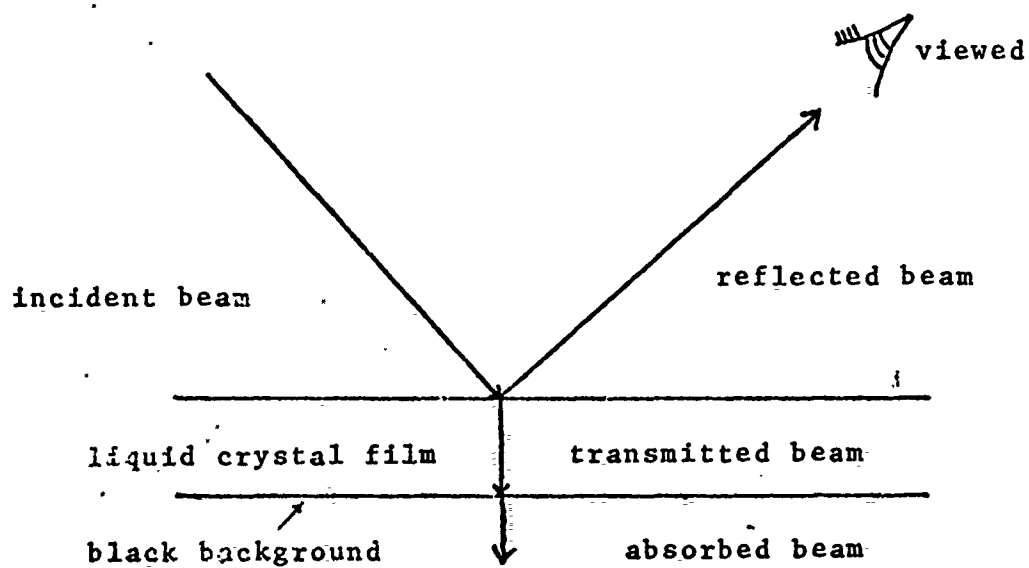


Figure 25. Light Reflection from Liquid Crystals.

basically flat, with a side chain of methyl groups ( $-\text{CH}_3$ ) projecting upward from the plane of each molecule. This configuration causes the direction of the long axis of the molecules in each layer to be displaced slightly from the corresponding direction in adjacent layers. This displacement, which averages about fifteen minutes of arc per layer, is cumulative through successive layers, and the overall displacement traces out a helical path.

The molecular structure of cholesteric liquid crystals gives rise to many peculiar optical properties. If linearly polarized light is transmitted perpendicularly to the molecular layers, the direction of the electric vector of the light will be rotated to the left in a helical path. Therefore, the plane of polarization will also be rotated to the left, through an angle proportional to the thickness of the transmitting material. Liquid crystals are the most optically active substances known. Another strictly crystalline optical property exhibited by cholesteric liquid crystals is circular dichroism. When ordinary white light is incident to a cholesteric material, the light is separated into two components, one with the electric vector rotating clockwise, the other rotating counterclockwise. Depending on the material, one of these components is transmitted, and the other is reflected. It is this property that gives the cholesteric phase its iridescent color when it is illuminated by white light. The particular combination of colors depends on the material, the temperature, and the angle of the incident light.

The molecular structure of a cholesteric substance is very delicately balanced and is easily upset. Any small disturbance that interferes with the weak forces between the molecules can produce marked changes in optical properties such as reflection, transmission, birefringence, circular dichroism, optical activity and color. The most striking optical transformation that occurs in a cholesteric substance, in response to small changes in its environment, is the variation of color with temperature. The crystal lattice is disrupted by the thermal vibrations giving successive transitions between the solid, the mesophase, and the isotropic liquid with rising temperature. The change from the three dimensional order of the crystal lattice to the disorder of the isotropic liquid occurs via one or more intermediate states, each of which has a particular temperature range at which it is stable [Ref. 10].

A cholesteric liquid crystal system responds to changes in temperature by sequentially passing through the complete visual spectrum (red through violet) in fractions or multi-degrees, depending on which cholesterol esters comprise the formulation. This color phenomenon is reversible and has been reported to function over a temperature range of  $-20^{\circ}\text{C}$  to  $250^{\circ}\text{C}$ . A very important point to note is that at a certain temperature a given material or combination of materials will always exhibit the same color. Also, the rate of change from color to color as well as the exact temperature at which the specific color changes occur are invariable. By



mixing cholesteric substances in various proportions, any desired temperature combination can be obtained. The thickness of the cholesteric film does not affect the predominant wave length of the reflected light; the light becomes circularly polarized [Ref. 11].

The colors scattered by the liquid crystals represent only a fraction of the incident light (Figure 25). The remaining portion of the incident light is transmitted by the liquid crystals. Therefore, an absorptive black background must be used to prevent reflection of the transmitted light, thereby enhancing the resolution of the scattered colors or wavelengths reflected by the liquid crystal system.

The cholesteric liquid crystal systems often present a number of problems due to the fact that they are viscous liquids. Some problems associated with the handling and the use of these materials are:

1. The tendency of the liquid crystal system to flow during application can cause variations in applied film thickness. This may result in non-uniform thermal patterns.

2. Direct exposure of liquid crystals to adverse environmental effects can cause variations in their sensitivity and deteriorate their color response in a few days.

These problems can be partially overcome by using an encapsulated liquid crystal material system. The capsules are 20-30 microns in diameter and are a water-based slurry suitable for application by conventional coating techniques such as brushing or spraying.

Encapsulated liquid crystals offer several advantages:

1. They convert the liquid crystal system to a pseudo-solid, which provides for easier handling, application, and use.
2. They provide longer shelf life by minimizing surface contamination and giving protection from ultraviolet light [Ref. 12].
3. They exhibit relatively unlimited fatigue life.
4. They reduce the angular dependence of the color observed.

## APPENDIX B

### Analytical Solution

The method of complex temperature as presented by Arpaci [Ref. 1] was used to find the steady periodic solution of a body experiencing a periodic sinusoidal disturbance. The general heat conduction equation in cylindrical coordinates was the basis for this derivation. It was assumed that no heat sources existed in this problem, that the rocket motor storage container system was infinitely long, that there was no heat conduction in the axial or circumferential directions, and that the container surface temperature was spatially uniform. Figure 26 gives a basic sketch of the system. The assumptions reduced the heat conduction equation to

$$\frac{1}{r} \frac{\partial (r \frac{\partial T}{\partial r})}{\partial r} = \frac{1}{\alpha} \frac{\partial T}{\partial t} \quad (1)$$

where  $r$  is the radial distance from the center of the rocket motor,  $T$  is the temperature of the rocket motor at time  $t$  and position  $r$ , and  $\alpha$  is the thermal diffusivity, a property of the conducting material.

$$\alpha = \frac{k}{\rho c} \quad (2)$$

where  $k$  is the thermal conductivity of the conducting material,  $\rho$  is the density of the material, and  $c$  is the specific heat. All thermal properties were assumed to be constant over the temperature range of this problem.

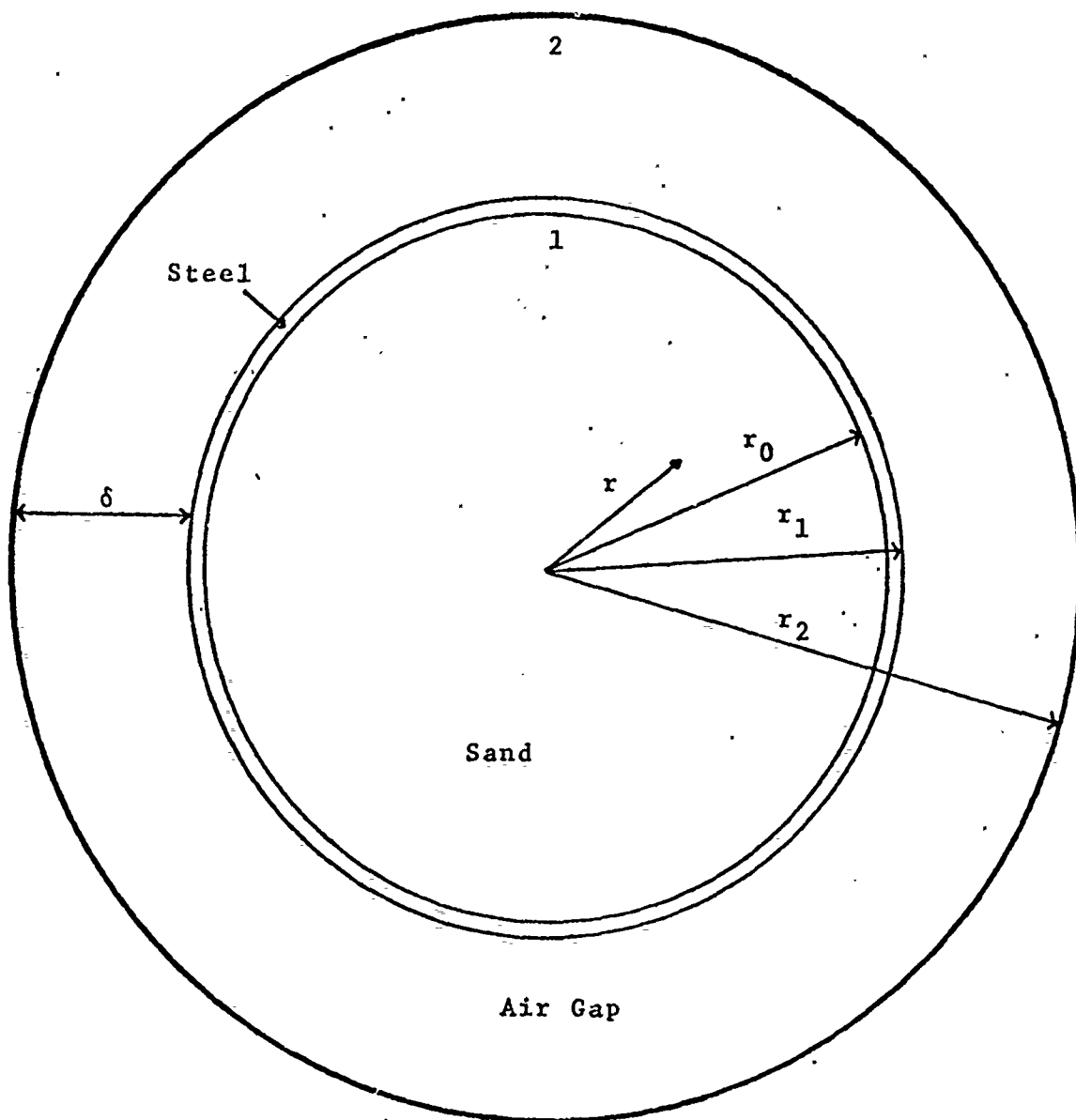


Figure 26. Analytical Model of Experimental System.

The boundary conditions used in this derivation were

$$\frac{dT}{dr} = 0 \quad \text{at } r = 0$$

$$\text{and } \frac{dT}{dr} = -\frac{\bar{h}}{k} (T - T_{\infty}) \quad \text{at } r = r_0$$

where  $r_0$  is the inner radius of the rocket motor.

$T_{\infty}$  is the known storage container temperature which is assumed to vary as

$$T_{\infty} = (T_M - T_A) \sin \omega t + T_A$$

where

$T_M$  = maximum bulk temperature of the storage container

$T_A$  = average bulk temperature of the storage container

$\omega$  = frequency of the sinusoidal variation ( $\frac{2\pi}{24 \text{ hours}}$ )

$t$  = time

$\bar{h}$  is the effective heat transfer coefficient across the air gap between the storage container and the rocket motor. It combines the heat transfer effects of radiation, convection, and conduction into one coefficient. The radiation coefficient was linearized by assuming constant temperatures ( $T_1, T_2$ ), representative of the average temperatures expected in the problem, in the equation

$$h_{\text{RAD}} = \mathcal{F}_{1-2} \sigma (T_1 + T_2) (T_1^2 + T_2^2)$$

where  $\sigma$  is the Stefan-Boltzmann constant and  $\mathcal{F}_{1-2}$  is the radiation exchange factor between surfaces 1 and 2. The convection coefficient is

$$h_{\text{CON}} = \frac{k_c}{\delta}$$

where  $k_c$  is the effective conductivity of air as obtained from the Beckmann and Liu correlations [Ref. 5 and 7] and  $\delta$  is the width of the air gap. In the analytical model,

the effective conductivity was assumed to equal the conductivity, thereby treating it as pure conduction and

$$\bar{h} = h_{\text{RAD}} + h_{\text{CON}}$$

Equation (1) was non-dimensionalized using the following relationships

$$\theta = \frac{T - T_A}{T_M - T_A} \quad (\text{a non-dimensional temperature})$$

$$\xi = \frac{r}{r_o} \quad (\text{a non-dimensional distance})$$

to give

$$\frac{1}{\xi} \frac{d(\xi \frac{d\theta}{d\xi})}{d\xi} = \frac{r_o^2}{\alpha} \frac{d\theta}{dt}$$

with boundary conditions

$$\frac{d\theta}{d\xi} = 0 \quad \text{at} \quad \xi = 0$$

$$\text{and} \quad \frac{d\theta}{d\xi} = -\beta(\theta - \sin \omega t) \text{ at } \xi = 1$$

where  $\beta = \frac{\bar{h}r_o}{k}$  is the Biot modulus (which compares the relative magnitudes of the effective heat transfer coefficient across the air gap and the internal conduction resistances to heat transfer).

An initial condition was not specified as the only concern was with the steady state, periodic behavior. Following Arpaci [Ref. 1], a complex temperature was defined as

$$\psi(r, t) = \theta^*(r, t) + i\theta(r, t)$$

where  $\psi(r, t)$  satisfied

$$\frac{1}{\xi} \frac{d(\xi \frac{d\psi}{d\xi})}{d\xi} = \frac{r_o^2}{\alpha} \frac{d\psi}{dt} \quad (3)$$

with boundary conditions

$$\frac{\partial \psi}{\partial \xi} = \frac{\partial \theta^*}{\partial \xi} + i \frac{\partial \theta}{\partial \xi} = 0 \quad \text{at } \xi = 0$$

$$\text{and } \frac{\partial \psi}{\partial \xi} = -\beta(\psi - e^{i\omega t}) = -\beta(\theta^* - \cos \omega t) + i\{-\beta(\theta - \sin \omega t)\} \text{ at } \xi = 1$$

This leads to  $\theta(r, t)$  which satisfied

$$\frac{1}{\xi} \frac{d(\xi \frac{\partial \theta}{\partial \xi})}{d\xi} = \frac{r_o^2}{\alpha} \frac{\partial \theta}{\partial t}$$

with boundary conditions

$$\frac{\partial \theta}{\partial \xi} = 0 \quad \text{at } \xi = 0$$

$$\text{and } \frac{\partial \theta}{\partial \xi} = -\beta(\theta - \sin \omega t) \quad \text{at } \xi = 1$$

also  $\theta^*(r, t)$  which satisfied

$$\frac{1}{\xi} \frac{d(\xi \frac{\partial \theta^*}{\partial \xi})}{d\xi} = \frac{r_o^2}{\alpha} \frac{\partial \theta^*}{\partial t}$$

with boundary conditions

$$\frac{\partial \theta^*}{\partial \xi} = 0 \quad \text{at } \xi = 0$$

$$\text{and } \frac{\partial \theta^*}{\partial \xi} = -\beta(\theta^* - \cos \omega t) \quad \text{at } \xi = 1$$

A solution of the form

$$\psi(r, t) = \phi(r) \tau(t)$$

was assumed, where for large values of time  $\tau(t)$  was assumed to equal  $e^{i\omega t}$ ; therefore,

$$\psi(r, t) = \phi(r) e^{i\omega t} \quad (4)$$

Equation (4) was then substituted into equation (3)

$$\frac{1}{\xi} \frac{d(\xi \frac{\partial \phi}{\partial \xi})}{d\xi} - \frac{i\omega r_o^2 \phi}{\alpha} = 0 \quad (5)$$

with boundary conditions

$$\frac{d\phi}{d\xi} = 0 \quad \text{at } \xi = 0$$

and 
$$\frac{d\phi}{d\xi} = -\beta(\phi-1) \quad \text{at } \xi = 1$$

Equation (5) was expanded to give

$$\frac{d^2\phi}{d\xi^2} + \frac{1}{\xi} \frac{d\phi}{d\xi} - \frac{i\omega r_o^2}{\alpha} \phi = 0 \quad (6)$$

$$\text{Now, let } Z = \sqrt{\frac{i\omega r_o^2}{\alpha}} \xi$$

and substitute into equation (6)

$$\frac{d^2\phi}{dZ^2} + \frac{1}{Z} \frac{d\phi}{dZ} - \phi = 0 \quad (7)$$

with boundary conditions

$$\frac{d\phi}{dZ} = 0 \quad \text{at } Z = 0$$

and

$$\frac{d\phi}{dZ} = -\frac{\beta}{\sqrt{\frac{i\omega r_o^2}{\alpha}}} (\phi-1) \quad \text{at } Z = \sqrt{\frac{i\omega r_o^2}{\alpha}}$$

The general solution of equation (7) is

$$\phi = C_1 I_0(Z) + C_2 K_0(Z) \quad (8)$$

as given in Ref. 13 with

$$I_0(Z) = 1 + \left(\frac{1}{2}Z\right)^2 + \frac{\left(\frac{1}{2}Z\right)^4}{(2!)^2} + \dots = \sum_{n=0}^{\infty} \frac{\left(\frac{1}{2}Z\right)^{2n}}{(n!)^2}$$

and

$$K_0(Z) = -\{\gamma + \log\left(\frac{1}{2}Z\right)\} I_0(Z) + \sum_{n=1}^{\infty} \frac{\left(\frac{1}{2}Z\right)^{2n}}{(n!)^2} \left\{1 + \frac{1}{2} + \frac{1}{3} + \dots + \frac{1}{n}\right\}$$

Now using the boundary condition

$$\frac{d\phi}{dZ} = 0 \quad \text{at } Z = 0$$



and differentiating equation (8) yields

$$\frac{d\phi}{dz} = c_1 \frac{d(I_o(z))}{dz} + c_2 \frac{d(K_o(z))}{dz}$$

where

$$\frac{d(I_o(z))}{dz} = 0 \quad \text{at } z = 0$$

and

$$\frac{d(K_o(z))}{dz} \neq 0 \quad \text{at } z = 0$$

therefore  $c_2 \equiv 0$

$$\text{and} \quad \phi = c_1 I_o(z) \quad (9)$$

Now using the second boundary condition that

$$\frac{d\phi}{dz} = - \frac{\beta}{\sqrt{\frac{i\omega r_o^2}{\alpha}}} (\phi - 1) \quad \text{at } z = \sqrt{\frac{i\omega r_o^2}{\alpha}} \quad (10)$$

and differentiating equation (9) gives

$$\frac{d\phi}{dz} = c_1 \frac{d(I_o(z))}{dz}$$

Noting that  $\frac{d(I_o(z))}{dz} = I_1(z)$  and substituting into equation (10)

$$c_1 I_1 \left( \sqrt{\frac{i\omega r_o^2}{\alpha}} \right) = \frac{\beta}{\sqrt{\frac{i\omega r_o^2}{\alpha}}} \left( c_1 I_o \left( \sqrt{\frac{i\omega r_o^2}{\alpha}} \right) - 1 \right)$$

Rearranging and solving for  $c_1$

$$c_1 = \frac{1}{\sqrt{\frac{i\omega r_o^2}{\alpha\beta^2}} I_1 \left( \sqrt{\frac{i\omega r_o^2}{\alpha}} \right) + I_o \left( \sqrt{\frac{i\omega r_o^2}{\alpha}} \right)}$$

and then substituting into equation (9)

$$\phi = \frac{I_0(z)}{I_0\left(\sqrt{\frac{i\omega r_o^2}{\alpha}}\right) + \frac{1}{\beta}\sqrt{\frac{i\omega r_o^2}{\alpha}} I_1\left(\sqrt{\frac{i\omega r_o^2}{\alpha}}\right)} \quad (11)$$

Now as

$$J_\nu(imx) = i^\nu I_\nu(mx) \quad [\text{Ref. 3, p. 135}]$$

$$I_0\left(\sqrt{\frac{\omega r_o^2}{\alpha}} i^{1/2} \xi\right) = J_0\left(\sqrt{\frac{\omega r_o^2}{\alpha}} i^{3/2} \xi\right)$$

and

$$I_1\left(\sqrt{\frac{\omega r_o^2}{\alpha}} i^{1/2} \xi\right) = \frac{1}{i} J_1\left(\sqrt{\frac{\omega r_o^2}{\alpha}} i^{3/2} \xi\right)$$

Let  $a = \sqrt{\frac{\omega r_o^2}{\alpha}}$  and substitute into equation (11)

$$\phi = \frac{J_0(i^{3/2} a \xi)}{J_0(i^{3/2} a) - \frac{a}{\beta} i^{3/2} J_1(i^{3/2} a)} \quad (12)$$

$$\text{Now } i^{3/2} = e^{i\frac{3\pi}{4}} = \cos \frac{3\pi}{4} + i \sin \frac{3\pi}{4} = \frac{1}{\sqrt{2}} (-1 + i)$$

Substituting this into equation (12)

$$\phi = \frac{J_0(i^{3/2} a \xi)}{J_0(i^{3/2} a) + \frac{a}{\sqrt{2}\beta} (1-i) J_1(i^{3/2} a)} \quad (13)$$

$$\text{As } J_0(a \xi i^{3/2}) = J_0(a \xi e^{i\frac{3\pi}{4}}) = \text{BER}_0(a \xi) + i \text{BEI}_0(a \xi)$$

and

$$J_1(a \xi i^{3/2}) = J_1(a \xi e^{i\frac{3\pi}{4}}) = \text{BER}_1(a \xi) + i \text{BEI}_1(a \xi)$$

Substituting these results into equation (13) yields

$$\phi = \frac{\text{BER}_0(a \xi) + i \text{BEI}_0(a \xi)}{\text{BER}_0(a) + i \text{BEI}_0(a) + \frac{a}{\sqrt{2}\beta} (1-i) (\text{BER}_1(a) + i \text{BEI}_1(a))} \quad (14)$$

After rearrangement.

$$\phi = \frac{\text{BER}_0(a\xi) + i\text{BEi}_0(a\xi)}{[\text{BER}_0(a) + \frac{a}{\sqrt{2\beta}}\text{BER}_1(a) + \frac{a}{\sqrt{2\beta}}\text{BEi}_1(a)] + i[\text{BEi}_0(a) + \frac{a}{\sqrt{2\beta}}\text{BEi}_1(a) - \frac{a}{\sqrt{2\beta}}\text{BER}_1(a)]}$$

Letting

$$X_R = \text{BER}_0(a) + \frac{a}{\sqrt{2\beta}}\text{BER}_1(a) + \frac{a}{\sqrt{2\beta}}\text{BEi}_1(a)$$

and

$$X_i = \text{BEi}_0(a) + \frac{a}{\sqrt{2\beta}}\text{BEi}_1(a) - \frac{a}{\sqrt{2\beta}}\text{BER}_1(a)$$

and substituting into equation (14) gives

$$\phi = \frac{\text{BER}_0(a\xi) + i\text{BEi}_0(a\xi)}{X_R + iX_i}$$

Rationalizing the denominator yields

$$\phi = \frac{\text{BER}_0(a\xi) + i\text{BEi}_0(a\xi)}{X_R^2 + X_i^2} (X_R - iX_i) \quad (15)$$

Now

$$\phi = \frac{(\text{BER}_0(a\xi)X_R + \text{BEi}_0(a\xi)X_i) + i(\text{BEi}_0(a\xi)X_R - \text{BER}_0(a\xi)X_i)}{X_R^2 + X_i^2}$$

which after rearrangement gives

$$\phi = \sqrt{\frac{\text{BER}_0^2(a\xi) + \text{BEi}_0^2(a\xi)}{X_R^2 + X_i^2}} e^{i\delta^*} \quad (16)$$

where

$$\delta^* = \tan^{-1} \frac{\text{BEi}_0(a\xi)X_R - \text{BER}_0(a\xi)X_i}{\text{BER}_0(a\xi)X_R + \text{BEi}_0(a\xi)X_i}$$

Substituting into equation (4) gives

$$\psi(r,t) = \sqrt{\frac{BER_o^2(a\xi) + BEi_o^2(a\xi)}{X_R^2 + X_i^2}} e^{i(\omega t + \delta^*)}$$

which also equals

$$\psi(r,t) = \sqrt{\frac{BER_o^2(a\xi) + BEi_o^2(a\xi)}{X_R^2 + X_i^2}} [\cos(\omega t + \delta^*) + i \sin(\omega t + \delta^*)]$$

As this problem was modeled as a sine wave, the imaginary part of  $\psi(r,t)$  was used.

$$I(\psi(r,t)) = \theta(r,t) = \sqrt{\frac{BER_o^2(a\xi) + BEi_o^2(a\xi)}{X_R^2 + X_i^2}} \sin(\omega t + \delta^*) \quad (17)$$

which is the analytical solution of infinitely long concentric cylinders experiencing a periodic sinusoidal temperature variation on its outermost surface when heat conduction is assumed to be radial only.

In summary

$$\theta(r,t) = \frac{T - T_A}{T_M - T_A} = \sqrt{\frac{BER_o^2(a\xi) + BEi_o^2(a\xi)}{X_R^2 + X_i^2}} \sin(\omega t + \delta^*)$$

where

$T$  = the temperature of a point  $r$  in the rocket motor at time  $t$

$T_A$  = average bulk temperature of the storage container

$T_M$  = maximum bulk temperature of the storage container

$\omega$  = frequency of the sinusoidal variation ( $2\pi/24$  hours)

$t$  = time

$\xi = \frac{r}{r_o}$  = dimensionless distance from the center of the rocket motor

$r_o$  = distance to the surface of the rocket motor

$r$  = distance from the center of the rocket motor

$a = \sqrt{\frac{\omega r_o^2}{\alpha}}$  = conduction parameter

$$\alpha = \frac{k}{\rho c} = \text{thermal diffusivity}$$

$\rho$  = density

$k$  = thermal conductivity

$c$  = specific heat

BER = real Bessel Function

BEi = imaginary Bessel Function

$$X_R = \text{BER}_0(a) + \frac{a}{\sqrt{2\beta}} \text{BER}_1(a) + \frac{a}{\sqrt{2\beta}} \text{BEi}_1(a)$$

$$X_i = \frac{\text{BEi}_0(a)}{hr_0} + \frac{a}{\sqrt{2\beta}} \text{BEi}_1(a) - \frac{a}{\sqrt{2\beta}} \text{BER}_1(a)$$

$$\beta = \frac{a}{k} = \text{Biot modulus}$$

$$\phi^* = \tan^{-1} \frac{\text{BEi}_0(a\xi)X_R - \text{BER}_0(a\xi)X_i}{\text{BER}_0(a\xi)X_R + \text{BEi}_0(a\xi)X_i}$$

The following computer programs were used to investigate a wide variety of parameters. The outputs are samples of some of these parameter studies.

# ANALYTICAL SOLUTION PARAMETER STUDY

```

DO 2 K=1,5
READ(5,11)A
11 FORMAT(F10.6)
31 WRITE(6,31)
31 FORMAT(1,19X,'A',4X,'B',4X,'DISTANCE FROM CENTER',4X,'TIME DELAY
1 IN RADIANS',3X,'RELATIVE AMPLITUDE')
DO 3 L=1,10
READ(5,11)B
FROM INPUT VALUES OF A AND B, CALCULATE THE DENOMINATOR(DENOM) OF EQUATION 17.
Y=SQRT(2.0)
Z=A
BEROZ=(1.0-(Z**4/64.0)+(Z**8/147500.0))
BERIOZ=0.25*Z**2*(1.0-(Z**4/576.0)+(Z**8/3790000.0))
BERIZ=-Z/((2.0*Y)*(1.0-(Z**4/128.0)-(Z**6/9216.0)+(Z**8/
1737280.0))
1BERIZ=Z/((2.0*Y)*(1.0-(Z**2/8.0)-(Z**4/128.0)+(Z**6/9216.0)+(Z**8/7
137280.0))
XR=BEROZ+A/(Y*8)*BERIZ+A/(Y*8)*BERIZ
XI=BERIOZ+A/(Y*8)*BERIZ-A/(Y*8)*BERIZ
V=XR**2+XI**2
DENOM=SQRT(V)
AT THE CENTER, HALF WAY TO THE SURFACE, AND AT THE SURFACE OF THE MOTOR,
CALCULATE DO 30 I=1,3
C=((1.-I)/2.0
Z=A*C
BEROZ=(1.0-(Z**4/64.0)+(Z**8/147500.0))
BERIOZ=0.25*Z**2*(1.0-(Z**4/576.0)+(Z**8/3790000.0))
U=BEROZ**2+BERIOZ**2
DNUM=SQRT(U)
CALCULATE THE TIME DELAY(DEL).
DNU=XR*BEROZ+XI*BERIOZ
DNO=XR*BEROZ+XI*BERIOZ
X=DNU/DNO
IF(DNO.LT.0.0)GO TO 22
DEL=ATAN(X)
GO TO 23
22 DEL=ATAN(X)-3.14159
CALCULATE THE RELATIVE AMPLITUDE(S).
23 S=DNUM/DENOM
32 WRITE(6,32)A,B,C,DEL,S
30 CONTINUE
2 CONTINUE
STOP
END

```

A.	B.	DISTANCE FROM CENTER	TIME DELAY IN RADIANS	RELATIVE AMPLITUDE
1.00	0.1	0.5	-1.50	0.19
1.00	0.1	0.5	-1.44	0.19
1.00	0.1	1.0	-1.27	0.16
1.00	0.5	0.5	-0.90	0.66
1.00	0.5	1.0	-0.72	0.67
1.00	1.0	0.5	-0.62	0.84
1.00	1.0	1.0	-0.43	0.84
1.00	2.0	0.5	-0.43	0.86
1.00	2.0	1.0	-0.23	0.93
1.00	3.0	0.5	-0.23	0.93
1.00	3.0	1.0	-0.14	0.94
1.00	4.0	0.5	-0.14	0.95
1.00	4.0	1.0	-0.07	0.95
1.00	5.0	0.5	-0.07	0.96
1.00	5.0	1.0	-0.03	0.96
1.00	6.0	0.5	-0.03	0.97
1.00	6.0	1.0	-0.02	0.97
1.00	7.0	0.5	-0.02	0.98
1.00	7.0	1.0	-0.01	0.98
1.00	8.0	0.5	-0.01	0.98
1.00	8.0	1.0	-0.00	0.98
1.00	9.0	0.5	-0.00	0.98
1.00	9.0	1.0	-0.00	0.98
1.00	10.0	0.5	-0.00	1.00
1.00	10.0	1.0	-0.00	1.00
1.00	11.0	0.5	-0.00	1.00
1.00	11.0	1.0	-0.00	1.00
1.00	12.0	0.5	-0.00	1.00
1.00	12.0	1.0	-0.00	1.00

A	B	DISTANCE FROM CENTER	TIME DELAY IN RADIAN	RELATIVE AMPLITUDE
2	0	0.5	2.78	0.05
2	0	1.0	1.12	0.06
2	0	1.5	1.59	0.22
2	0	2.0	1.92	0.27
2	0	2.5	1.66	0.37
2	0	3.0	1.47	0.45
2	1	0.5	1.74	0.54
2	1	1.0	1.43	0.66
2	1	1.5	1.18	0.62
2	1	2.0	1.52	0.63
2	1	2.5	1.03	0.76
2	1	3.0	1.32	0.67
2	1	3.5	1.03	0.82
2	1	4.0	1.37	0.70
2	1	4.5	1.19	0.71
2	1	5.0	1.20	0.86
2	1	5.5	1.08	0.76
2	1	6.0	1.31	0.77
2	1	6.5	1.14	0.93
2	1	7.0	1.49	0.80
2	1	7.5	1.60	0.82
2	1	8.0	1.38	0.89
2	1	8.5	1.60	0.81
2	1	9.0	1.00	0.99
2	1	9.5	1.00	0.00



A	B
3.00	0.00
3.00	1.11
3.00	1.55
3.00	5.00
3.00	1.00
3.00	2.00
3.00	2.00
3.00	3.00
3.00	3.00
3.00	4.00
3.00	4.00
3.00	5.00
3.00	5.00
3.00	10.00
3.00	10.00
3.00	50.00
3.00	50.00
3.00	100.00
3.00	100.00

A	B	DISTANCE FROM CENTER	TIME DELAY IN RADIAN	RELATIVE AMPLITUDE
4.0	0.1	0.5	3.65	0.01
4.0	0.1	0.5	3.74	0.01
4.0	0.1	1.0	3.22	0.02
4.0	0.1	1.0	3.25	0.03
4.0	0.1	1.0	3.26	0.04
4.0	0.1	1.0	3.15	0.06
4.0	0.1	1.0	3.45	0.08
4.0	0.1	1.0	3.55	0.22
4.0	0.1	1.0	3.02	0.11
4.0	0.1	1.0	3.38	0.14
4.0	0.1	1.0	3.38	0.33
4.0	0.1	1.0	3.15	0.15
4.0	0.1	1.0	3.25	0.18
4.0	0.1	1.0	3.05	0.12
4.0	0.1	1.0	3.55	0.20
4.0	0.1	1.0	3.07	0.22
4.0	0.1	1.0	3.20	0.47
4.0	0.1	1.0	3.07	0.26
4.0	0.1	1.0	3.25	0.40
4.0	0.1	1.0	3.49	0.38
4.0	0.1	1.0	3.58	0.28
4.0	0.1	1.0	3.45	0.37
4.0	0.1	1.0	3.05	0.29
4.0	0.1	1.0	3.54	0.35
4.0	0.1	1.0	3.10	0.39
4.0	0.1	1.0	3.20	0.00
4.0	0.1	1.0	3.10	0.00

A	B	DISTANCE FROM CENTER	TIME DELAY IN RADIAN	RELATIVE AMPLITUDE
0	0	0.5	4.99	0.00
5	0	1.0	4.21	0.01
5	0	1.0	4.17	0.01
5	0	1.0	4.25	0.02
5	0	1.0	4.13	0.02
5	0	1.0	4.19	0.03
5	0	1.0	4.18	0.10
5	0	1.0	4.09	0.06
5	0	1.0	4.07	0.06
5	0	1.0	4.09	0.24
5	0	1.0	4.06	0.05
5	0	1.0	4.09	0.03
5	0	1.0	4.08	0.03
5	0	1.0	4.09	0.10
5	0	1.0	4.07	0.18
5	0	1.0	4.05	0.00
5	0	1.0	4.08	0.12
5	0	1.0	4.05	0.48
5	0	1.0	4.07	0.17
5	0	1.0	4.09	0.17
5	0	1.0	4.03	0.19
5	0	1.0	4.04	0.15
5	0	1.0	4.03	0.23
5	0	1.0	4.05	0.34
5	0	1.0	4.03	0.16
5	0	1.0	4.01	0.29
5	0	1.0	4.01	0.00

# ANALYTICAL SOLUTION - SAMPLE PROBLEM

```

//WIR11687 JOB (1687,0860ET,NF12),'WIRZBURGER,ALLEN'
// EXEC FOR TCLGP,REGION=150K
//FORT SYSIN DD *
REAL LABEL
REAL#8 ITITLE(12)
REAL#4 J2
VALUES ARE A, B, MAXIMUM TEMPERATURE AND AVERAGE TEMPERATURE.
DIMENSION J2(49),TINF(49),T(7,49),TI(49),T2(49)
READ(5,11)A,B,TM,TA
FORMAT(4F10.6)
11 READ(5,10) (ITITLE(I), I=1, 12)
10 FORMAT(6A8)
FROM INPUT VALUES OF A AND B, CALCULATE THE DENOMINATOR(DENOM) OF EQUATION 17.
Y=SQRT(2.0)
Z=A
BEROZ=(1.0-(Z**4/64.0)+(Z**8/147500.0))
BERIOZ=0.25*Z**2*(1.0-(Z**4/576.0)+(Z**8/3790000.0))
BER1Z=-Z/(2.0*Y)*(1.0-(Z**2/8.0)-(Z**4/128.0)-(Z**6/9216.0)+(Z**8/
1737280.0))
BER1IZ=Z/(2.0*Y)*(1.0-(Z**2/8.0)-(Z**4/128.0)+(Z**6/9216.0)+(Z**8/7
137280.0))
XR=BEROZ+A/(Y*B)*BER1Z+A/(Y*B)*BER1IZ
XI=BERIOZ+A/(Y*B)*BER1Z-A/(Y*B)*BER1IZ
V=XR**2+XI**2
DENOM=SQRT(V)
N=0
THE TEMPERATURE OF THE CONTAINER(TINF) IS CALCULATED AT 30 MINUTE INTERVALS.
DO 40 J=1,1441,30
N=N+1
J2(N)=J-1
TEMP=DMEGA*J2(N)
TINF(N)=(TM-TA)*SIN(TEMP)+TA
IF(J.EQ.1441) GO TO 31
L=(N-1)/6
N2=N-1
L2=6*L
IF(N2.EQ.L2) GO TO 21
FOR SEVEN POSITIONS BETWEEN THE CENTER OF THE ROCKET MOTOR AND THE SURFACE, THE
NUMERATOR(DNUM) OF EQUATION 17 AND THE TIME DELAY(DEL) ARE CALCULATED.
DO 30 I=1,7
C=(I-1)/5.75
IF(C.GT.1.0) C=1.0
Z=A*C
BEROZ=(1.0-(Z**4/64.0)+(Z**8/147500.0))
BERIOZ=0.25*Z**2*(1.0-(Z**4/576.0)+(Z**8/3790000.0))

```



DISTANCE FROM CENTER	TIME	TEMPERATURE	TEMPERATURE OF CONTAINER	TIME DELAY
0.00	0.00	88.20	104.00	363.40
1.00	0.00	88.20	104.00	378.17
2.00	0.00	88.20	104.00	347.61
3.00	0.00	88.20	104.00	297.89
4.00	0.00	88.20	104.00	232.81
5.00	0.00	88.20	104.00	159.10
6.00	0.00	88.20	104.00	102.29
7.00	0.00	88.20	104.00	388.47
8.00	0.00	88.20	104.00	378.17
9.00	0.00	88.20	104.00	347.61
10.00	0.00	88.20	104.00	297.89
11.00	0.00	88.20	104.00	232.81
12.00	0.00	88.20	104.00	159.10
13.00	0.00	88.20	104.00	102.29
14.00	0.00	88.20	104.00	388.47
15.00	0.00	88.20	104.00	378.17
16.00	0.00	88.20	104.00	347.61
17.00	0.00	88.20	104.00	297.89
18.00	0.00	88.20	104.00	232.81
19.00	0.00	88.20	104.00	159.10
20.00	0.00	88.20	104.00	102.29
21.00	0.00	88.20	104.00	388.47
22.00	0.00	88.20	104.00	378.17
23.00	0.00	88.20	104.00	347.61
24.00	0.00	88.20	104.00	297.89
25.00	0.00	88.20	104.00	232.81
26.00	0.00	88.20	104.00	159.10
27.00	0.00	88.20	104.00	102.29
28.00	0.00	88.20	104.00	388.47
29.00	0.00	88.20	104.00	378.17
30.00	0.00	88.20	104.00	347.61
31.00	0.00	88.20	104.00	297.89
32.00	0.00	88.20	104.00	232.81
33.00	0.00	88.20	104.00	159.10
34.00	0.00	88.20	104.00	102.29
35.00	0.00	88.20	104.00	388.47
36.00	0.00	88.20	104.00	378.17
37.00	0.00	88.20	104.00	347.61
38.00	0.00	88.20	104.00	297.89
39.00	0.00	88.20	104.00	232.81
40.00	0.00	88.20	104.00	159.10
41.00	0.00	88.20	104.00	102.29
42.00	0.00	88.20	104.00	388.47
43.00	0.00	88.20	104.00	378.17
44.00	0.00	88.20	104.00	347.61
45.00	0.00	88.20	104.00	297.89
46.00	0.00	88.20	104.00	232.81
47.00	0.00	88.20	104.00	159.10
48.00	0.00	88.20	104.00	102.29
49.00	0.00	88.20	104.00	388.47
50.00	0.00	88.20	104.00	378.17
51.00	0.00	88.20	104.00	347.61
52.00	0.00	88.20	104.00	297.89
53.00	0.00	88.20	104.00	232.81
54.00	0.00	88.20	104.00	159.10
55.00	0.00	88.20	104.00	102.29
56.00	0.00	88.20	104.00	388.47
57.00	0.00	88.20	104.00	378.17
58.00	0.00	88.20	104.00	347.61
59.00	0.00	88.20	104.00	297.89
60.00	0.00	88.20	104.00	232.81
61.00	0.00	88.20	104.00	159.10
62.00	0.00	88.20	104.00	102.29
63.00	0.00	88.20	104.00	388.47
64.00	0.00	88.20	104.00	378.17
65.00	0.00	88.20	104.00	347.61
66.00	0.00	88.20	104.00	297.89
67.00	0.00	88.20	104.00	232.81
68.00	0.00	88.20	104.00	159.10
69.00	0.00	88.20	104.00	102.29
70.00	0.00	88.20	104.00	388.47
71.00	0.00	88.20	104.00	378.17
72.00	0.00	88.20	104.00	347.61
73.00	0.00	88.20	104.00	297.89
74.00	0.00	88.20	104.00	232.81
75.00	0.00	88.20	104.00	159.10
76.00	0.00	88.20	104.00	102.29
77.00	0.00	88.20	104.00	388.47
78.00	0.00	88.20	104.00	378.17
79.00	0.00	88.20	104.00	347.61
80.00	0.00	88.20	104.00	297.89
81.00	0.00	88.20	104.00	232.81
82.00	0.00	88.20	104.00	159.10
83.00	0.00	88.20	104.00	102.29
84.00	0.00	88.20	104.00	388.47
85.00	0.00	88.20	104.00	378.17
86.00	0.00	88.20	104.00	347.61
87.00	0.00	88.20	104.00	297.89
88.00	0.00	88.20	104.00	232.81
89.00	0.00	88.20	104.00	159.10
90.00	0.00	88.20	104.00	102.29
91.00	0.00	88.20	104.00	388.47
92.00	0.00	88.20	104.00	378.17
93.00	0.00	88.20	104.00	347.61
94.00	0.00	88.20	104.00	297.89
95.00	0.00	88.20	104.00	232.81
96.00	0.00	88.20	104.00	159.10
97.00	0.00	88.20	104.00	102.29
98.00	0.00	88.20	104.00	388.47
99.00	0.00	88.20	104.00	378.17
100.00	0.00	88.20	104.00	347.61

DISTANCE FROM CENTER	TIME	TEMPERATURE	TEMPERATURE OF CONTAINER	TIME DELAY
0.00	180.00	91.50	128.04	388.40
1.00	180.00	91.34	128.04	378.17
2.00	180.00	93.90	128.04	347.61
3.00	180.00	99.94	128.04	297.81
4.00	180.00	99.85	128.04	232.10
5.00	180.00	105.71	128.04	152.42
6.00	210.00	111.88	130.97	102.47
7.00	210.00	92.35	130.97	88.17
8.00	210.00	94.98	130.97	47.61
9.00	210.00	97.84	130.97	29.81
10.00	210.00	102.23	130.97	23.15
11.00	210.00	108.42	130.97	15.15
12.00	224.00	114.44	133.44	102.40
13.00	224.00	95.01	133.44	88.17
14.00	224.00	95.77	133.44	47.61
15.00	224.00	96.85	133.44	29.81
16.00	224.00	104.56	133.44	23.15
17.00	224.00	111.10	133.44	15.15
18.00	224.00	117.18	133.44	102.40
19.00	227.00	96.70	135.41	88.17
20.00	227.00	98.79	135.41	47.61
21.00	227.00	102.87	135.41	29.81
22.00	227.00	113.48	135.41	23.15
23.00	227.00	119.40	135.41	15.15
24.00	230.00	98.70	136.84	102.40
25.00	230.00	100.71	136.84	88.17
26.00	230.00	104.15	136.84	47.61
27.00	230.00	109.70	136.84	29.81
28.00	230.00	115.60	136.84	23.15
29.00	230.00	121.60	136.84	15.15
30.00	233.00	100.69	137.71	102.40
31.00	233.00	102.77	137.71	88.17
32.00	233.00	106.31	137.71	47.61
33.00	233.00	111.74	137.71	29.81
34.00	233.00	117.42	137.71	23.15
35.00	233.00	123.42	137.71	15.15

DISTANCE FROM CENTER	TIME	TEMPERATURE	TEMPERATURE DE CONTAINER	TIME DELAY
0.00	360.00	102.04	138.00	388.40
1.00	360.00	102.74	138.00	378.17
2.00	360.00	104.86	138.00	347.61
3.00	360.00	108.41	138.00	297.89
4.00	360.00	113.59	138.00	232.81
5.00	360.00	124.90	138.00	152.29
0.00	390.00	104.12	137.71	388.17
1.00	390.00	106.94	137.71	378.17
2.00	390.00	110.45	137.71	347.61
3.00	390.00	115.25	137.71	297.89
4.00	390.00	121.03	137.71	232.81
5.00	390.00	126.18	137.71	152.29
0.00	420.00	106.85	136.84	388.17
1.00	420.00	108.37	136.84	378.17
2.00	420.00	112.62	136.84	347.61
3.00	420.00	116.78	136.84	297.89
4.00	420.00	122.91	136.84	232.81
5.00	420.00	128.90	136.84	152.29
0.00	450.00	110.80	135.41	388.17
1.00	450.00	114.37	135.41	378.17
2.00	450.00	118.37	135.41	347.61
3.00	450.00	123.71	135.41	297.89
4.00	450.00	127.16	135.41	232.81
5.00	450.00	130.81	135.41	152.29
0.00	480.00	111.02	133.44	388.17
1.00	480.00	115.59	133.44	378.17
2.00	480.00	121.69	133.44	347.61
3.00	480.00	127.99	133.44	297.89
4.00	480.00	133.10	133.44	232.81
5.00	480.00	137.62	133.44	152.29
0.00	510.00	111.47	130.97	388.17
1.00	510.00	117.20	130.97	378.17
2.00	510.00	124.67	130.97	347.61
3.00	510.00	132.26	130.97	297.89
4.00	510.00	140.27	130.97	232.81
5.00	510.00	146.61	130.97	152.29



DISTANCE FROM CENTER	TIME	TEMPERATURE	TEMPERATURE OF CONTAINER	TIME DELAY
0.00	540.00	113.73	128.04	388.49
1.00	540.00	114.28	128.04	378.17
2.00	540.00	115.34	128.04	347.61
3.00	540.00	118.30	128.04	297.81
4.00	540.00	121.20	128.04	232.10
5.00	540.00	125.58	128.04	159.29
0.00	570.00	115.27	124.70	102.40
1.00	570.00	117.17	124.70	378.17
2.00	570.00	119.27	124.70	347.61
3.00	570.00	121.68	124.70	297.81
4.00	570.00	123.66	124.70	232.10
5.00	570.00	124.66	124.70	159.29
0.00	600.00	116.06	124.00	102.40
1.00	600.00	117.06	121.00	378.17
2.00	600.00	118.25	121.00	347.61
3.00	600.00	119.76	121.00	297.81
4.00	600.00	121.03	121.00	232.10
5.00	600.00	123.17	121.00	159.29
0.00	630.00	118.10	117.01	102.40
1.00	630.00	119.35	117.01	378.17
2.00	630.00	120.59	117.01	347.61
3.00	630.00	121.92	117.01	297.81
4.00	630.00	121.68	117.01	232.10
5.00	630.00	118.64	117.01	159.29
0.00	660.00	119.01	112.80	102.40
1.00	660.00	120.47	112.80	378.17
2.00	660.00	121.50	112.80	347.61
3.00	660.00	119.57	112.80	297.81
4.00	660.00	119.35	112.80	232.10
5.00	660.00	119.30	112.80	159.29
0.00	690.00	119.30	108.44	102.40
1.00	690.00	119.59	108.44	378.17
2.00	690.00	120.31	108.44	347.61
3.00	690.00	116.64	108.44	297.81
4.00	690.00	116.64	108.44	232.10
5.00	690.00	116.64	108.44	159.29

DISTANCE FROM CENTER	TIME	TEMPERATURE	TEMPERATURE OF CONTAINER	TIME DELAY
0.00	720.00	119.72	104.30	-388.40
1.00	720.00	119.80	104.00	-378.17
2.00	720.00	119.87	104.00	-347.89
3.00	720.00	119.90	104.00	-297.81
4.00	720.00	119.98	104.00	-232.10
5.00	720.00	119.99	104.00	-152.29
6.00	750.00	119.84	99.56	-102.40
7.00	750.00	119.83	99.56	-378.17
8.00	750.00	119.70	99.56	-347.89
9.00	750.00	119.16	99.56	-297.81
10.00	750.00	119.75	99.56	-232.10
11.00	750.00	119.83	99.56	-152.29
12.00	750.00	119.44	99.56	-378.17
13.00	750.00	119.75	99.56	-347.89
14.00	750.00	119.83	99.56	-297.81
15.00	780.00	119.59	99.56	-232.10
16.00	780.00	119.59	99.56	-152.29
17.00	780.00	119.59	99.56	-378.17
18.00	780.00	119.59	99.56	-347.89
19.00	780.00	119.59	99.56	-297.81
20.00	780.00	119.59	99.56	-232.10
21.00	780.00	119.59	99.56	-152.29
22.00	780.00	119.59	99.56	-378.17
23.00	780.00	119.59	99.56	-347.89
24.00	780.00	119.59	99.56	-297.81
25.00	780.00	119.59	99.56	-232.10
26.00	780.00	119.59	99.56	-152.29
27.00	810.00	119.59	99.56	-378.17
28.00	810.00	119.59	99.56	-347.89
29.00	810.00	119.59	99.56	-297.81
30.00	810.00	119.59	99.56	-232.10
31.00	810.00	119.59	99.56	-152.29
32.00	810.00	119.59	99.56	-378.17
33.00	810.00	119.59	99.56	-347.89
34.00	810.00	119.59	99.56	-297.81
35.00	810.00	119.59	99.56	-232.10
36.00	810.00	119.59	99.56	-152.29
37.00	810.00	119.59	99.56	-378.17
38.00	810.00	119.59	99.56	-347.89
39.00	810.00	119.59	99.56	-297.81
40.00	810.00	119.59	99.56	-232.10
41.00	810.00	119.59	99.56	-152.29
42.00	810.00	119.59	99.56	-378.17
43.00	810.00	119.59	99.56	-347.89
44.00	810.00	119.59	99.56	-297.81
45.00	810.00	119.59	99.56	-232.10
46.00	810.00	119.59	99.56	-152.29
47.00	810.00	119.59	99.56	-378.17
48.00	810.00	119.59	99.56	-347.89
49.00	810.00	119.59	99.56	-297.81
50.00	810.00	119.59	99.56	-232.10
51.00	810.00	119.59	99.56	-152.29
52.00	810.00	119.59	99.56	-378.17
53.00	810.00	119.59	99.56	-347.89
54.00	810.00	119.59	99.56	-297.81
55.00	810.00	119.59	99.56	-232.10
56.00	810.00	119.59	99.56	-152.29
57.00	810.00	119.59	99.56	-378.17
58.00	810.00	119.59	99.56	-347.89
59.00	810.00	119.59	99.56	-297.81
60.00	810.00	119.59	99.56	-232.10
61.00	810.00	119.59	99.56	-152.29
62.00	810.00	119.59	99.56	-378.17
63.00	810.00	119.59	99.56	-347.89
64.00	810.00	119.59	99.56	-297.81
65.00	810.00	119.59	99.56	-232.10
66.00	810.00	119.59	99.56	-152.29
67.00	810.00	119.59	99.56	-378.17
68.00	810.00	119.59	99.56	-347.89
69.00	810.00	119.59	99.56	-297.81
70.00	810.00	119.59	99.56	-232.10
71.00	810.00	119.59	99.56	-152.29
72.00	810.00	119.59	99.56	-378.17
73.00	810.00	119.59	99.56	-347.89
74.00	810.00	119.59	99.56	-297.81
75.00	810.00	119.59	99.56	-232.10
76.00	810.00	119.59	99.56	-152.29
77.00	810.00	119.59	99.56	-378.17
78.00	810.00	119.59	99.56	-347.89
79.00	810.00	119.59	99.56	-297.81
80.00	810.00	119.59	99.56	-232.10
81.00	810.00	119.59	99.56	-152.29
82.00	810.00	119.59	99.56	-378.17
83.00	810.00	119.59	99.56	-347.89
84.00	810.00	119.59	99.56	-297.81
85.00	810.00	119.59	99.56	-232.10
86.00	810.00	119.59	99.56	-152.29
87.00	810.00	119.59	99.56	-378.17
88.00	810.00	119.59	99.56	-347.89
89.00	810.00	119.59	99.56	-297.81
90.00	810.00	119.59	99.56	-232.10
91.00	810.00	119.59	99.56	-152.29
92.00	810.00	119.59	99.56	-378.17
93.00	810.00	119.59	99.56	-347.89
94.00	810.00	119.59	99.56	-297.81
95.00	810.00	119.59	99.56	-232.10
96.00	810.00	119.59	99.56	-152.29
97.00	810.00	119.59	99.56	-378.17
98.00	810.00	119.59	99.56	-347.89
99.00	810.00	119.59	99.56	-297.81
100.00	810.00	119.59	99.56	-232.10

DISTANCE FROM CENTER	TIME	TEMPERATURE	TEMPERATURE OF CONTAINER	TIME DELAY
0.00	900.00	116.50	79.96	-388.40
1.00	900.00	116.06	79.96	-378.17
2.00	900.00	114.66	79.96	-347.89
3.00	900.00	112.10	79.96	-232.81
4.00	900.00	108.06	79.96	-159.29
5.00	900.00	102.15	79.96	-102.40
0.00	930.00	115.12	77.03	-388.17
1.00	930.00	113.02	77.03	-378.17
2.00	930.00	110.16	77.03	-347.89
3.00	930.00	105.53	77.03	-232.81
4.00	930.00	99.51	77.03	-159.29
5.00	930.00	93.56	77.03	-102.40
0.00	960.00	111.11	74.56	-388.17
1.00	960.00	108.12	74.56	-378.17
2.00	960.00	103.44	74.56	-347.89
3.00	960.00	96.59	74.56	-232.81
4.00	960.00	90.59	74.56	-159.29
5.00	960.00	83.10	74.56	-102.40
0.00	990.00	111.23	72.59	-388.17
1.00	990.00	109.00	72.59	-378.17
2.00	990.00	106.00	72.59	-347.89
3.00	990.00	101.13	72.59	-232.81
4.00	990.00	94.52	72.59	-159.29
5.00	990.00	88.56	72.59	-102.40
0.00	1020.00	109.30	71.16	-388.17
1.00	1020.00	107.28	71.16	-378.17
2.00	1020.00	103.87	71.16	-347.89
3.00	1020.00	98.30	71.16	-232.81
4.00	1020.00	92.49	71.16	-159.29
5.00	1020.00	87.31	71.16	-102.40
0.00	1050.00	107.20	70.29	-388.17
1.00	1050.00	105.20	70.29	-378.17
2.00	1050.00	101.69	70.29	-347.89
3.00	1050.00	96.25	70.29	-232.81
4.00	1050.00	90.84	70.29	-159.29
5.00	1050.00	84.84	70.29	-102.40



DISTANCE FROM CENTER	TIME	TEMPERATURE	TEMPERATURE OF CONTAINER	TIME DELAY
0.00	1260.00	94.27	79.96	388.40
1.00	1260.00	93.12	79.96	378.17
2.00	1260.00	92.66	79.96	347.61
3.00	1260.00	89.70	79.96	297.89
4.00	1260.00	88.15	79.96	232.81
5.00	1260.00	82.72	79.96	159.10
6.00	1260.00	52.33	83.30	102.29
7.00	1260.00	50.73	83.30	88.47
8.00	1260.00	50.33	83.30	378.17
9.00	1260.00	50.33	83.30	347.61
10.00	1260.00	50.33	83.30	297.89
11.00	1260.00	50.33	83.30	159.10
12.00	1260.00	50.33	83.30	102.29
13.00	1260.00	50.33	83.30	88.47
14.00	1260.00	50.33	83.30	378.17
15.00	1260.00	50.33	83.30	347.61
16.00	1260.00	50.33	83.30	297.89
17.00	1260.00	50.33	83.30	159.10
18.00	1260.00	50.33	83.30	102.29
19.00	1260.00	50.33	83.30	88.47
20.00	1260.00	50.33	83.30	378.17
21.00	1260.00	50.33	83.30	347.61
22.00	1260.00	50.33	83.30	297.89
23.00	1260.00	50.33	83.30	159.10
24.00	1260.00	50.33	83.30	102.29
25.00	1260.00	50.33	83.30	88.47
26.00	1260.00	50.33	83.30	378.17
27.00	1260.00	50.33	83.30	347.61
28.00	1260.00	50.33	83.30	297.89
29.00	1260.00	50.33	83.30	159.10
30.00	1260.00	50.33	83.30	102.29
31.00	1260.00	50.33	83.30	88.47
32.00	1260.00	50.33	83.30	378.17
33.00	1260.00	50.33	83.30	347.61
34.00	1260.00	50.33	83.30	297.89
35.00	1260.00	50.33	83.30	159.10
36.00	1260.00	50.33	83.30	102.29
37.00	1260.00	50.33	83.30	88.47
38.00	1260.00	50.33	83.30	378.17
39.00	1260.00	50.33	83.30	347.61
40.00	1260.00	50.33	83.30	297.89
41.00	1260.00	50.33	83.30	159.10
42.00	1260.00	50.33	83.30	102.29
43.00	1260.00	50.33	83.30	88.47
44.00	1260.00	50.33	83.30	378.17
45.00	1260.00	50.33	83.30	347.61
46.00	1260.00	50.33	83.30	297.89
47.00	1260.00	50.33	83.30	159.10
48.00	1260.00	50.33	83.30	102.29
49.00	1260.00	50.33	83.30	88.47
50.00	1260.00	50.33	83.30	378.17
51.00	1260.00	50.33	83.30	347.61
52.00	1260.00	50.33	83.30	297.89
53.00	1260.00	50.33	83.30	159.10
54.00	1260.00	50.33	83.30	102.29
55.00	1260.00	50.33	83.30	88.47
56.00	1260.00	50.33	83.30	378.17
57.00	1260.00	50.33	83.30	347.61
58.00	1260.00	50.33	83.30	297.89
59.00	1260.00	50.33	83.30	159.10
60.00	1260.00	50.33	83.30	102.29
61.00	1260.00	50.33	83.30	88.47
62.00	1260.00	50.33	83.30	378.17
63.00	1260.00	50.33	83.30	347.61
64.00	1260.00	50.33	83.30	297.89
65.00	1260.00	50.33	83.30	159.10
66.00	1260.00	50.33	83.30	102.29
67.00	1260.00	50.33	83.30	88.47
68.00	1260.00	50.33	83.30	378.17
69.00	1260.00	50.33	83.30	347.61
70.00	1260.00	50.33	83.30	297.89
71.00	1260.00	50.33	83.30	159.10
72.00	1260.00	50.33	83.30	102.29
73.00	1260.00	50.33	83.30	88.47
74.00	1260.00	50.33	83.30	378.17
75.00	1260.00	50.33	83.30	347.61
76.00	1260.00	50.33	83.30	297.89
77.00	1260.00	50.33	83.30	159.10
78.00	1260.00	50.33	83.30	102.29
79.00	1260.00	50.33	83.30	88.47
80.00	1260.00	50.33	83.30	378.17
81.00	1260.00	50.33	83.30	347.61
82.00	1260.00	50.33	83.30	297.89
83.00	1260.00	50.33	83.30	159.10
84.00	1260.00	50.33	83.30	102.29
85.00	1260.00	50.33	83.30	88.47
86.00	1260.00	50.33	83.30	378.17
87.00	1260.00	50.33	83.30	347.61
88.00	1260.00	50.33	83.30	297.89
89.00	1260.00	50.33	83.30	159.10
90.00	1260.00	50.33	83.30	102.29
91.00	1260.00	50.33	83.30	88.47
92.00	1260.00	50.33	83.30	378.17
93.00	1260.00	50.33	83.30	347.61
94.00	1260.00	50.33	83.30	297.89
95.00	1260.00	50.33	83.30	159.10
96.00	1260.00	50.33	83.30	102.29
97.00	1260.00	50.33	83.30	88.47
98.00	1260.00	50.33	83.30	378.17
99.00	1260.00	50.33	83.30	347.61
100.00	1260.00	50.33	83.30	297.89

## APPENDIX C

### TRUMP Solution

TRUMP is a computer program for solving transient and steady-state temperature distributions in multidimensional systems. This program was developed in 1965 at the Lawrence Radiation Laboratory by A. L. Edwards [Ref. 2] for their CDC/3600 computer. The program was adapted to the Naval Postgraduate School IBM/360 Model 67 computer system in 1971 by C. Erbayrum [Ref. 3] from a version used by the B. F. Goodrich Corporation.

TRUMP is a multi-purpose program able to solve a wide variety of problems involving flow in various kinds of potential fields such as heat flow in a temperature field. TRUMP allows the solution of general nonlinear parabolic partial differential equations both in steady-state and transient problems. Complex geometric configurations with multidimensional flow may be solved using various coordinate systems. Initial conditions may vary with spatial position. Material properties, boundary conditions, and other problem parameters may vary with spatial position, time, or the primary dependent variable.

Input data are fed to TRUMP in "Block" form through its 12 input data blocks. A complete description of each of these blocks is given in Ref. 2. A model of the problem must be constructed and data from this model read into TRUMP through the data blocks.

Two models were used to simulate the rocket motor storage container system and several variations of each model were investigated.

The first model assumed one dimensional heat transfer (radial) with the assumptions that the system was infinitely long and that the container surface temperature was spatially uniform. The system was modeled as two infinitely long concentric cylinders separated by a 2.94 inch air gap. The inner cylinder was constructed of 4130 steel and was filled with dry wind blown sand. The thermal properties of the materials used in the experimental system are given in Table II with units most easily compared to the actual data obtained from the system at China Lake.

TABLE II  
Thermal Properties of Materials

Material	Density	Specific Heat	Thermal Conductivity
Sand	0.05486 lbm/in <sup>3</sup>	0.195 BTU/lbm°F	0.00026 BTU/min-in-°F
Steel	0.2807 lbm/in <sup>3</sup>	0.109 BTU/lbm°F	0.364 BTU/min-in-°F
Air	0.0000436 "	0.240 BTU/lbm°F	0.0000225 "

The model was subdivided into volume elements or nodes with the representative nodal points given in Figure 27. Although the representative nodal point may be located anywhere in the node or on the surface of the node, in transient problems it is usually located so that the lines connecting the nodal points are perpendicularly bisected by the connected area. This gives maximum accuracy. Two boundary conditions were given to the surface node. The first was a sinusoidal disturbance which closely modeled the actual

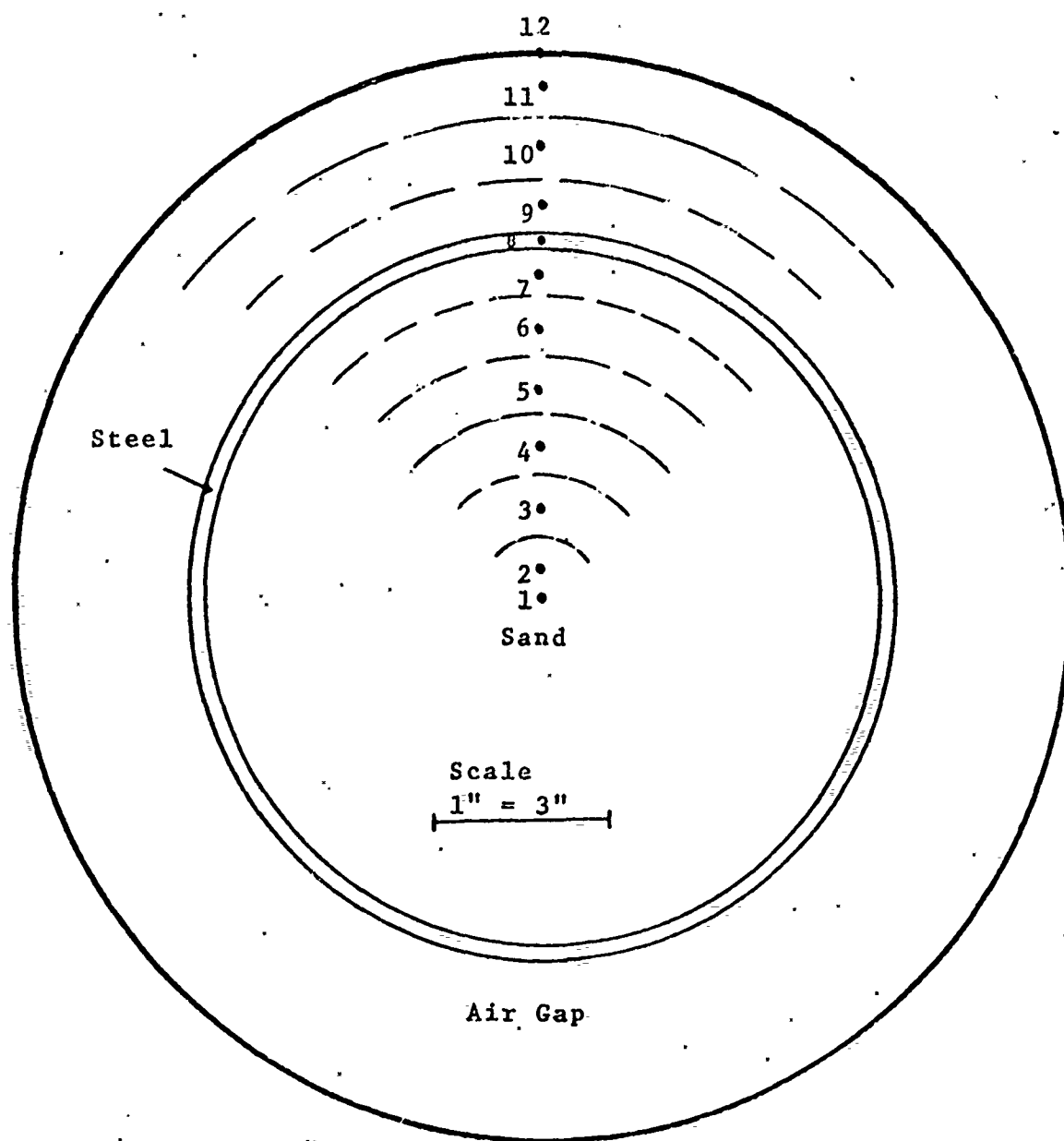


Figure 27. Location of Nodes for One Dimensional TRUMP Model.



average experimental data obtained at China Lake as given in Appendix D. The sine wave exhibited a maximum temperature of 138°F and an average temperature of 104°F. Its period was 24 hours (1440 minutes). The second boundary condition was the actual average surface temperature of the storage container given at two hour intervals. Both these boundary conditions are approximations of the actual surface temperature. Two hour intervals were the minimum allowable for the tabular data as this version of TRUMP has a maximum table size of 12.

Several assumptions were initially made. The thermocouple data obtained from the experiment at China Lake gave the average temperature at a point on the storage container and not the actual outside surface temperature. As this container wall was only 1/16 of an inch thick and made of a good thermal conductor, it was decided to model this data as a zero volume boundary node with a known temperature impressed on it. It was also assumed that heat transfer across the air gap occurred only by radiation and conduction, neglecting the effects of free convection.

It was estimated that the surface emissivities for the rocket motor and the storage container were 0.9 [Ref. 6] based on their haze gray surfaces. The radiation exchange factor for this geometry is given by

$$J_{1-2} = \frac{1}{\frac{1}{\epsilon_1} + \frac{r_1}{r_2} \left( \frac{1}{\epsilon_2} - 1 \right)} = 0.84$$

A sample input deck for the tabular approximation of the boundary condition is given at the end of this appendix. Several cycles of output data for the one dimensional model are also given.

The second model assumed two dimensional heat transfer (radial and circumferential) with the assumption that the system was infinitely long. The same physical model was assumed for the system except 48 nodes were used instead of 12. The representative nodal points are given in Figure 28. The four surface nodes (12, 24, 36, and 48) each had two different temperature approximations applied, a sinusoidal representation and a tabular input taken at two hour intervals. The four surface nodes were also modeled as zero volume boundary nodes. Each internal thermal connection between nodes is described in the input data by specifying the two node identification numbers, two connector lengths, and two interface dimensional factors. An example of the thermal connections of node 4 is shown in Figure 28 and the input data in BLOCK 5 of the two dimensional TRUMP program.

The calculation of the radiosities in the two dimensional case was accomplished by using a radiation-network and the method of crossed-strings.

The radiation shape factors for the two dimensional system were determined by the method of crossed-strings [Ref. 14]. The graphical construction for this method is given in Figure 29.

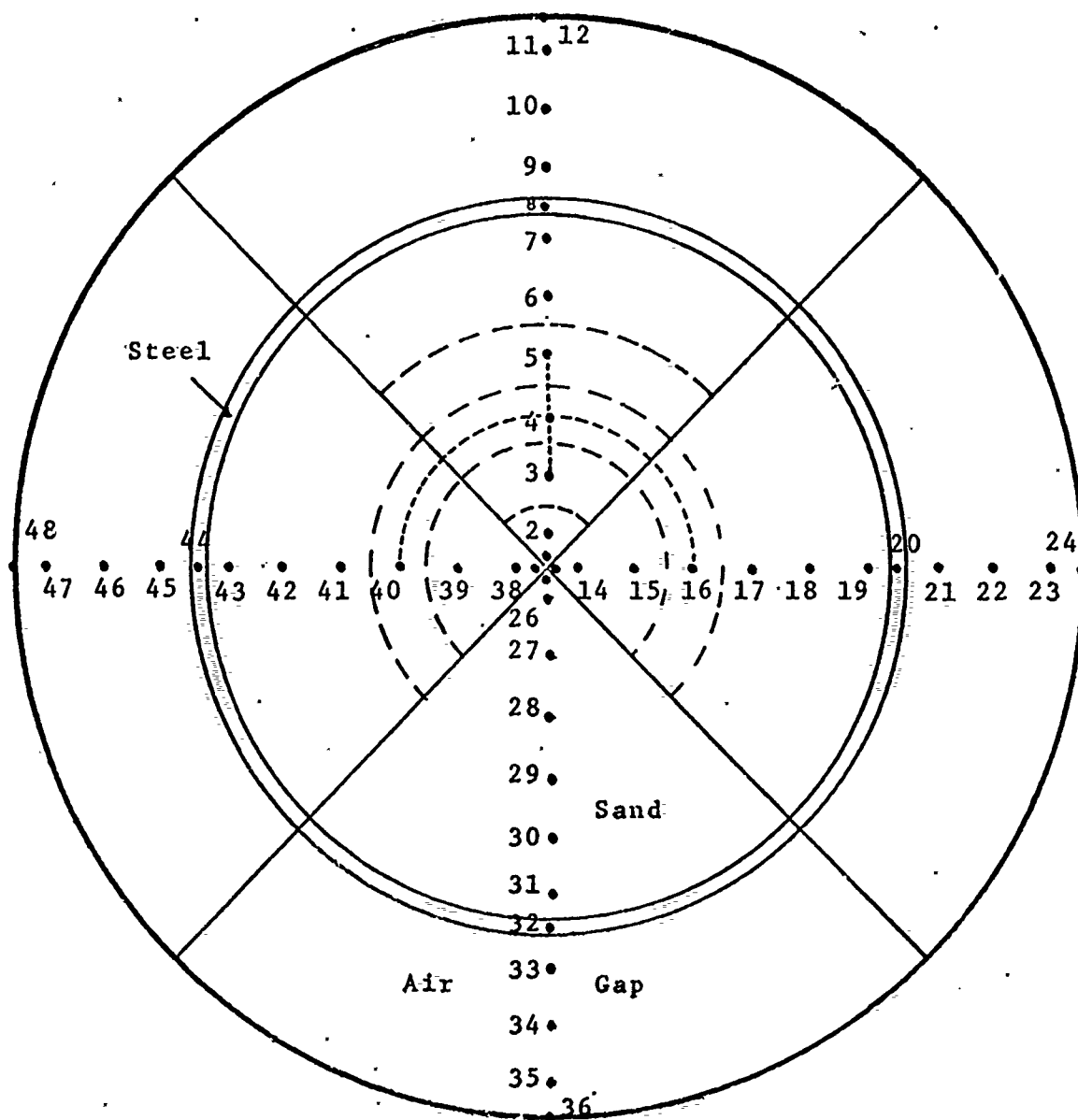


Figure 28: Location of Nodes for Two Dimensional TRUMP Model.



$F_{m-n}$  is defined as the fraction of energy leaving surface  $m$  which directly reaches surface  $n$ . From the physical dimensions of the model  $A_1 = A_4 = A_6 = 9.45 \frac{\text{sq.in}}{\text{in.}}$ ,  $A_2 = A_3 = A_5 = 14.05 \frac{\text{sq.in}}{\text{in.}}$ ,  $A_{2'} = 12.65 \frac{\text{sq.in}}{\text{in.}}$ , assuming unit depth. Let  $S_1$  equal the length of  $A_1$ .

The crossed-string method lets each surface represent the effective surface obtained by stretching a string tightly over the radiating face between the bounding edges, to produce a surface that cannot see any of itself. For example, surface  $2'$  in Figure 29 stretched over surface 2. By definition  $F_{2'2} \equiv 1$ , which by reciprocity leads to

$$F_{22'} = \frac{A_{2'}}{A_2} F_{2'2} = 0.9$$

and therefore since

$$F_{22} + F_{22'} = 1 \quad \text{then } F_{22} = 0.10$$

To calculate the direct radiant heat exchanged between surfaces 1 and 2, a minimum-length line was stretched connecting edge B of  $A_1$  to edge E of  $A_2$  and a second minimum length line from edge L of  $A_1$  to edge F of  $A_2$ . These lines are labeled  $L_1$  in Figure 29 and are equal to the width of the air gap,  $L_1 = 2.9375$  in. Minimum length lines were also stretched from point B on  $A_1$  to F on  $A_2$  and L on  $A_1$  to E on  $A_2$ . The length of these lines is  $D_1$  and is made up of two parts;  $D_1'$ , the tangential distance from F to surface  $A_1$  and  $D_1''$ , the arc length from the point the tangent hits  $A_1$  to B. From geometry  $D_1' = \sqrt{r_1^2 - r_o^2} = 6.62''$

$$D_1'' = r_o \theta_a = 4.42''$$

therefore

$$D_1 = D_1' + D_1'' = 11.04''$$

$$\text{Now } F_{12} = \frac{2D_1 - 2L_1}{2S_1} = 0.86$$

From reciprocity,  $A_1 F_{12} = A_2 F_{21}$

$$F_{21} = \frac{r_o}{r_1} F_{12} = 0.578$$

Now  $F_{13}$  is calculated from

$$F_{12} + 2F_{13} = 1$$

therefore  $F_{13} = 0.07$

From symmetry  $F_{42} = F_{13}$

and then by reciprocity

$$F_{24} = \frac{r_o}{r_1} F_{42} = 0.047$$

Now  $F_{23}$  was calculated by stretching minimum length lines from F to E, from E to G, from F to G and from E to E; where the length of the line from F to E = from E to G =  $S_2'$ , from F to G =  $2D_1$ , and from E to E = 0

$$F_{23} = \frac{2S_2' - 2D_1}{2S_2} = .113$$

$F_{25}$  was now calculated from

$$F_{21} + F_{22} + F_{23} + F_{24} + F_{25} = 1$$

therefore  $F_{25} = 0.002$

As  $F_{25}$  was much smaller than the other  $F_{m-n}$ , it was not included in the radiation-network diagram in Figure 30

[Ref. 15].

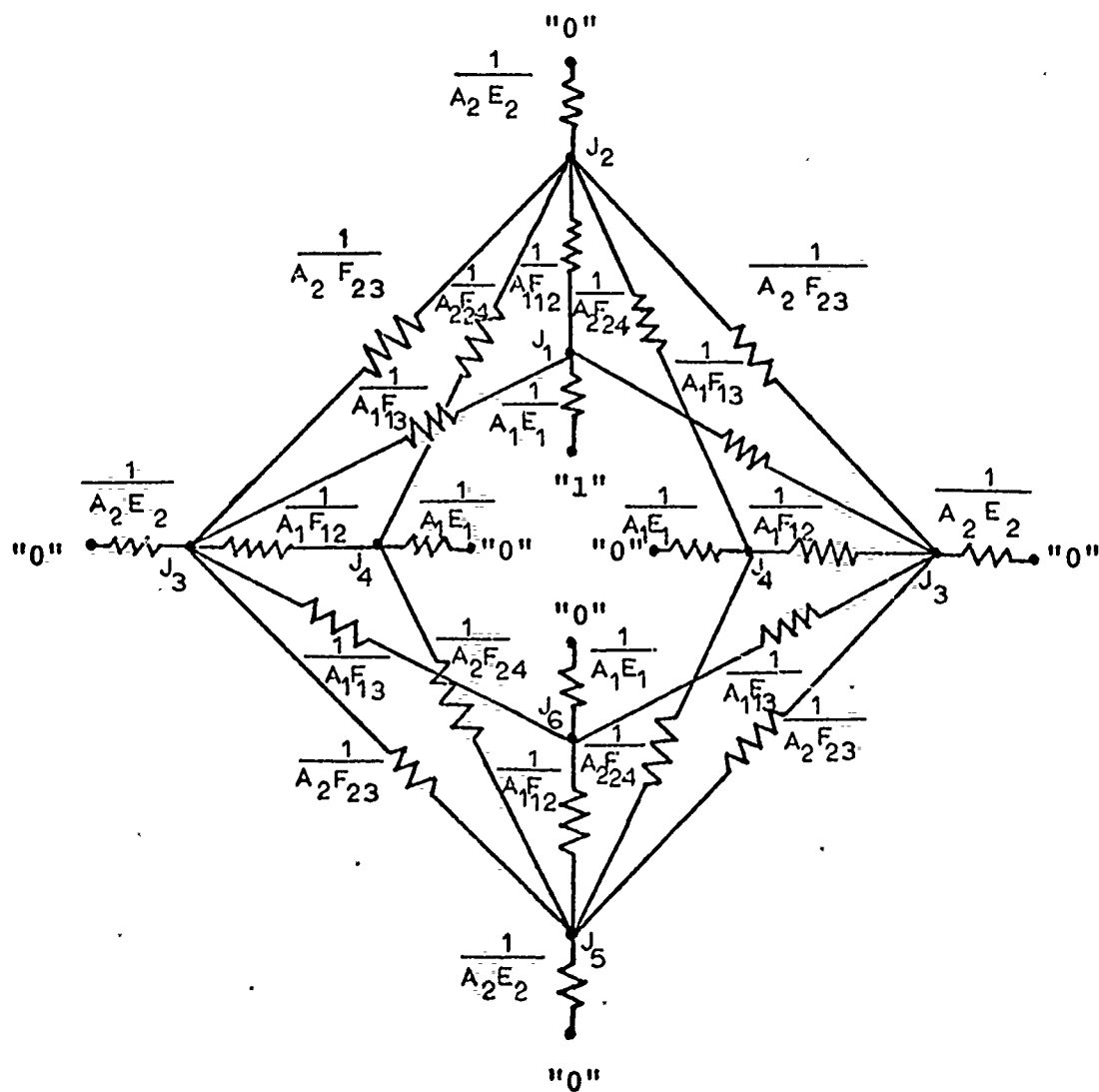


Figure 30: Radiation Network.

To calculate  $F_{1-n}$ , the blackbody potential of area 1 is set to unity and all other blackbody potentials are set as zero. An energy balance was written at each node giving a set of six simultaneous equations as follows:

Node 1

$$E_1 A_1 (1 - J_1) = A_1 F_{12} (J_1 - J_2) + 2 A_1 F_{13} (J_1 - J_3)$$

Node 2

$$E_2 A_2 (0 - J_2) = A_1 F_{12} (J_2 - J_1) + 2 A_2 F_{24} (J_2 - J_4) + 2 A_2 F_{23} (J_2 - J_3)$$

Node 3

$$E_2 A_2 (0 - J_3) = A_1 F_{12} (J_3 - J_4) + A_2 F_{23} (J_3 - J_2) + A_1 F_{13} (J_3 - J_1) + A_1 F_{13} (J_3 - J_6) + A_2 F_{23} (J_3 - J_5)$$

Node 4

$$E_1 A_1 (0 - J_4) = A_2 F_{24} (J_4 - J_2) + A_1 F_{12} (J_4 - J_3) + A_2 F_{24} (J_4 - J_5)$$

Node 5

$$E_2 A_2 (0 - J_5) = 2 A_2 F_{23} (J_5 - J_3) + 2 A_2 F_{24} (J_5 - J_4) + A_1 F_{12} (J_5 - J_6)$$

Node 6

$$E_1 A_1 (0 - J_6) = 2 A_1 F_{13} (J_6 - J_3) + A_1 F_{12} (J_6 - J_5)$$

where  $J_n$  = radiosity of node n

$$E_1 A_1 = \frac{\epsilon_1}{1 - \epsilon_1} A_1$$

$$E_2 A_2 = \frac{\epsilon_2}{1 - \epsilon_2} A_2$$

$F_{nm}$  = radiation shape factors previously calculated.

Now the values of  $A_1$ ,  $A_2$  and  $F_{nm}$  were substituted into the energy balance equations which were then put into matrix form as shown in Table III.



TABLE III  
Matrix Form of Energy Balance Equations

$\left(\frac{1}{1-\epsilon_1}\right)$	$(-0.86)$	$(-0.14)$	$(0.0)$	$(0.0)$	$(0.0)$	$J_1$	$\left(\frac{\epsilon_1}{1-\epsilon_1}\right)$
$(-0.86)$	$\left(1.33 + \frac{3\epsilon_2}{2(1-\epsilon_2)}\right)$	$(-0.33)$	$(-0.14)$	$(0.0)$	$(0.0)$	$J_2$	$(0.0)$
$(-0.07)$	$(-0.165)$	$\left(1.33 + \frac{3\epsilon_2}{2(1-\epsilon_2)}\right)$	$(-0.86)$	$(-0.165)$	$(-0.07)$	$J_3$	$(0.0)$
$(0.0)$	$(-0.07)$	$(-0.86)$	$\left(\frac{1}{1-\epsilon_1}\right)$	$(-0.07)$	$(0.0)$	$J_4$	$(0.0)$
$(0.0)$	$(0.0)$	$(-0.14)$	$(0.0)$	$(-0.86)$	$\left(\frac{1}{1-\epsilon_1}\right)$	$J_5$	$(0.0)$
$(0.0)$	$(0.0)$	$(-0.33)$	$(-0.14)$	$\left(1.33 + \frac{3\epsilon_2}{2(1-\epsilon_2)}\right)$	$(-0.86)$	$J_6$	$(0.0)$

Letting  $\epsilon_1 = \epsilon_2 = 0.9$ , a standard computer solution for matrix problems gave the radiosities as listed in Table IV.

TABLE IV  
Radiosities at Nodes

$J_1$	= .9046
$J_2$	= .0529
$J_3$	= .00495
$J_4$	= .000797
$J_5$	= .000125
$J_6$	= .000080

Now to find the radiation exchange factors from node 1 to nodes n, the radiation network shown in Figure 30 was reduced to the equivalent network shown in Figure 31. Where the nodal equations are

$$F_{1-2} A_1 (1-0) = E_2 A_2 (J_2 - 0)$$

where

$$F_{1-2} = \frac{E_2 A_2}{A_1} J_2 = .71$$

$$F_{1-3} A_1 (1-0) = E_2 A_2 (J_3 - 0)$$

$$F_{1-3} = \frac{E_2 A_2}{A_1} J_3 = .066$$

These values of the radiation exchange factor are used in the two-dimensional program. A sample input deck for the sinusoidal boundary condition is included at the end of this appendix. Several cycles of output data for the tabular boundary condition are also given.

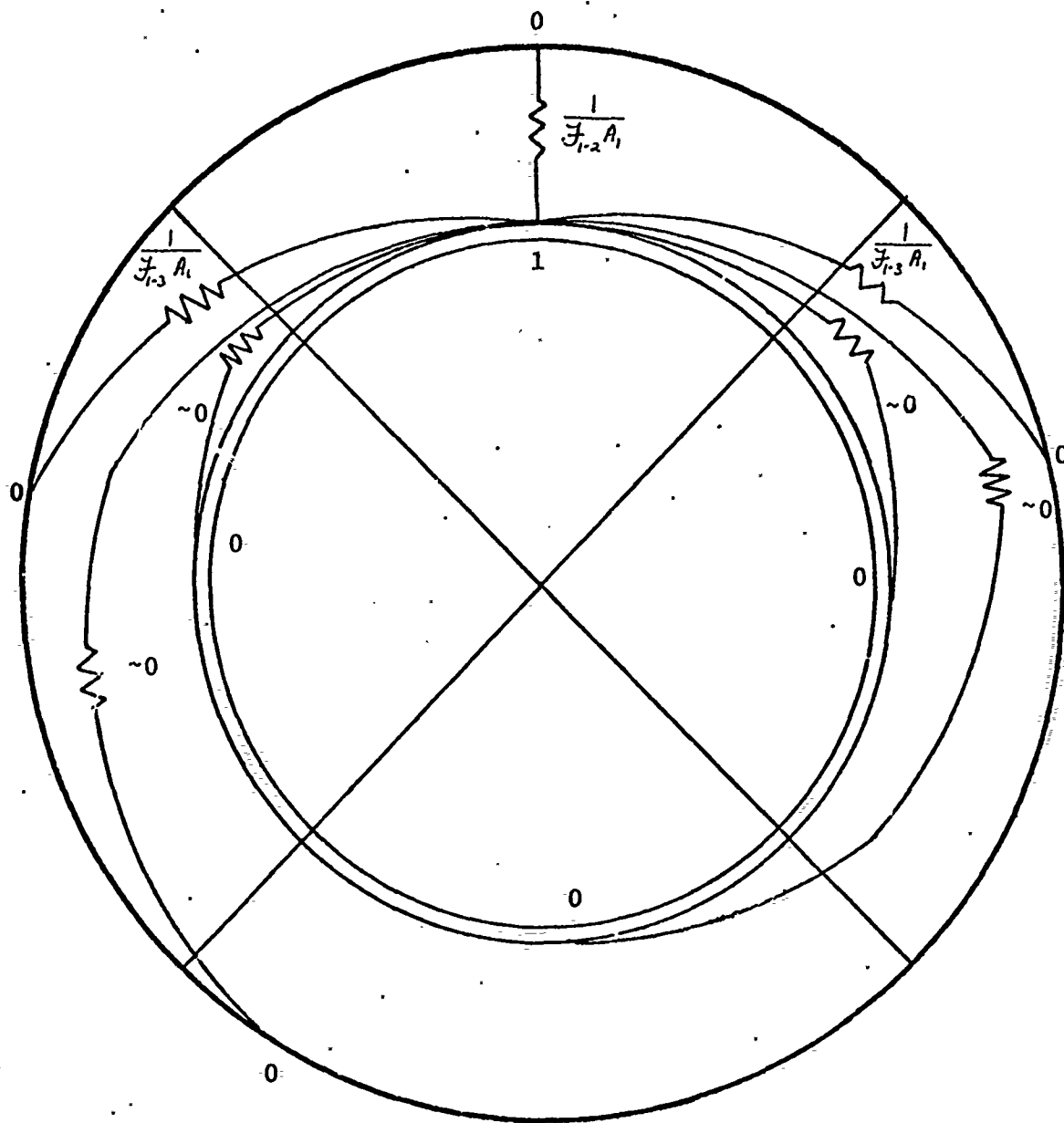


Figure 31: Equivalent Radiation Network

```

//WIR31687 JOB (1687,0860FT,NF12),WIRZBURGER.A. BOX W',TIME=(2,00)
//JOB118 DD UNIT=2321,DSNAME=SI734.KATZ,
// DISP=(OLD,PASS),VOLUME=SER=CELOO1
// EXEC PGM=TRUMP,REGION=350K
//FT06FOO1 DD SYSDUT=A.DC8=(RECFM=FBA,LRECL=133,BLKSIZE=3325),
//SPACE=(CYL,(5,1))
//FT05FOO1 DD

```

\* MISSLE PROBLEM ONE DIMENSIONAL

BLOCK 1 CONTROLS, LIMITS, CONSTANTS

1	1.000 E 00	1.000E 00	1440.0
2			
3			

BLOCK 2 MATERIAL NAMES, NUMBERS, THERMAL PROPERTIES

1	0.0544	0.19	0.00027
2	0.2807	0.109	0.0364
3	0.0000436	0.240	0.0000225

BLOCK 4 NODE NUMBERS, MATERIAL REFERENCES, TYPES, VOLUMES.

1	1.0	0.002	0.001
2	1.0	0.998	0.501
3	1.0	1.0	1.5
4	1.0	1.0	2.5
5	1.0	1.0	3.5
6	1.0	0.75	4.5
7	1.0	0.25	5.375
8	1.0	1.0	5.875
9	1.0	1.0	6.5
10	1.0	0.9375	7.5
11	1.0	0.0	8.46875
12	0.0	0.0	8.9375

BLOCK 5 INTERNAL THERMAL CONNECTION NODE NUMBERS.

1	0.001	0.499	0.002
2	0.499	0.5	1.0
3	0.5	0.5	1.0
4	0.5	0.5	1.0
5	0.5	0.375	1.0
6	0.3750	0.125	1.0
7	0.1250	0.5	1.0
8	0.125	0.5	1.0
9	0.500	0.56875	1.0
10	0.56875	0.0	1.0
11	0.46875	0.0	1.0
12	0.0	0.0	8.9375

0.00009760

BLOCK 6	EXTERNAL THERMAL CONNECTIONS	1.0	8.9375	1.00	E6
12 2001					
BLOCK 7	BOUNDARY TEMPERATURE VARIATION				
2001		89.5	84.5	240.0	79.25
76.0		69.75	82.25	720.0	103.75
119.0		130.0	138.0	1200.0	132.25
103.5		1440.0			360.0
					840.0
					1320.0
BLOCK 9	INITIAL TEMPERATURES				
1		115.2			
2		115.3			
3		116.0			
4		117.2			
5		118.4			
6		118.7			
7		117.3			
8		115.8			
9		113.2			
10		108.9			
11		105.1			
12		103.5			

ENDED-1 LAST CARD OF DATA DECK









118



DATA DECK 1

```

=====
* MISSILE PROBLEM ONE DIMENSIONAL
=====
PRINTOUT CYCLE TOO FAST TOO SLOW KWT DELTIX 12 SMALL IVARY NUTS
4 30 0 1.00000E 00 1.00000E 00 1.00000E 00
TOTAL TIME 1.54166E 01 HEAT FLOW 7.70604E 02 TEMP RATE 2.38003E 00
2.38531E 02
AVG TEMP 1.04224E 02 HEAT CAPACITY 1.35799D 00 GEN RATE 0.0 HEAT GEN 0.0 TEMP FROM GEN 0.0
=====
NODE TEMP DT DDT GE N RATE W H F CURE AT 280 F
1 0.11200 03 -0.79100 00 -0.40740 -01 0.0 0.1483E-04 0.3370E-06 0.3373E-06 0.0
2 0.11200 03 -0.79100 00 -0.40740 -01 0.0 0.3666E-04 0.3755E-06 0.3752E-06 0.0
3 0.11200 03 -0.82450 00 -0.42190 -01 0.0 0.1089E-04 0.4084E-06 0.4081E-06 0.0
4 0.10700 03 -0.82670 00 -0.42190 -01 0.0 0.2747E-04 0.4244E-06 0.4241E-06 0.0
5 0.10700 03 -0.82670 00 -0.42190 -01 0.0 0.3024E-04 0.4255E-06 0.4252E-06 0.0
6 0.10700 03 -0.82670 00 -0.42190 -01 0.0 0.2776E-04 0.4466E-06 0.4463E-06 0.0
7 0.09830 02 -0.81550 00 -0.41500 -01 0.0 0.2776E-04 0.4466E-06 0.4463E-06 0.0
8 0.09830 02 -0.81550 00 -0.41500 -01 0.0 0.2776E-04 0.4466E-06 0.4463E-06 0.0
9 0.09050 02 -0.85550 00 -0.46020 -01 0.0 0.4379E-04 0.4589E-06 0.4586E-06 0.0
10 0.09050 02 -0.85550 00 -0.46020 -01 0.0 0.4379E-04 0.4589E-06 0.4586E-06 0.0
11 0.08630 02 -0.82310 00 -0.42390 -01 0.0 0.4379E-04 0.4589E-06 0.4586E-06 0.0
12 0.08450 02 -0.80930 00 -0.41670 -01 0.0 0.4379E-04 0.4589E-06 0.4586E-06 0.0
=====
MATERIAL DATA
NAME MATL TOT CAP TOT HEAT TOT TEMP TMELT HMELT
SAND 1 1.07359E 00 1.13585E 02 1.05800E 02 0.0 0.0
STFL 2 2.82356E-03 2.71569E 01 9.83936E 01 0.0 0.0
AIR 3 1.44246E-03 1.30534E-01 9.04932E 01 0.0 0.0
=====
NODE DATA
NODE MATL NTYPE VOLUME MASS CAPACITY CONDUCTIVITY ZIP SLIM
1 1 1 4 0.1257E-04 0.68360D-06 0.1599D-06 0.2700D-03 0.6740E-05 0.1900D-01
2 1 1 4 0.3142E-01 0.1790D-00 0.3741D-01 0.2700D-03 0.5091E-02 0.1900D-01
3 1 1 4 0.1471E 02 0.8554D-00 0.2740D 00 0.2700D-03 0.8820E-02 0.1900D-01
4 1 1 4 0.2297E 02 0.1530D 01 0.2700D-03 0.1188E-01 0.1900D-01
5 1 1 4 0.2297E 02 0.1530D 01 0.2700D-03 0.1188E-01 0.1900D-01
6 1 1 4 0.2297E 02 0.1530D 01 0.2700D-03 0.1188E-01 0.1900D-01
7 1 1 4 0.2297E 02 0.1530D 01 0.2700D-03 0.1188E-01 0.1900D-01
8 1 1 4 0.2297E 02 0.1530D 01 0.2700D-03 0.1188E-01 0.1900D-01
9 1 1 4 0.2297E 02 0.1530D 01 0.2700D-03 0.1188E-01 0.1900D-01
10 1 1 4 0.2297E 02 0.1530D 01 0.2700D-03 0.1188E-01 0.1900D-01
11 1 1 4 0.2297E 02 0.1530D 01 0.2700D-03 0.1188E-01 0.1900D-01
12 1 1 4 0.2297E 02 0.1530D 01 0.2700D-03 0.1188E-01 0.1900D-01
=====
INTERNAL CONNECTION DATA
NODE1 NODE2 AREA HINT00E PINT00E TRAN HEAT FLOW AVG RATE
1 2 0.1257E-04 0.1000E 13 0.0 0.1698D-05 0.3733E-06 0.1414E-08
2 3 0.3142E-01 0.1000E 13 0.0 0.3930D-02 0.4955E-06 0.3778E-03
3 4 0.1471E 02 0.1000E 13 0.0 0.5089D-02 0.1638E-06 0.2055E-02
4 5 0.2297E 02 0.1000E 13 0.0 0.6786D-02 0.4089E-06 0.1414E-01
5 6 0.2297E 02 0.1000E 13 0.0 0.6786D-02 0.4089E-06 0.1414E-01
6 7 0.2297E 02 0.1000E 13 0.0 0.6786D-02 0.4089E-06 0.1414E-01
7 8 0.2297E 02 0.1000E 13 0.0 0.6786D-02 0.4089E-06 0.1414E-01
8 9 0.2297E 02 0.1000E 13 0.0 0.6786D-02 0.4089E-06 0.1414E-01
9 10 0.2297E 02 0.1000E 13 0.0 0.6786D-02 0.4089E-06 0.1414E-01
10 11 0.2297E 02 0.1000E 13 0.0 0.6786D-02 0.4089E-06 0.1414E-01
11 12 0.2297E 02 0.1000E 13 0.0 0.6786D-02 0.4089E-06 0.1414E-01
=====
BOUNDARY NODE DATA
NODE TEMPR HEAT FLCH AVG RATE
2001 8.4561E 01 7.7060D 02 3.2306E 00
=====
SYSTEM TOTAL 7.7060E 02 3.2306E 00
EXTERNAL CONNECTION DATA
=====
NODE NODE5 AREAS HSURE RSURE TRANS HEAT FLOW AVG RATE
2001 2005 5.4156D 01 1.0000D 06 0.0 0.0 5.6156D 07 7.7060E 02 3.2306E 00
=====

```

121







# DATA DECK 1

## TRUMP OUTPUT DATA

\* MISSILE PROBLEM ONE DIMENSIONAL

```

PRINTOUT CYCLE TOO FAST TOO SLOW KHIT DELTAX SMALL TVARY NUTS
9 105 6 0 0 1.00000E 12 1.00000E 00 1.00000E 00 00 5

TOTAL TIME 1.07468E 01 HEAT FLOW -1.15326E 04 TEMP RATE -8.59233E 00
1.01237E 03

AVG TEMP 9.89246E 01 HEAT CAPACITY 1.34279E 02 GEN RATE 0.0 HEAT GEN TEMP FROM GEN
0.0

=====
CURE AT 280 F
=====

```

MATERIAL DATA

```

NAME MATL TOI CAP TOI HEAT TOI TEMP TMELT HMELT
SAND 1 1.07359E 00 1.04172E 02 9.7038E 01 0.0 0.0
STEL 2 2.82356E 01 2.99406E 01 1.06038E 02 0.0 0.0
AIR 3 1.44246E 03 1.67498E 01 1.16120E 02 0.0 0.0
=====

```

MODE DATA

```

MODE MATL NTYPE RADIUS VOLUME MASS CAPACITY CONDUCTIVITY ZIP SLIM
1 1 1 4 0.50100E 01 0.34422E 01 0.157E 04 0.1299D 06 0.2733E 03 0.678D 02 0.1914E 01
2 1 1 4 0.50100E 01 0.34422E 01 0.157E 04 0.1299D 06 0.2733E 03 0.678D 02 0.1914E 01
3 1 1 4 0.50100E 01 0.34422E 01 0.157E 04 0.1299D 06 0.2733E 03 0.678D 02 0.1914E 01
4 1 1 4 0.50100E 01 0.34422E 01 0.157E 04 0.1299D 06 0.2733E 03 0.678D 02 0.1914E 01
5 1 1 4 0.50100E 01 0.34422E 01 0.157E 04 0.1299D 06 0.2733E 03 0.678D 02 0.1914E 01
6 1 1 4 0.50100E 01 0.34422E 01 0.157E 04 0.1299D 06 0.2733E 03 0.678D 02 0.1914E 01
7 1 1 4 0.50100E 01 0.34422E 01 0.157E 04 0.1299D 06 0.2733E 03 0.678D 02 0.1914E 01
8 1 1 4 0.50100E 01 0.34422E 01 0.157E 04 0.1299D 06 0.2733E 03 0.678D 02 0.1914E 01
9 1 1 4 0.50100E 01 0.34422E 01 0.157E 04 0.1299D 06 0.2733E 03 0.678D 02 0.1914E 01
10 1 1 4 0.50100E 01 0.34422E 01 0.157E 04 0.1299D 06 0.2733E 03 0.678D 02 0.1914E 01
11 1 1 4 0.50100E 01 0.34422E 01 0.157E 04 0.1299D 06 0.2733E 03 0.678D 02 0.1914E 01
12 1 1 4 0.50100E 01 0.34422E 01 0.157E 04 0.1299D 06 0.2733E 03 0.678D 02 0.1914E 01
=====

```

INTERNAL CONNECTION DATA

```

NOD1 NOD2 AREA TOI HINT RINT TRAN RINT
1 2 0.1258D 01 0.1000E 01 0.1000E 01 0.678D 05 0.334E 03
2 3 0.1258D 01 0.1000E 01 0.1000E 01 0.678D 05 0.334E 03
3 4 0.1258D 01 0.1000E 01 0.1000E 01 0.678D 05 0.334E 03
4 5 0.1258D 01 0.1000E 01 0.1000E 01 0.678D 05 0.334E 03
5 6 0.1258D 01 0.1000E 01 0.1000E 01 0.678D 05 0.334E 03
6 7 0.1258D 01 0.1000E 01 0.1000E 01 0.678D 05 0.334E 03
7 8 0.1258D 01 0.1000E 01 0.1000E 01 0.678D 05 0.334E 03
8 9 0.1258D 01 0.1000E 01 0.1000E 01 0.678D 05 0.334E 03
9 10 0.1258D 01 0.1000E 01 0.1000E 01 0.678D 05 0.334E 03
10 11 0.1258D 01 0.1000E 01 0.1000E 01 0.678D 05 0.334E 03
11 12 0.1258D 01 0.1000E 01 0.1000E 01 0.678D 05 0.334E 03
=====

```

BOUNDARY NODE DATA

```

NODR TEMPR8 HEAT FLOW AVG RATE
2001 1.2380E 02 -1.1533D 04 -1.1592E 01

SYSTEM TOTAL -1.1533E 04 -1.1392E 01
EXTERNAL CONNECTION DATA

NODS NODSB AREAS HSURE PSURE POWER TRANS HEAT FLOW AVG RATE
12 2001 5.6156D 01 1.0000D 06 0.0 0.8 5.4156D 07 -1.1533E 04 -1.1392E 01
=====

```



### TRAINING OUTPUT DATA

126





## TRUMP OUTPUT DATA

[illegible]

```

//WIR71687 JOB (1687,0860FT,NF12),WIRZBURGER.A. BOX W',TIME=(4,00)
//JOBLIB DD UNIT=2321,DSNAME=SI734.KATZ,
//DISP=(OLD,PASS),VOLUME=SER=CELOO1
//EXEC PGM=TRUMP,REGION=350K
//FT06F001 DD SYSOUT=A,DCB=(RECFM=FBA,LRECL=133,BLKSIZE=3325),
//SPACE=(CYL,(6,1))
//FT05F001 DD *

```

\* MISSILE PROBLEM TWO DIMENSIONAL

BLOCK 1 CONTROLS, LIMITS, CONSTANTS

5	1	1.000 E 00	1.000E 00	1380.0	8000.0
2	3				
114.0					

BLOCK 2 MATERIAL NAMES, NUMBERS, THERMAL PROPERTIES.

ASAND	1	0.0544	0.19	0.00027
ASTEL	2	0.2807	0.109	0.0364
AAIR	3	0.0000436	0.240	0.0000225

BLOCK 4 NODE NUMBERS, MATERIAL REFERENCES, TYPES, VOLUMES.

1	12	1	0.25	0.002	0.001
2	12	1	0.25	0.998	0.501
3	12	1	0.25	1.00	1.50
4	12	1	0.25	1.00	2.50
5	12	1	0.25	1.00	3.50
6	12	1	0.25	1.00	4.50
7	12	1	0.25	0.75	5.375
8	12	1	0.25	0.25	5.875
9	12	1	0.25	1.00	6.50
10	12	1	0.25	1.00	7.50
11	12	1	0.25	0.9375	8.46875
12	12	1	0.0	0.0	8.9375

BLOCK 5 INTERNAL THERMAL CONNECTION NODE NUMBERS.

1	3	12	12	0.001	0.499	0.25	0.002
2	3	12	12	0.499	0.500	0.25	1.00
3	3	12	12	0.500	0.500	0.25	2.00
4	3	12	12	0.500	0.500	0.25	3.00
5	3	12	12	0.500	0.500	0.25	4.00
6	3	12	12	0.500	0.375	0.25	5.00
7	3	12	12	0.375	0.125	0.25	5.75
8	3	12	12	0.125	0.500	0.25	6.00
9	3	12	12	0.500	0.0	0.25	6.00
10	3	12	12	0.500	0.500	0.25	7.00
11	3	12	12	0.500	0.46875	0.25	8.00
12	3	12	12	0.46875	0.0	0.25	8.9375
13	3	12	12	0.000785	0.000785	0.25	0.001273

0.00008478

BLOCK 6		EXTERNAL THERMAL CONNECTIONS		BLOCK 7		BOUNDARY TEMPERATURE VARIATION		BLOCK 8		BOUNDARY TEMPERATURE VARIATION	
12	2001	3	12	1	8.9375	1.00	E6	12	2001	3	12
2	3	39	0	393	0	393	0	393	2	3	39
3	4	40	1	178	1	178	1	178	3	4	40
4	5	41	2	748	2	748	2	748	4	5	41
5	6	42	3	534	3	534	3	534	5	6	42
6	7	43	4	271	4	271	4	271	6	7	43
7	8	44	5	665	5	665	5	665	7	8	44
8	9	45	6	890	6	890	6	890	8	9	45
9	10	46	7	651	7	651	7	651	9	10	46
10	11	47	8	0	0	0	0	0	10	11	47
11	12	48	9	0	0	0	0	0	11	12	48
12	13	49	10	0	0	0	0	0	12	13	49
13	14	50	11	0	0	0	0	0	13	14	50
14	15	51	12	0	0	0	0	0	14	15	51
15	16	52	13	0	0	0	0	0	15	16	52
16	17	53	14	0	0	0	0	0	16	17	53
17	18	54	15	0	0	0	0	0	17	18	54
18	19	55	16	0	0	0	0	0	18	19	55
19	20	56	17	0	0	0	0	0	19	20	56
20	21	57	18	0	0	0	0	0	20	21	57
21	22	58	19	0	0	0	0	0	21	22	58
22	23	59	20	0	0	0	0	0	22	23	59
23	24	60	21	0	0	0	0	0	23	24	60
24	25	61	22	0	0	0	0	0	24	25	61
25	26	62	23	0	0	0	0	0	25	26	62
26	27	63	24	0	0	0	0	0	26	27	63
27	28	64	25	0	0	0	0	0	27	28	64
28	29	65	26	0	0	0	0	0	28	29	65
29	30	66	27	0	0	0	0	0	29	30	66
30	31	67	28	0	0	0	0	0	30	31	67
31	32	68	29	0	0	0	0	0	31	32	68
32	33	69	30	0	0	0	0	0	32	33	69
33	34	70	31	0	0	0	0	0	33	34	70
34	35	71	32	0	0	0	0	0	34	35	71
35	36	72	33	0	0	0	0	0	35	36	72
36	37	73	34	0	0	0	0	0	36	37	73
37	38	74	35	0	0	0	0	0	37	38	74
38	39	75	36	0	0	0	0	0	38	39	75
39	40	76	37	0	0	0	0	0	39	40	76
40	41	77	38	0	0	0	0	0	40	41	77
41	42	78	39	0	0						







DATA BLOCK 60										EXTERNAL THERMAL CONNECTIONS										PSUPE									
NOD1	NOD2	INDEX	DEL1	DEL2	C- LONG	GRAD	HINT	AREA	RINT	NODS	NODS8	INDEX	LTABH	POWER	DLONG	DRAD	HSURE	PSUPE	AREA5										
10	46	58	5.89105D	5.89050D	00	00	00	1.33777D	0.0	10	2001	1	0	0.0	5000E-01	8.9375E-00	1.0000D	0.0	1.4039D										
11	47	59	6.65110D	6.65110D	00	00	00	1.33777D	0.0	11	2002	2	0	0.0	5000E-01	8.9375E-00	1.0000D	0.0	1.4039D										
20	48	60	6.65110D	6.65110D	00	00	00	1.33777D	0.0	20	2003	3	0	0.0	5000E-01	8.9375E-00	1.0000D	0.0	1.4039D										
30	49	61	6.65110D	6.65110D	00	00	00	1.33777D	0.0	30	2004	4	0	0.0	5000E-01	8.9375E-00	1.0000D	0.0	1.4039D										
40	50	62	6.65110D	6.65110D	00	00	00	1.33777D	0.0	40	2005	5	0	0.0	5000E-01	8.9375E-00	1.0000D	0.0	1.4039D										
50	51	63	6.65110D	6.65110D	00	00	00	1.33777D	0.0	50	2006	6	0	0.0	5000E-01	8.9375E-00	1.0000D	0.0	1.4039D										
60	52	64	6.65110D	6.65110D	00	00	00	1.33777D	0.0	60	2007	7	0	0.0	5000E-01	8.9375E-00	1.0000D	0.0	1.4039D										
70	53	65	6.65110D	6.65110D	00	00	00	1.33777D	0.0	70	2008	8	0	0.0	5000E-01	8.9375E-00	1.0000D	0.0	1.4039D										
80	54	66	6.65110D	6.65110D	00	00	00	1.33777D	0.0	80	2009	9	0	0.0	5000E-01	8.9375E-00	1.0000D	0.0	1.4039D										
90	55	67	6.65110D	6.65110D	00	00	00	1.33777D	0.0	90	2010	10	0	0.0	5000E-01	8.9375E-00	1.0000D	0.0	1.4039D										
100	56	68	6.65110D	6.65110D	00	00	00	1.33777D	0.0	100	2011	11	0	0.0	5000E-01	8.9375E-00	1.0000D	0.0	1.4039D										
110	57	69	6.65110D	6.65110D	00	00	00	1.33777D	0.0	110	2012	12	0	0.0	5000E-01	8.9375E-00	1.0000D	0.0	1.4039D										
120	58	70	6.65110D	6.65110D	00	00	00	1.33777D	0.0	120	2013	13	0	0.0	5000E-01	8.9375E-00	1.0000D	0.0	1.4039D										
130	59	71	6.65110D	6.65110D	00	00	00	1.33777D	0.0	130	2014	14	0	0.0	5000E-01	8.9375E-00	1.0000D	0.0	1.4039D										
140	60	72	6.65110D	6.65110D	00	00	00	1.33777D	0.0	140	2015	15	0	0.0	5000E-01	8.9375E-00	1.0000D	0.0	1.4039D										
150	61	73	6.65110D	6.65110D	00	00	00	1.33777D	0.0	150	2016	16	0	0.0	5000E-01	8.9375E-00	1.0000D	0.0	1.4039D										
160	62	74	6.65110D	6.65110D	00	00	00	1.33777D	0.0	160	2017	17	0	0.0	5000E-01	8.9375E-00	1.0000D	0.0	1.4039D										
170	63	75	6.65110D	6.65110D	00	00	00	1.33777D	0.0	170	2018	18	0	0.0	5000E-01	8.9375E-00	1.0000D	0.0	1.4039D										
180	64	76	6.65110D	6.65110D	00	00	00	1.33777D	0.0	180	2019	19	0	0.0	5000E-01	8.9375E-00	1.0000D	0.0	1.4039D										
190	65	77	6.65110D	6.65110D	00	00	00	1.33777D	0.0	190	2020	20	0	0.0	5000E-01	8.9375E-00	1.0000D	0.0	1.4039D										
200	66	78	6.65110D	6.65110D	00	00	00	1.33777D	0.0	200	2021	21	0	0.0	5000E-01	8.9375E-00	1.0000D	0.0	1.4039D										
210	67	79	6.65110D	6.65110D	00	00	00	1.33777D	0.0	210	2022	22	0	0.0	5000E-01	8.9375E-00	1.0000D	0.0	1.4039D										
220	68	80	6.65110D	6.65110D	00	00	00	1.33777D	0.0	220	2023	23	0	0.0	5000E-01	8.9375E-00	1.0000D	0.0	1.4039D										
230	69	81	6.65110D	6.65110D	00	00	00	1.33777D	0.0	230	2024	24	0	0.0	5000E-01	8.9375E-00	1.0000D	0.0	1.4039D										
240	70	82	6.65110D	6.65110D	00	00	00	1.33777D	0.0	240	2025	25	0	0.0	5000E-01	8.9375E-00	1.0000D	0.0	1.4039D										
250	71	83	6.65110D	6.65110D	00	00	00	1.33777D	0.0	250	2026	26	0	0.0	5000E-01	8.9375E-00	1.0000D	0.0	1.4039D										
260	72	84	6.65110D	6.65110D	00	00	00	1.33777D	0.0	260	2027	27	0	0.0	5000E-01	8.9375E-00	1.0000D	0.0	1.4039D										
270	73	85	6.65110D	6.65110D	00	00	00	1.33777D	0.0	270	2028	28	0	0.0	5000E-01	8.9375E-00	1.0000D	0.0	1.4039D										
280	74	86	6.65110D	6.65110D	00	00	00	1.33777D	0.0	280	2029	29	0	0.0	5000E-01	8.9375E-00	1.0000D	0.0	1.4039D										
290	75	87	6.65110D	6.65110D	00	00	00	1.33777D	0.0	290	2030	30	0	0.0	5000E-01	8.9375E-00	1.0000D	0.0	1.4039D										
300	76	88	6.65110D	6.65110D	00	00	00	1.33777D	0.0	300	2031	31	0	0.0	5000E-01	8.9375E-00	1.0000D	0.0	1.4039D										
310	77	89	6.65110D	6.65110D	00	00	00	1.33777D	0.0	310	2032	32	0	0.0	5000E-01	8.9375E-00	1.0000D	0.0	1.4039D										
320	78	90	6.65110D	6.65110D	00	00	00	1.33777D	0.0	320	2033	33	0	0.0	5000E-01	8.9375E-00	1.0000D	0.0	1.4039D										
330	79	91	6.65110D	6.65110D	00	00	00	1.33777D	0.0	330	2034	34	0	0.0	5000E-01	8.9375E-00	1.0000D	0.0	1.4039D										
340	80	92	6.65110D	6.65110D	00	00	00	1.33777D	0.0	340	2035	35	0	0.0	5000E-01	8.9375E-00	1.0000D	0.0	1.4039D										
350	81	93	6.65110D	6.65110D	00	00	00	1.33777D	0.0	350	2036	36	0	0.0	5000E-01	8.9375E-00	1.0000D	0.0	1.4039D										
360	82	94	6.65110D	6.65110D	00	00	00	1.33777D	0.0	360	2037	37	0	0.0	5000E-01	8.9375E-00	1.0000D	0.0	1.4039D										
370	83	95	6.65110D	6.65110D	00	00	00	1.33777D	0.0	370	2038	38	0	0.0	5000E-01	8.9375E-00	1.0000D	0.0	1.4039D										
380	84	96	6.65110D	6.65110D	00	00	00	1.33777D	0.0	380	2039	39	0	0.0	5000E-01	8.9375E-00	1.0000D	0.0	1.4039D										
390	85	97	6.65110D	6.65110D	00	00	00	1.33777D	0.0	390	2040	40	0	0.0	5000E-01	8.9375E-00	1.0000D	0.0	1.4039D										
400	86	98	6.65110D	6.65110D	00	00	00	1.33777D	0.0	400	2041	41	0	0.0	5000E-01	8.9375E-00	1.0000D	0.0	1.4039D										
410	87	99	6.65110D	6.65110D	00	00	00	1.33777D	0.0	410	2042	42	0	0.0	5000E-01	8.9375E-00	1.0000D	0.0	1.4039D										
420	88	100	6.65110D	6.65110D	00	00	00	1.33777D	0.0	420	2043	43	0	0.0	5000E-01	8.9375E-00	1.0000D	0.0	1.4039D										
430	89		6.65110D	6.65110D	00	00	00	1.33777D	0.0	430	2044	44	0	0.0	5000E-01	8.9375E-00	1.0000D	0.0	1.4039D										
440	90		6.65110D	6.65110D	00	00	00	1.33777D	0.0	440	2045	45	0	0.0	5000E-01	8.9375E-00	1.0000D	0.0	1.4039D										
450	91		6.65110D	6.65110D	00	00	00	1.33777D	0.0	450	2046	46	0	0.0	5000E-01	8.9375E-00	1.0000D	0.0	1.4039D										
460	92		6.65110D	6.65110D	00	00	00	1.33777D	0.0	460	2047	47	0	0.0	5000E-01	8.9375E-00	1.0000D	0.0	1.4039D										
470	93		6.65110D	6.65110D	00	00	00	1.33777D	0.0	470	2048	48	0	0.0	5000E-01	8.9375E-00	1.0000D	0.0	1.4039D										
480	94		6.65110D	6.65110D	00	00	00	1.33777D	0.0	480	2049	49	0	0.0	5000E-01	8.9375E-00	1.0000D	0.0	1.4039D										
490	95		6.65110D	6.65110D	00	00	00	1.33777D	0.0	490	2050	50	0	0.0	5000E-01	8.9375E-00	1.0000D	0.0	1.4039D										
500	96		6.65110D	6.65110D	00	00	00	1.33777D	0.0	500	2051	51	0	0.0	5000E-01	8.9375E-00	1.0000D	0.0	1.4039D										
510	97		6.65110D	6.65110D	00	00	00	1.33777D	0.0	510	2052	52	0	0.0	5000E-01	8.9375E-00	1.0000D	0.0	1.4039D										
520	98		6.65110D	6.65110D	00	00	00	1.33777D	0.0	520	2053	53	0	0.0	5000E-01	8.9375E-00	1.0000D	0.0	1.4039D										
530	99		6.65110D	6.65110D	00	00	00	1.33777D	0.0	530	2054	54	0	0.0	5000E-01	8.9375E-00	1.0000D	0.0	1.4039D										
540	100		6.65110D	6.65110D	00	00	00	1.33777D	0.0	540	2055	55	0	0.0	5000E-01	8.9375E-00	1.0000D	0.0	1.4039D										
550			6.65110D	6.65110D	00	00	00	1.33777D	0.0	550	2056	56	0	0.0	5000E-01	8.9375E-00	1.0000D	0.0	1.4039D										
560			6.65110D	6.65110D	00	00	00	1.33777D	0.0	560	2057	57	0	0.0	5000E-01	8.9375E-00	1.0000D	0.0	1.4039D										
570			6.65110D	6.65110D	00	00	00	1.33777D	0.0	570	2058	58	0	0.0	5000E-01	8.9375E-00	1.0000D	0.0	1.4039D										
580			6.65110D	6.65110D	00	00	00	1.33777D	0.0	580	2059	59	0	0.0	5000E-01	8.9375E-00	1.0000D	0.0	1.4039D										
590			6.65110D	6.65110D	00	00	00	1.33777D	0.0	590	2060	60	0	0.0	5000E-01	8.9375E-00	1.0000D	0.0	1.4039D										
600			6.65110D	6.65110D	00	00	00	1.33777D	0.0	600	2061	61	0	0.0	5000E-01	8.9375E-00	1.0000D	0.0	1.4039D										
610			6.65110D	6.65110D	00	00	00	1.33777D	0.0	610	2062	62	0	0.0	5000E-01	8.9375E-00	1.0000D	0.0	1.4039D										
620			6.65110D	6.65110D	00	00	00	1.33777D	0.0	620	2063	63	0	0.0	5000E-01	8.9375E-00	1.0000D	0.0	1.4039D										
630			6.65110D	6.65110D	00	00	00	1.33777D	0.0	630	2064	64	0	0.0	5000E-01	8.9375E-00	1.0000D	0.0	1.4039D										
640			6.																										

DATA BLOCK 70 BOUNDARY TEMPERATURE VARIATION.									
NODB INDEX	LTABT	TEMPB	SLOPE	TIMEB	TIMEB	TIMEB	TIMEB	TIMEB	TIMEB
2001	1	12							
		8.400000E	01	1.200000E	02	1.200000E	02	1.200000E	02
		7.900000E	01	1.400000E	02	1.400000E	02	1.400000E	02
		7.200000E	01	3.600000E	02	3.600000E	02	3.600000E	02
		7.100000E	01	4.800000E	02	4.800000E	02	4.800000E	02
		6.400000E	01	6.000000E	02	6.000000E	02	6.000000E	02
		6.200000E	01	7.200000E	02	7.200000E	02	7.200000E	02
		1.100000E	02	8.400000E	02	8.400000E	02	8.400000E	02
		1.400000E	02	9.600000E	02	9.600000E	02	9.600000E	02
		1.500000E	02	1.080000E	03	1.080000E	03	1.080000E	03
		1.300000E	02	1.200000E	03	1.200000E	03	1.200000E	03
		9.900000E	01	1.440000E	03	1.440000E	03	1.440000E	03
2002	2	12							
		8.700000E	01	1.200000E	02	1.200000E	02	1.200000E	02
		8.200000E	01	1.400000E	02	1.400000E	02	1.400000E	02
		7.300000E	01	3.600000E	02	3.600000E	02	3.600000E	02
		7.700000E	01	4.800000E	02	4.800000E	02	4.800000E	02
		6.700000E	01	6.000000E	02	6.000000E	02	6.000000E	02
		7.900000E	01	7.200000E	02	7.200000E	02	7.200000E	02
		1.100000E	02	8.400000E	02	8.400000E	02	8.400000E	02
		1.300000E	02	9.600000E	02	9.600000E	02	9.600000E	02
		1.400000E	02	1.080000E	03	1.080000E	03	1.080000E	03
		1.300000E	02	1.200000E	03	1.200000E	03	1.200000E	03
		1.030000E	02	1.440000E	03	1.440000E	03	1.440000E	03
2003	3	12							
		9.100000E	01	1.200000E	02	1.200000E	02	1.200000E	02
		8.700000E	01	1.400000E	02	1.400000E	02	1.400000E	02
		8.500000E	01	3.600000E	02	3.600000E	02	3.600000E	02
		8.900000E	01	4.800000E	02	4.800000E	02	4.800000E	02
		7.300000E	01	6.000000E	02	6.000000E	02	6.000000E	02
		8.800000E	01	7.200000E	02	7.200000E	02	7.200000E	02
		1.000000E	02	8.400000E	02	8.400000E	02	8.400000E	02
		1.100000E	02	9.600000E	02	9.600000E	02	9.600000E	02
		1.200000E	02	1.080000E	03	1.080000E	03	1.080000E	03
		1.100000E	02	1.200000E	03	1.200000E	03	1.200000E	03
		1.030000E	02	1.440000E	03	1.440000E	03	1.440000E	03
2004	4	12							
		9.600000E	01	1.200000E	02	1.200000E	02	1.200000E	02
		9.000000E	01	1.400000E	02	1.400000E	02	1.400000E	02
		8.500000E	01	3.600000E	02	3.600000E	02	3.600000E	02
		8.100000E	01	4.800000E	02	4.800000E	02	4.800000E	02
		7.500000E	01	6.000000E	02	6.000000E	02	6.000000E	02
		8.400000E	01	7.200000E	02	7.200000E	02	7.200000E	02
		1.000000E	02	8.400000E	02	8.400000E	02	8.400000E	02
		1.100000E	02	9.600000E	02	9.600000E	02	9.600000E	02
		1.200000E	02	1.080000E	03	1.080000E	03	1.080000E	03
		1.300000E	02	1.200000E	03	1.200000E	03	1.200000E	03
		1.090000E	02	1.440000E	03	1.440000E	03	1.440000E	03
LAST CARD OF DATA DECK									
DATA ENDED -10									





### TRUMP OUTPUT DATA

* MISSILE PROBLEM TWO DIMENSIONAL														
PRINTOUT	CYCLE	TOO FAST	TOO SLOW	HEAT FLOW	HEAT CONTENT	GEN RATE	HEAT GEN	FLUX RATE	FLUX	DELTMX	SMALL	TVARY	NUTS	
TOTAL TIME	TIME STEP	4.86662E 00	2.52999E 03	2.52999E 03	1.32592E 02	0.0	0.0	1.86387E 03	1.08086E 01	1.00000E 00	1.00000E 00	1.00000E 00	12	
AVG TEMP	HEAT CAPACITY	1.35739D 00	1.32592E 02	1.32592E 02	1.32592E 02	0.0	0.0	1.86387E 03	1.01876E 02	7.50532E 01				
1.12416E 02	1.35739D 00	1.32592E 02	1.32592E 02	1.32592E 02	1.32592E 02	0.0	0.0	1.86387E 03	1.01876E 02	7.50532E 01				
1.12416E 02	1.35739D 00	1.32592E 02	1.32592E 02	1.32592E 02	1.32592E 02	0.0	0.0	1.86387E 03	1.01876E 02	7.50532E 01				
1.12416E 02	1.35739D 00	1.32592E 02	1.32592E 02	1.32592E 02	1.32592E 02	0.0	0.0	1.86387E 03	1.01876E 02	7.50532E 01				
1.12416E 02	1.35739D 00	1.32592E 02	1.32592E 02	1.32592E 02	1.32592E 02	0.0	0.0	1.86387E 03	1.01876E 02	7.50532E 01				
1.12416E 02	1.35739D 00	1.32592E 02	1.32592E 02	1.32592E 02	1.32592E 02	0.0	0.0	1.86387E 03	1.01876E 02	7.50532E 01				
1.12416E 02	1.35739D 00	1.32592E 02	1.32592E 02	1.32592E 02	1.32592E 02	0.0	0.0	1.86387E 03	1.01876E 02	7.50532E 01				
1.12416E 02	1.35739D 00	1.32592E 02	1.32592E 02	1.32592E 02	1.32592E 02	0.0	0.0	1.86387E 03	1.01876E 02	7.50532E 01				
1.12416E 02	1.35739D 00	1.32592E 02	1.32592E 02	1.32592E 02	1.32592E 02	0.0	0.0	1.86387E 03	1.01876E 02	7.50532E 01				
1.12416E 02	1.35739D 00	1.32592E 02	1.32592E 02	1.32592E 02	1.32592E 02	0.0	0.0	1.86387E 03	1.01876E 02	7.50532E 01				
1.12416E 02	1.35739D 00	1.32592E 02	1.32592E 02	1.32592E 02	1.32592E 02	0.0	0.0	1.86387E 03	1.01876E 02	7.50532E 01				
1.12416E 02	1.35739D 00	1.32592E 02	1.32592E 02	1.32592E 02	1.32592E 02	0.0	0.0	1.86387E 03	1.01876E 02	7.50532E 01				
1.12416E 02	1.35739D 00	1.32592E 02	1.32592E 02	1.32592E 02	1.32592E 02	0.0	0.0	1.86387E 03	1.01876E 02	7.50532E 01				
1.12416E 02	1.35739D 00	1.32592E 02	1.32592E 02	1.32592E 02	1.32592E 02	0.0	0.0	1.86387E 03	1.01876E 02	7.50532E 01				
1.12416E 02	1.35739D 00	1.32592E 02	1.32592E 02	1.32592E 02	1.32592E 02	0.0	0.0	1.86387E 03	1.01876E 02	7.50532E 01				
1.12416E 02	1.35739D 00	1.32592E 02	1.32592E 02	1.32592E 02	1.32592E 02	0.0	0.0	1.86387E 03	1.01876E 02	7.50532E 01				
1.12416E 02	1.35739D 00	1.32592E 02	1.32592E 02	1.32592E 02	1.32592E 02	0.0	0.0	1.86387E 03	1.01876E 02	7.50532E 01				
1.12416E 02	1.35739D 00	1.32592E 02	1.32592E 02	1.32592E 02	1.32592E 02	0.0	0.0	1.86387E 03	1.01876E 02	7.50532E 01				
1.12416E 02	1.35739D 00	1.32592E 02	1.32592E 02	1.32592E 02	1.32592E 02	0.0	0.0	1.86387E 03	1.01876E 02	7.50532E 01				
1.12416E 02	1.35739D 00	1.32592E 02	1.32592E 02	1.32592E 02	1.32592E 02	0.0	0.0	1.86387E 03	1.01876E 02	7.50532E 01				
1.12416E 02	1.35739D 00	1.32592E 02	1.32592E 02	1.32592E 02	1.32592E 02	0.0	0.0	1.86387E 03	1.01876E 02	7.50532E 01				
1.12416E 02	1.35739D 00	1.32592E 02	1.32592E 02	1.32592E 02	1.32592E 02	0.0	0.0	1.86387E 03	1.01876E 02	7.50532E 01				
1.12416E 02	1.35739D 00	1.32592E 02	1.32592E 02	1.32592E 02	1.32592E 02	0.0	0.0	1.86387E 03	1.01876E 02	7.50532E 01				
1.12416E 02	1.35739D 00	1.32592E 02	1.32592E 02	1.32592E 02	1.32592E 02	0.0	0.0	1.86387E 03	1.01876E 02	7.50532E 01				
1.12416E 02	1.35739D 00	1.32592E 02	1.32592E 02	1.32592E 02	1.32592E 02	0.0	0.0	1.86387E 03	1.01876E 02	7.50532E 01				
1.12416E 02	1.35739D 00	1.32592E 02	1.32592E 02	1.32592E 02	1.32592E 02	0.0	0.0	1.86387E 03	1.01876E 02	7.50532E 01				
1.12416E 02	1.35739D 00	1.32592E 02	1.32592E 02	1.32592E 02	1.32592E 02	0.0	0.0	1.86387E 03	1.01876E 02	7.50532E 01				
1.12416E 02	1.35739D 00	1.32592E 02	1.32592E 02	1.32592E 02	1.32592E 02	0.0	0.0	1.86387E 03	1.01876E 02	7.50532E 01				
1.12416E 02	1.35739D 00	1.32592E 02	1.32592E 02	1.32592E 02	1.32592E 02	0.0	0.0	1.86387E 03	1.01876E 02	7.50532E 01				
1.12416E 02	1.35739D 00	1.32592E 02	1.32592E 02	1.32592E 02	1.32592E 02	0.0	0.0	1.86387E 03	1.01876E 02	7.50532E 01				
1.12416E 02	1.35739D 00	1.32592E 02	1.32592E 02	1.32592E 02	1.32592E 02	0.0	0.0	1.86387E 03	1.01876E 02	7.50532E 01				
1.12416E 02	1.35739D 00	1.32592E 02	1.32592E 02	1.32592E 02	1.32592E 02	0.0	0.0	1.86387E 03	1.01876E 02	7.50532E 01				
1.12416E 02	1.35739D 00	1.32592E 02	1.32592E 02	1.32592E 02	1.32592E 02	0.0	0.0	1.86387E 03	1.01876E 02	7.50532E 01				
1.12416E 02	1.35739D 00	1.32592E 02	1.32592E 02	1.32592E 02	1.32592E 02	0.0	0.0	1.86387E 03	1.01876E 02	7.50532E 01				
1.12416E 02	1.35739D 00	1.32592E 02	1.32592E 02	1.32592E 02	1.32592E 02	0.0	0.0	1.86387E 03	1.01876E 02	7.50532E 01				
1.12416E 02	1.35739D 00	1.32592E 02	1.32592E 02	1.32592E 02	1.32592E 02	0.0	0.0	1.86387E 03	1.01876E 02	7.50532E 01				
1.12416E 02	1.35739D 00	1.32592E 02	1.32592E 02	1.32592E 02	1.32592E 02	0.0	0.0	1.86387E 03	1.01876E 02	7.50532E 01				
1.12416E 02	1.35739D 00	1.32592E 02	1.32592E 02	1.32592E 02	1.32592E 02	0.0	0.0	1.86387E 03	1.01876E 02	7.50532E 01				
1.12416E 02	1.35739D 00	1.32592E 02	1.32592E 02	1.32592E 02	1.32592E 02	0.0	0.0	1.86387E 03	1.01876E 02	7.50532E 01				
1.12416E 02	1.35739D 00	1.32592E 02	1.32592E 02	1.32592E 02	1.32592E 02	0.0	0.0	1.86387E 03	1.01876E 02	7.50532E 01				
1.12416E 02	1.35739D 00	1.32592E 02	1.32592E 02	1.32592E 02	1.32592E 02	0.0	0.0	1.86387E 03	1.01876E 02	7.50532E 01				
1.12416E 02	1.35739D 00	1.32592E 02	1.32592E 02	1.32592E 02	1.32592E 02	0.0	0.0	1.86387E 03	1.01876E 02	7.50532E 01				
1.12416E 02	1.35739D 00	1.32592E 02	1.32592E 02	1.32592E 02	1.32592E 02	0.0	0.0	1.86387E 03	1.01876E 02	7.50532E 01				
1.12416E 02	1.35739D 00	1.32592E 02	1.32592E 02	1.32592E 02	1.32592E 02	0.0	0.0	1.86387E 03	1.01876E 02	7.50532E 01				
1.12416E 02	1.35739D 00	1.32592E 02	1.32592E 02	1.32592E 02	1.32592E 02	0.0	0.0	1.86387E 03	1.01876E 02	7.50532E 01				
1.12416E 02	1.35739D 00	1.32592E 02	1.32592E 02	1.32592E 02	1.32592E 02	0.0	0.0	1.86387E 03	1.01876E 02	7.50532E 01				
1.12416E 02	1.35739D 00	1.32592E 02	1.32592E 02	1.32592E 02	1.32592E 02	0.0	0.0	1.86387E 03	1.01876E 02	7.50532E 01				
1.														









TRUMP OUTPUT DATA

* MISSILE PROBLEM TWO DIMENSIONAL									
PRINTOUT	CYCLE	TOO FAST	TOO SLOW	SWIT	DELTMX	SMALL	TVARY	NUTS	
	100	11	0	0	1.0000E 12	1.0000E 00	1.0000E 00	00	
TOTAL TIME	TIME STEP	HEAT FLOW	HEAT CONTENT	GEN RATE	HEAT GEN	FLUX RATE	TEMP RATE		
7.84895E 02	3.2434E 00	-2.06335E 04	1.17042E 02	0.0	0.0	-2.62883E 01	-1.9368E 01		
AVS TEMP	HEAT CAPACITY	HEAT CONTENT	GEN RATE	HEAT GEN	FLUX RATE	TEMP RATE	TEMP FROM GEN		
5.62263E 01	1.357390 00	1.17042E 02	0.0	0.0	0.0	0.0	0.0		
=====									
TEMP	DT	OT	DDT	GE N RATE	HEAT GEN	FLUX RATE	TEMP RATE	TEMP FROM GEN	CURE AT 280 F
0.87723E 00	0.9000	0.0000	0.0000	0.0000	0.0000	0.0000	0.0000	0.0000	0.0000
0.87723E 00	0.9100	0.0000	0.0000	0.0000	0.0000	0.0000	0.0000	0.0000	0.0000
0.87723E 00	0.9200	0.0000	0.0000	0.0000	0.0000	0.0000	0.0000	0.0000	0.0000
0.87723E 00	0.9300	0.0000	0.0000	0.0000	0.0000	0.0000	0.0000	0.0000	0.0000
0.87723E 00	0.9400	0.0000	0.0000	0.0000	0.0000	0.0000	0.0000	0.0000	0.0000
0.87723E 00	0.9500	0.0000	0.0000	0.0000	0.0000	0.0000	0.0000	0.0000	0.0000
0.87723E 00	0.9600	0.0000	0.0000	0.0000	0.0000	0.0000	0.0000	0.0000	0.0000
0.87723E 00	0.9700	0.0000	0.0000	0.0000	0.0000	0.0000	0.0000	0.0000	0.0000
0.87723E 00	0.9800	0.0000	0.0000	0.0000	0.0000	0.0000	0.0000	0.0000	0.0000
0.87723E 00	0.9900	0.0000	0.0000	0.0000	0.0000	0.0000	0.0000	0.0000	0.0000
0.87723E 00	1.0000	0.0000	0.0000	0.0000	0.0000	0.0000	0.0000	0.0000	0.0000
0.87723E 00	1.0100	0.0000	0.0000	0.0000	0.0000	0.0000	0.0000	0.0000	0.0000
0.87723E 00	1.0200	0.0000	0.0000	0.0000	0.0000	0.0000	0.0000	0.0000	0.0000
0.87723E 00	1.0300	0.0000	0.0000	0.0000	0.0000	0.0000	0.0000	0.0000	0.0000
0.87723E 00	1.0400	0.0000	0.0000	0.0000	0.0000	0.0000	0.0000	0.0000	0.0000
0.87723E 00	1.0500	0.0000	0.0000	0.0000	0.0000	0.0000	0.0000	0.0000	0.0000
0.87723E 00	1.0600	0.0000	0.0000	0.0000	0.0000	0.0000	0.0000	0.0000	0.0000
0.87723E 00	1.0700	0.0000	0.0000	0.0000	0.0000	0.0000	0.0000	0.0000	0.0000
0.87723E 00	1.0800	0.0000	0.0000	0.0000	0.0000	0.0000	0.0000	0.0000	0.0000
0.87723E 00	1.0900	0.0000	0.0000	0.0000	0.0000	0.0000	0.0000	0.0000	0.0000
0.87723E 00	1.1000	0.0000	0.0000	0.0000	0.0000	0.0000	0.0000	0.0000	0.0000
0.87723E 00	1.1100	0.0000	0.0000	0.0000	0.0000	0.0000	0.0000	0.0000	0.0000
0.87723E 00	1.1200	0.0000	0.0000	0.0000	0.0000	0.0000	0.0000	0.0000	0.0000
0.87723E 00	1.1300	0.0000	0.0000	0.0000	0.0000	0.0000	0.0000	0.0000	0.0000
0.87723E 00	1.1400	0.0000	0.0000	0.0000	0.0000	0.0000	0.0000	0.0000	0.0000
0.87723E 00	1.1500	0.0000	0.0000	0.0000	0.0000	0.0000	0.0000	0.0000	0.0000
0.87723E 00	1.1600	0.0000	0.0000	0.0000	0.0000	0.0000	0.0000	0.0000	0.0000
0.87723E 00	1.1700	0.0000	0.0000	0.0000	0.0000	0.0000	0.0000	0.0000	0.0000
0.87723E 00	1.1800	0.0000	0.0000	0.0000	0.0000	0.0000	0.0000	0.0000	0.0000
0.87723E 00	1.1900	0.0000	0.0000	0.0000	0.0000	0.0000	0.0000	0.0000	0.0000
0.87723E 00	1.2000	0.0000	0.0000	0.0000	0.0000	0.0000	0.0000	0.0000	0.0000
0.87723E 00	1.2100	0.0000	0.0000	0.0000	0.0000	0.0000	0.0000	0.0000	0.0000
0.87723E 00	1.2200	0.0000	0.0000	0.0000	0.0000	0.0000	0.0000	0.0000	0.0000
0.87723E 00	1.2300	0.0000	0.0000	0.0000	0.0000	0.0000	0.0000	0.0000	0.0000
0.87723E 00	1.2400	0.0000	0.0000	0.0000	0.0000	0.0000	0.0000	0.0000	0.0000
0.87723E 00	1.2500	0.0000	0.0000	0.0000	0.0000	0.0000	0.0000	0.0000	0.0000
0.87723E 00	1.2600	0.0000	0.0000	0.0000	0.0000	0.0000	0.0000	0.0000	0.0000
0.87723E 00	1.2700	0.0000	0.0000	0.0000	0.0000	0.0000	0.0000	0.0000	0.0000
0.87723E 00	1.2800	0.0000	0.0000	0.0000	0.0000	0.0000	0.0000	0.0000	0.0000
0.87723E 00	1.2900	0.0000	0.0000	0.0000	0.0000	0.0000	0.0000	0.0000	0.0000
0.87723E 00	1.3000	0.0000	0.0000	0.0000	0.0000	0.0000	0.0000	0.0000	0.0000
0.87723E 00	1.3100	0.0000	0.0000	0.0000	0.0000	0.0000	0.0000	0.0000	0.0000
0.87723E 00	1.3200	0.0000	0.0000	0.0000	0.0000	0.0000	0.0000	0.0000	0.0000
0.87723E 00	1.3300	0.0000	0.0000	0.0000	0.0000	0.0000	0.0000	0.0000	0.0000
0.87723E 00	1.3400	0.0000	0.0000	0.0000	0.0000	0.0000	0.0000	0.0000	0.0000
0.87723E 00	1.3500	0.0000	0.0000	0.0000	0.0000	0.0000	0.0000	0.0000	0.0000
0.87723E 00	1.3600	0.0000	0.0000	0.0000	0.0000	0.0000	0.0000	0.0000	0.0000
0.87723E 00	1.3700	0.0000	0.0000	0.0000	0.0000	0.0000	0.0000	0.0000	0.0000
0.87723E 00	1.3800	0.0000	0.0000	0.0000	0.0000	0.0000	0.0000	0.0000	0.0000
0.87723E 00	1.3900	0.0000	0.0000	0.0000	0.0000	0.0000	0.0000	0.0000	0.0000
0.87723E 00	1.4000	0.0000	0.0000	0.0000	0.0000	0.0000	0.0000	0.0000	0.0000
0.87723E 00	1.4100	0.0000	0.0000	0.0000	0.0000	0.0000	0.0000	0.0000	0.0000
0.87723E 00	1.4200	0.0000	0.0000	0.0000	0.0000	0.0000	0.0000	0.0000	0.0000
0.87723E 00	1.4300	0.0000	0.0000	0.0000	0.0000	0.0000	0.0000	0.0000	0.0000
0.87723E 00	1.4400	0.0000	0.0000	0.0000	0.0000	0.0000	0.0000	0.0000	0.0000
0.87723E 00	1.4500	0.0000	0.0000	0.0000	0.0000	0.0000	0.0000	0.0000	0.0000
0.87723E 00	1.4600	0.0000	0.0000	0.0000	0.0000	0.0000	0.0000	0.0000	0.0000
0.87723E 00	1.4700	0.0000	0.0000	0.0000	0.0000	0.0000	0.0000	0.0000	0.0000
0.87723E 00	1.4800	0.0000	0.0000	0.0000	0.0000	0.0000	0.0000	0.0000	0.0000
0.87723E 00	1.4900	0.0000	0.0000	0.0000	0.0000	0.0000	0.0000	0.0000	0.0000
0.87723E 00	1.5000	0.0000	0.0000	0.0000	0.0000	0.0000	0.0000	0.0000	0.0000
0.87723E 00	1.5100	0.0000	0.0000	0.0000	0.0000	0.0000	0.0000	0.0000	0.0000
0.87723E 00	1.5200	0.0000	0.0000	0.0000	0.0000	0.0000	0.0000	0.0000	0.0000
0.87723E 00	1.5300	0.0000	0.0000	0.0000	0.0000	0.0000	0.0000	0.0000	0.0000
0.87723E 00	1.5400	0.0000	0.0000	0.0000	0.0000	0.0000	0.0000	0.0000	0.0000
0.87723E 00	1.5500	0.0000	0.0000	0.0000	0.0000	0.0000	0.0000	0.0000	0.0000
0.87723E 00	1.5600	0.0000	0.0000	0.0000	0.0000	0.0000	0.0000	0.0000	0.0000
0.87723E 00	1.5700	0.0000	0.0000	0.0000	0.0000	0.0000	0.0000	0.0000	0.0000
0.87723E 00	1.5800	0.0000	0.0000	0.0000	0.0000	0.0000	0.0000	0.0000	0.0000
0.87723E 00	1.5900	0.0000	0.0000	0.0000	0.0000	0.0000	0.0000	0.0000	0.0000
0.87723E 00	1.6000	0.0000	0.0000	0.0000	0.0000	0.0000	0.0000	0.0000	0.0000
0.87723E 00	1.6100	0.0000	0.0000	0.0000	0.0000	0.0000	0.0000	0.0000	0.0000
0.87723E 00	1.6200	0.0000	0.0000	0.0000	0.0000	0.0000	0.0000	0.0000	0.0000
0.87723E 00	1.6300	0.0000	0.0000	0.0000	0.0000	0.0000	0.0000	0.0000	0.0000
0.87723E 00	1.6400	0.0000	0.0000	0.0000	0.0000	0.0000	0.0000	0.0000	0.0000
0.87723E 00	1.6500	0.0000	0.0000	0.0000	0.0000	0.0000	0.0000	0.0000	0.0000
0.87723E 00	1.6600	0.0000	0.0000	0.0000	0.0000	0.0000	0.0000	0.0000	0.0000
0.87723E 00	1.6700	0.0000	0.0000	0.0000	0.0000	0.0000	0.0000	0.0000	0.0000
0.87723E 00	1.6800	0.0000	0.0000	0.0000	0.0000	0.0000	0.0000	0.0000	0.0000
0.87723E 00	1.6900	0.0000	0.0000	0.0000	0.0000	0.0000	0.0000	0.0000	0.0000
0.87723E 00	1.7000	0.0000	0.0000	0.0000	0.0000	0.0000	0.0000	0.0000	0.0000
0.87723E 00	1.7100	0.0000	0.0000	0.0000	0.0000	0.0000	0.0000	0.0000	0.0000
0.87723E 00	1.7200	0.0000	0.0000	0.0000	0.0000	0.0000	0.0000	0.0000	0.0000
0.87723E 00	1.7300	0.0000	0.0000	0.0000	0.0000	0.0000	0.0000	0.0000	0.0000
0.87723E 00	1.7400	0.0000	0.0000	0.0000	0.0000	0.0000	0.0000	0.0000	0.0000
0.87723E 00	1.7500	0.0000	0.0000	0.0000	0.0000	0.0000	0.0000	0.0000	0.0000
0.87723E 00	1.7600	0.0000	0.0000	0.0000	0.0000	0.0000	0.0000	0.0000	0.0000
0.87723E 00	1.7700	0.0000	0.0000	0.0000	0.0000	0.0000	0.0000	0.0000	0.0000
0.87723E 00	1.7800	0.0000	0.0000	0.0000	0.0000	0.0000	0.0000	0.0000	0.0000
0.87723E 00	1.7900	0.0000	0.0000	0.0000	0.0000	0.0000	0.0000	0.0000	0.0000
0.87723E 00	1.8000	0.0000	0.0000	0.0000	0.0000	0.0000	0.0000	0.0000	0.0000
0.87723E 00	1.8100	0.0000	0.0000	0.0000	0.0000	0.0000	0.0000	0.0000	0.0000
0.87723E 00	1.8200	0.0000	0.0000	0.0000	0.0000	0.0000	0.0000	0.0000	0.0000
0.87723E 00	1.8300	0.0000	0.0000	0.0000	0.0000	0.0000	0.0000	0.0000	0.0000
0.87723E 00	1.8400	0.0000	0.0000	0.0000	0.0000	0.0000	0.0000	0.0000	0.0000
0.87723E 00	1.8500	0.0000	0.0000	0.0000	0.0000	0.0000	0.0000	0.0000	0.0000
0.87723E 00	1.8600	0.0000	0.0000	0.0000	0.0000	0.0000	0.0000	0.0000	0.0000
0.87723E 00	1.8700	0.0000	0.0000	0.0000	0.0000	0.0000	0.0000	0.0000	0.0000
0.87723E 00	1.8800	0.0000	0.0000	0.0000	0.00				

===== MATERIAL DATA =====						
NAME	MATL	TOT CAP	TOT HEAT	AVG TEMP	TMELT	HMELT
STEL	1	1.0735E-01	9.24379E-01	8.62137E-01	0.0	0.0
STAL	2	1.8225E-01	2.43140E-01	8.6252E-01	0.0	0.0
AIR	3	1.44224E-03	1.3003E-01	9.0541E-01	0.0	0.0

## TRUMP OUTPUT DATA

MISSILE PROBLEM TWO DIMENSIONAL

## TWO DIMENSIONAL

PRINTOUT	8	TOO	FAST	TOO	SLTW	KWIT	DELTHX	SMALL	TVARY	NUTS
	120	11	0	0	0	0	1.00000E 12	1.20000E 03	1.00000E 00	3

TOTAL TIME	TIME STEP	HEAT FLOW	TEMP FROM FLUX	FLUX RATE	TEMP RATE
8.51641E 02	4.38834E 00	-2.30600E 04	-1.69885E 04	-2.70777E 01	-1.99480E 01

AVG TEMP	HEAT CAPACITY	HEAT CONTENT	GEN RATE	HEAT GEN	TEMP FROM GEN
----------	---------------	--------------	----------	----------	---------------

Account Number	Amount	Currency
3.88432E 01	1.357390 00	0.0
	1.20594E 02	0.0
		0.0

NODE	TEMP	DT	DDT	GEN RATE	W	H	F	CURE AT 280 F
1	0.0000	0.000000-01	0.000000-01	0.0000	0.2832E-05	-0.8702E-06	-0.1147E-02	0.0

[illegible][illegible][illegible][illegible][illegible][illegible][illegible][illegible][illegible][illegible][illegible][illegible][illegible][illegible][illegible][illegible][illegible]

Case No.	Case Name	Case Type	Case Status	Case Date	Case Time	Case Location	Case Description	Case Details	Case Notes
46	0.9704D 02	0.39270 00	0.8948D-01	0.0	0.0	0.0	0.0	0.0	0.0
47	C.1196D 03	0.8910D 00	0.2030D 00	0.0	0.0	0.0	0.0	0.0	0.0
48	0.9704D 02	0.39270 00	0.8948D-01	0.0	0.0	0.0	0.0	0.0	0.0
49	0.9704D 02	0.39270 00	0.8948D-01	0.0	0.0	0.0	0.0	0.0	0.0
50	0.9704D 02	0.39270 00	0.8948D-01	0.0	0.0	0.0	0.0	0.0	0.0
51	0.9704D 02	0.39270 00	0.8948D-01	0.0	0.0	0.0	0.0	0.0	0.0
52	0.9704D 02	0.39270 00	0.8948D-01	0.0	0.0	0.0	0.0	0.0	0.0
53	0.9704D 02	0.39270 00	0.8948D-01	0.0	0.0	0.0	0.0	0.0	0.0
54	0.9704D 02	0.39270 00	0.8948D-01	0.0	0.0	0.0	0.0	0.0	0.0
55	0.9704D 02	0.39270 00	0.8948D-01	0.0	0.0	0.0	0.0	0.0	0.0
56	0.9704D 02	0.39270 00	0.8948D-01	0.0	0.0	0.0	0.0	0.0	0.0
57	0.9704D 02	0.39270 00	0.8948D-01	0.0	0.0	0.0	0.0	0.0	0.0
58	0.9704D 02	0.39270 00	0.8948D-01	0.0	0.0	0.0	0.0	0.0	0.0
59	0.9704D 02	0.39270 00	0.8948D-01	0.0	0.0	0.0	0.0	0.0	0.0
60	0.9704D 02	0.39270 00	0.8948D-01	0.0	0.0	0.0	0.0	0.0	0.0
61	0.9704D 02	0.39270 00	0.8948D-01	0.0	0.0	0.0	0.0	0.0	0.0
62	0.9704D 02	0.39270 00	0.8948D-01	0.0	0.0	0.0	0.0	0.0	0.0
63	0.9704D 02	0.39270 00	0.8948D-01	0.0	0.0	0.0	0.0	0.0	0.0
64	0.9704D 02	0.39270 00	0.8948D-01	0.0	0.0	0.0	0.0	0.0	0.0
65	0.9704D 02	0.39270 00	0.8948D-01	0.0	0.0	0.0	0.0	0.0	0.0
66	0.9704D 02	0.39270 00	0.8948D-01	0.0	0.0	0.0	0.0	0.0	0.0
67	0.9704D 02	0.39270 00	0.8948D-01	0.0	0.0	0.0	0.0	0.0	0.0
68	0.9704D 02	0.39270 00	0.8948D-01	0.0	0.0	0.0	0.0	0.0	0.0
69	0.9704D 02	0.39270 00	0.8948D-01	0.0	0.0	0.0	0.0	0.0	0.0
70	0.9704D 02	0.39270 00	0.8948D-01	0.0	0.0	0.0	0.0	0.0	0.0
71	0.9704D 02	0.39270 00	0.8948D-01	0.0	0.0	0.0	0.0	0.0	0.0
72	0.9704D 02	0.39270 00	0.8948D-01	0.0	0.0	0.0	0.0	0.0	0.0
73	0.9704D 02	0.39270 00	0.8948D-01	0.0	0.0	0.0	0.0	0.0	0.0
74	0.9704D 02	0.39270 00	0.8948D-01	0.0	0.0	0.0	0.0	0.0	0.0
75	0.9704D 02	0.39270 00	0.8948D-01	0.0	0.0	0.0	0.0	0.0	0.0
76	0.9704D 02	0.39270 00	0.8948D-01	0.0	0.0	0.0	0.0	0.0	0.0
77	0.9704D 02	0.39270 00	0.8948D-01	0.0	0.0	0.0	0.0	0.0	0.0
78	0.9704D 02	0.39270 00	0.8948D-01	0.0	0.0	0.0	0.0	0.0	0.0
79	0.9704D 02	0.39270 00	0.8948D-01	0.0	0.0	0.0	0.0	0.0	0.0
80	0.9								

[illegible]

MODE	TEMP	DT	DDT	GEN RATE	W	H	F	CURE AT 280 F
47	0.39010 02	0.40000 00	0.02000 01	0.00000 00	0.00000 00	0.00000 00	0.00000 00	0.00000 00

[illegible]

	02	03	00	01	-23	-24	04	08	09
36	0.98786		0.29260	0.66670-01	0.30222E-23	0.4038E-24	0.3307E-04		
48	0.10110		0.40230	0.91670-01	0.30925E-23	-0.3957E-24	+0.3669E-04		

## MATERIAL DATA

NAME	MATL	TOT CAP	TOT HEAT	AVG TEMP	TMELT	HMELT
SAND	1	1.37359E 03	9.45373E 01	8.80574E 01	0.0	0.0

3	2.82356E-01	2.59139E 01	9.17777E 01	0.0	0.0
3	1.44246E-03	1.43372E-01	9.93947E 01	0.0	0.0
STFL					
AIR					

1  
2  
3  
4  
5  
6  
7  
8  
9  
10  
11  
12  
13  
14  
15  
16  
17  
18  
19  
20  
21  
22  
23  
24  
25  
26  
27  
28  
29  
30  
31  
32  
33  
34  
35  
36  
37  
38  
39  
40  
41  
42  
43  
44  
45  
46  
47  
48  
49  
50  
51  
52  
53  
54  
55  
56  
57  
58  
59  
60  
61  
62  
63  
64  
65  
66  
67  
68  
69  
70  
71  
72  
73  
74  
75  
76  
77  
78  
79  
80  
81  
82  
83  
84  
85  
86  
87  
88  
89  
90  
91  
92  
93  
94  
95  
96  
97  
98  
99  
100

[illegible]

2

```

=====
TRUMP OUTPUT DATA
* MISSILE PROBLEM TWO DIMENSIONAL
=====
PRINTOUT CYCLE 140 TIME STEP 11 DELTAX 1.00000E 12 DELTAY 1.00000E 00 NUTS 3
TOTAL TIME 9.47229E 02 4.80006E 00 -2.34107E 04 -1.72459E 04 -2.47150E 01 -1.82078E 01
AVG TEMP 9.43739E 01 HEAT CAPACITY 1.35739D 00 HEAT CONTENT 1.28102E 02 GEN RATE 0.0 HEAT GEN 0.0 TEMP FROM GEN 0.0
=====
CURE AT 280 F
=====
NODE 1 2 3 4 5 6 7 8 9 10 11 12 13 14 15 16 17 18 19 20 21 22 23 24 25 26 27 28 29 30 31 32 33 34 35 36 37 38
TEMP 0.87850 0.87850 0.87850 0.87850 0.87850 0.87850 0.87850 0.87850 0.87850 0.87850 0.87850 0.87850 0.87850 0.87850 0.87850 0.87850 0.87850 0.87850 0.87850 0.87850 0.87850 0.87850 0.87850 0.87850 0.87850 0.87850 0.87850 0.87850 0.87850 0.87850 0.87850 0.87850 0.87850 0.87850
DT 0.30740D 01 0.30740D 01 0.30740D 01 0.30740D 01 0.30740D 01 0.30740D 01 0.30740D 01 0.30740D 01 0.30740D 01 0.30740D 01 0.30740D 01 0.30740D 01 0.30740D 01 0.30740D 01 0.30740D 01 0.30740D 01 0.30740D 01 0.30740D 01 0.30740D 01 0.30740D 01 0.30740D 01 0.30740D 01 0.30740D 01 0.30740D 01
DOT -0.6419D -02 -0.6419D -02 -0.6419D -02 -0.6419D -02 -0.6419D -02 -0.6419D -02 -0.6419D -02 -0.6419D -02 -0.6419D -02 -0.6419D -02 -0.6419D -02 -0.6419D -02 -0.6419D -02 -0.6419D -02 -0.6419D -02 -0.6419D -02 -0.6419D -02 -0.6419D -02 -0.6419D -02
GE N RATE 0.0 0.0 0.0 0.0 0.0 0.0 0.0 0.0 0.0 0.0 0.0 0.0 0.0 0.0 0.0 0.0 0.0 0.0 0.0 0.0 0.0 0.0 0.0 0.0 0.0 0.0 0.0 0.0 0.0 0.0 0.0 0.0 0.0 0.0
H 0.8499E -06 0.8499E -06 0.8499E -06 0.8499E -06 0.8499E -06 0.8499E -06 0.8499E -06 0.8499E -06 0.8499E -06 0.8499E -06 0.8499E -06 0.8499E -06 0.8499E -06 0.8499E -06 0.8499E -06 0.8499E -06 0.8499E -06 0.8499E -06 0.8499E -06 0.8499E -06 0.8499E -06 0.8499E -06 0.8499E -06 0.8499E -06 0.8499E -06 0.8499E -06 0.8499E -06 0.8499E -06 0.8499E -06
H 0.8499E -06 0.8499E -06 0.8499E -06 0.8499E -06 0.8499E -06 0.8499E -06 0.8499E -06 0.8499E -06 0.8499E -06 0.8499E -06 0.8499E -06 0.8499E -06 0.8499E -06 0.8499E -06 0.8499E -06 0.8499E -06 0.8499E -06 0.8499E -06 0.8499E -06 0.8499E -06 0.8499E -06 0.8499E -06 0.8499E -06 0.8499E -06 0.8499E -06 0.8499E -06 0.8499E -06 0.8499E -06 0.8499E -06 0.8499E -06
F 0.1222E -01 0.1222E -01 0.1222E -01 0.1222E -01 0.1222E -01 0.1222E -01 0.1222E -01 0.1222E -01 0.1222E -01 0.1222E -01 0.1222E -01 0.1222E -01 0.1222E -01 0.1222E -01 0.1222E -01 0.1222E -01 0.1222E -01 0.1222E -01 0.1222E -01 0.1222E -01 0.1222E -01 0.1222E -01 0.1222E -01 0.1222E -01 0.1222E -01 0.1222E -01 0.1222E -01 0.1222E -01 0.1222E -01 0.1222E -01 0.1222E -01 0.1222E -01
F 0.1222E -01 0.1222E -01 0.1222E -01 0.1222E -01 0.1222E -01 0.1222E -01 0.1222E -01 0.1222E -01 0.1222E -01 0.1222E -01 0.1222E -01 0.1222E -01 0.1222E -01 0.1222E -01 0.1222E -01 0.1222E -01 0.1222E -01 0.1222E -01 0.1222E -01 0.1222E -01 0.1222E -01 0.1222E -01 0.1222E -01 0.1222E -01 0.1222E -01 0.1222E -01 0.1222E -01 0.1222E -01 0.1222E -01 0.1222E -01 0.1222E -01 0.1222E -01 0.1222E -01
CURE AT 280 F
=====
CURE AT 280 F
=====
MATERIAL DATA
NAME MATL 1
STEEL 2
AIR 3
=====
NAME MATL 1
STEEL 2
AIR 3
=====

```

TRUMP OUTPUT DATA

MISSILE PROBLEM

TW1 DIMENSIONAL

DATA DECK 1

PRINTOUT CYCLE 160

TOTAL TIME 1.06258E 03

AVG TEMP 1.02454F 02

HEAT CAPACITY 1.35739D 00

HEAT CONTENT 1.39070E 02

HEAT FLOW -2.49402E 04

TEMP FROM FLUX -1.83737E 04

FLUX RATE -2.34713E 01

TEMP RATE -1.72915E 01

DELIM 1.00000E 12

SMALL 1.00000E 00

TVARY 1.00000E 00

NUTS 3

GE N RATE

GE N RATE

GE N RATE

GE N RATE

GE N RATE

GE N RATE

GE N RATE

GE N RATE

GE N RATE

GE N RATE

GE N RATE

GE N RATE

GE N RATE

GE N RATE

GE N RATE

GE N RATE

GE N RATE

GE N RATE





DATA DECK 1

TRUMP OUTPUT DATA

\* MISSILE PROBLEM TWO DIMENSIONAL

PRINTOUT CYCLE 220 TIME STEP 11 DELTAX 1.00000E 12 SMALL 1.00000E 00 TVARY 1.00000E 00 NUTS 3

TOTAL TIME 1.36145E 03 HEAT FLOW 1.10823E 04 TEMP FROM FLUX 8.14007E 00 FLUX RATE 5.99687E 00 TEMP RATE

1.18861E 02 HEAT CAPACITY 1.61341E 02 GEN RATE 0.0 HEAT GEN 0.0 TEMP FROM GEN 0.0

NODE	TEMP	DT	DI	DDI	GE N RATE	H	H	F	CURE AT 280 F
1	0.10920	0.00000	0.00000	0.00000	0.00000	0.00000	0.00000	0.00000	0.00000
2	0.10920	0.00000	0.00000	0.00000	0.00000	0.00000	0.00000	0.00000	0.00000
3	0.10920	0.00000	0.00000	0.00000	0.00000	0.00000	0.00000	0.00000	0.00000
4	0.10920	0.00000	0.00000	0.00000	0.00000	0.00000	0.00000	0.00000	0.00000
5	0.10920	0.00000	0.00000	0.00000	0.00000	0.00000	0.00000	0.00000	0.00000
6	0.10920	0.00000	0.00000	0.00000	0.00000	0.00000	0.00000	0.00000	0.00000
7	0.10920	0.00000	0.00000	0.00000	0.00000	0.00000	0.00000	0.00000	0.00000
8	0.10920	0.00000	0.00000	0.00000	0.00000	0.00000	0.00000	0.00000	0.00000
9	0.10920	0.00000	0.00000	0.00000	0.00000	0.00000	0.00000	0.00000	0.00000
10	0.10920	0.00000	0.00000	0.00000	0.00000	0.00000	0.00000	0.00000	0.00000
11	0.10920	0.00000	0.00000	0.00000	0.00000	0.00000	0.00000	0.00000	0.00000
12	0.10920	0.00000	0.00000	0.00000	0.00000	0.00000	0.00000	0.00000	0.00000
13	0.10920	0.00000	0.00000	0.00000	0.00000	0.00000	0.00000	0.00000	0.00000
14	0.10920	0.00000	0.00000	0.00000	0.00000	0.00000	0.00000	0.00000	0.00000
15	0.10920	0.00000	0.00000	0.00000	0.00000	0.00000	0.00000	0.00000	0.00000
16	0.10920	0.00000	0.00000	0.00000	0.00000	0.00000	0.00000	0.00000	0.00000
17	0.10920	0.00000	0.00000	0.00000	0.00000	0.00000	0.00000	0.00000	0.00000
18	0.10920	0.00000	0.00000	0.00000	0.00000	0.00000	0.00000	0.00000	0.00000
19	0.10920	0.00000	0.00000	0.00000	0.00000	0.00000	0.00000	0.00000	0.00000
20	0.10920	0.00000	0.00000	0.00000	0.00000	0.00000	0.00000	0.00000	0.00000
21	0.10920	0.00000	0.00000	0.00000	0.00000	0.00000	0.00000	0.00000	0.00000
22	0.10920	0.00000	0.00000	0.00000	0.00000	0.00000	0.00000	0.00000	0.00000
23	0.10920	0.00000	0.00000	0.00000	0.00000	0.00000	0.00000	0.00000	0.00000
24	0.10920	0.00000	0.00000	0.00000	0.00000	0.00000	0.00000	0.00000	0.00000
25	0.10920	0.00000	0.00000	0.00000	0.00000	0.00000	0.00000	0.00000	0.00000
26	0.10920	0.00000	0.00000	0.00000	0.00000	0.00000	0.00000	0.00000	0.00000
27	0.10920	0.00000	0.00000	0.00000	0.00000	0.00000	0.00000	0.00000	0.00000
28	0.10920	0.00000	0.00000	0.00000	0.00000	0.00000	0.00000	0.00000	0.00000
29	0.10920	0.00000	0.00000	0.00000	0.00000	0.00000	0.00000	0.00000	0.00000
30	0.10920	0.00000	0.00000	0.00000	0.00000	0.00000	0.00000	0.00000	0.00000
31	0.10920	0.00000	0.00000	0.00000	0.00000	0.00000	0.00000	0.00000	0.00000
32	0.10920	0.00000	0.00000	0.00000	0.00000	0.00000	0.00000	0.00000	0.00000
33	0.10920	0.00000	0.00000	0.00000	0.00000	0.00000	0.00000	0.00000	0.00000
34	0.10920	0.00000	0.00000	0.00000	0.00000	0.00000	0.00000	0.00000	0.00000
35	0.10920	0.00000	0.00000	0.00000	0.00000	0.00000	0.00000	0.00000	0.00000
36	0.10920	0.00000	0.00000	0.00000	0.00000	0.00000	0.00000	0.00000	0.00000
37	0.10920	0.00000	0.00000	0.00000	0.00000	0.00000	0.00000	0.00000	0.00000

NAME	MATL	TOT CAP	TOT HEAT	AVG TEMP	TMELT	HMELT	CURE AT 280 F
SAND	1	1.07359E 00	1.26427E 02	1.17762E 02	0.0	0.0	0.0
STEL	2	2.82356E 01	3.47344E 01	1.23024E 02	0.0	0.0	0.0
AIR	3	1.44245E 03	1.76973E 01	1.22689E 02	0.0	0.0	0.0

MATERIAL DATA

NAME	MATL	TOT CAP	TOT HEAT	AVG TEMP	THELT	HNELT
SAND	1	1.37359E+03	1.26225E+02	1.17605E+02	3.3	0.0
ST-IL	1	1.42337E+01	1.36337E+01	1.18407E+02	0.0	0.0
AIR	3	1.44246E+03	1.63386E+01	1.13259E+02	0.0	0.0



TRUMP OUTPUT CAT A

\* MISSILE PROBLEM TWO DIMENSIONAL

PRINTOUT	CYCLE	TOO FAST	TOO SLOW	KNIT	DELTMX	SMALL	TVARY	NUTS
	30.0	1	0	1	1.00000E 12	1.00000E 00	1.00000E 00	2

TOTAL TIME	TIME STEP	HEAT FLOW	TEMP FROM FLUX	FLUX RATE	TEMP RATE
1.44000E 03	2.21753E 00	1.04904E 04	7.72841E 03	7.28502E 00	5.36695E 00
=====					
AVG TEMP	HEAT CAPACITY	HEAT CONTENT	GEN RATE	HEAT GEN	TEMP FROM GEN
1.16772E 02	1.35739D 00	1.58504E 02	0.0	0.0	0.0
=====					

CURE AT 280 °C

E

T

H

N

RATE

Z

G

I

D

O

T

N

NOB

[illegible]

## APPENDIX D

### Experimental Data

The data presented in this appendix were obtained from the thermocouples on the rocket motor storage container system located at China Lake, California. The thermocouple output was read out on a Honeywell Electronik 25, 24 channel recorder which had been calibrated at 50, 100 and 150°F. The data was taken on two consecutive, typical summer days (August 1 and 2, 1972) at China Lake. Each thermocouple was read once every 24 minutes. The first set of data presents the storage container temperature at four locations plus three different ways of averaging this data. It also presents the ambient temperature and the approximate time of day. The second set of data presents the surface temperature of the rocket motor and three ways to average this data. It also presents the temperature at the center of the rocket motor and the approximate time of day. Figure 32 shows the location of the thermocouples used to collect this temperature data.

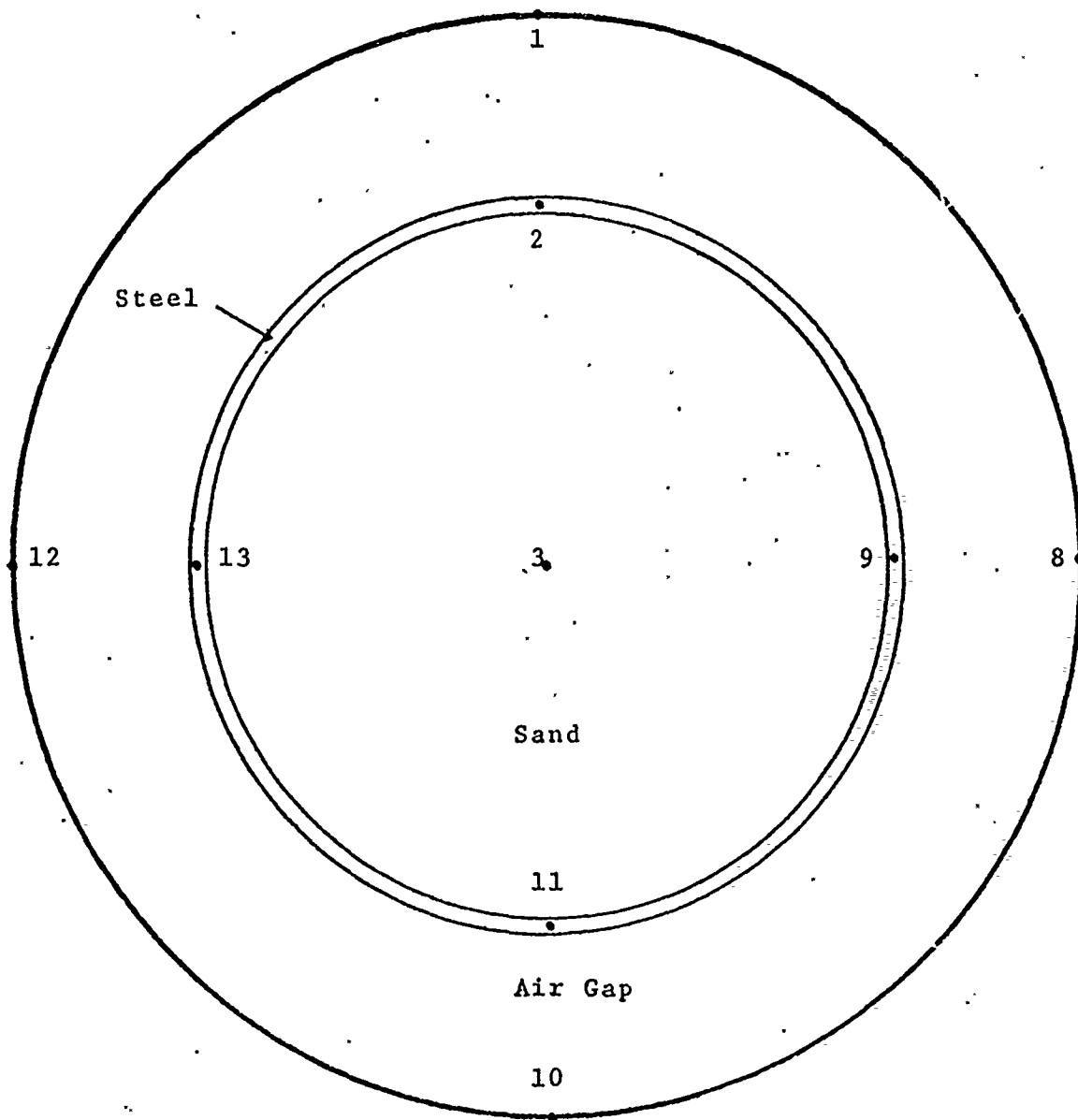


Figure 32: Thermocouple Locations for Experimental Data.

Series 1

Time (Approximate) Aug. 1, 1972	Ambient (°F)	#1 (°F)	#8 (°F)	#10 (°F)	#12 (°F)	Avg. #1 & #10 (°F)	Avg. #8 & #12 (°F)	all 4 "Bulk"
0536	76	69	72	79	80	74	76	75
0600	77	68	72	79	80	73.5	76	74.75
0624	80	73	75	81	82	77	78.5	77.75
0648	80	81	79	87	85	84	82	83
0712	83	90	82	90	89	90	85.5	87.75
0736	85	98	87	93	92	95.5	89.5	92.5
0800	87	105	90	94	94	99.5	92	95.75
	89	110	93	96	97	103	95	99
	91	116	96	98	99	107	97.5	102.25
	92	121	100	101	102	111	101	106
	94	129	103	102	105	115.5	104	109.75
1000	96	133	107	105	108	119	107.5	113.25
	97	139	110	107	110	123	110	116.5
	100	143	113	107	112	125	112.5	118.75
	101	147	117	109	115	128	116	122
	103	150	119	109	116	129.5	117.5	123.5
1200	104	153	124	110	119	131.5	121.5	126.5
	106	156	128	112	122	134	125	129.5
	106	157	131	113	124	135	127.5	131.25
	106	154	133	114	125	134	129	131.5
	107	157	138	115	127	136	132.5	134.25
1400	108	154	143	117	129	135.5	136	135.75
	109	153	142	118	129	135.5	135.5	135.5
	110	148	142	119	129	133.5	135.5	134.5
	110	143	141	118	128	130.5	134.5	132.5
	109	142	143	119	128	130.5	135.5	133
1600	107	137	143	119	128	128	135.5	131.75
	108	134	139	117	127	125.5	133	129.25
	108	130	139	117	127	123.5	133	128.25
	106	126	138	116	126	121	132	126.5
	104	123	136	115	125	119	130.5	124.75

Time (Approximate) Aug. 1, 1972	Ambient (°F)	#1 (°F)	#8 (°F)	#10 (°F)	#12 (°F)	Avg. #1 & #10 (°F)	Avg. #8 & #12 (°F)	Avg. all 4 "Bulk"
1800	103	118	131	113	123	115.5	127	121.25
	101	113	127	111	120	112	123.5	117.75
	99	107	121	108	117	107.5	119	113.25
	96	101	106	103	111	102	108.5	105.25
	95	91	93	98	104	94.5	98.5	96.5
2000	93	88	91	95	101	91.5	96	93.75
	91	86	89	94	99	90	94	92
	90	85	88	92	97	88.5	92.5	90.5
	89	84	87	91	96	87.5	91.5	89.5
	87	83	85	89	94	86	89.5	87.75
2200	87	81	84	88	93	84.5	88.5	86.5
	85	80	83	87	91	83.5	87	85.25
	86	79	82	86	91	82.5	86.5	84.5
	86	79	82	87	90	83	86	84.5
	84	79	82	86	89	82.5	85.5	84
0000 2 Aug.	82	77	80	85	88	81	84	82.5
	81	74	78	84	86	79	82	80.5
	81	72	76	83	85	77.5	80.5	79
	81	72	77	83	85	77.5	81	79.25
0200	79	72	75	81	83	76.5	79	77.75
	79	72	75	80	83	76	79	77.5
	79	72	74	80	82	76	78	77
	78	72	74	79	82	75.5	78	76.75
	77	71	73	79	81	75	77	76
	75	70	72	78	80	74	76	75
0400	73	67	69	77	78	72	73.5	72.75
	72	66	69	75	77	70.5	73	71.75
	73	65	68	75	76	70	72	71
	69	64	67	73	75	68.5	71	69.75
	69	63	66	72	74	67.5	70	68.75
0600	68	63	66	71	73	67	69.5	68.25
	71	65	67	75	76	70	71.5	70.75
	77	74	71	80	79	77	75	76
	79	84	77	84	84	84	80.5	82.25

Time (Approximate) Aug. 2, 1972	Ambient (°F)	#1 (°F)	#8 (°F)	#10 (°F)	#12 (°F)	Avg. #1 & #10 (°F)	Avg. #8 & #12 (°F)	all 4 "Bulk"
0800	80	93	81	89	87	91	84	87.5
	83	101	85	92	91	96.5	88	92.25
	85	108	89	93	93	100.5	91	95.75
	86	114	93	96	97	105	95	100
	88	121	96	98	100	109.5	98	103.75
1000	89	126	98	98	101	112	99.5	105.75
	91	130	101	100	103	115	102	108.5
	94	137	106	102	106	119.5	106	112.75
	96	143	109	104	109	123.5	109	116.25
	100	146	113	106	111	126	112	119
1200	100	149	117	107	114	128	115.5	121.75
	101	151	121	108	117	129.5	119	124.25
	103	150	127	110	119	130	123	126.5
	104	156	129	110	121	133	125	129
	104	154	133	111	122	132.5	127.5	130
1400	105	155	137	112	125	133.5	131	132.25
	105	156	141	114	126	135	133.5	134.25
	107	149	143	114	127	131.5	135	133.25
	107	149	146	115	128	132	137	134.5
	106	151	152	118	131	134.5	141.5	138
1600	107	144	152	120	132	132	142	137
	108	139	152	119	131	129	141.5	135.25
	107	136	147	120	130	128	138.5	133.25
	107	136	147	121	130	128.5	138.5	133.5
	105	131	147	121	130	126	138.5	132.25
1800	103	124	144	120	128	122	136	129
	103	117	134	117	124	117	129	123
	100	111	119	113	121	112	120	116
	98	105	118	108	117	106.5	117.5	112
	95	99	103	103	109	101	106	103.5
2000	93	91	93	97	103	94	98	96
	91	87	90	94	100	90.5	95	92.75
	90	85	88	93	98	89	93	91
	88	83	86	91	96	87	91	89



Series 2

Time (Approximate) Aug. 1, 1972	#3 (°F)	#2 (°F)	#9 (°F)	#11 (°F)	#13 (°F)	Avg. #2 & #11 (°F)	Avg. #9 & #13 (°F)	all 4 (°F)
0536	97	83	84	85	85	84	84.5	84.25
0600	96	82	83	85	84	83.5	83.5	83.5
0624	95	82	83	84	85	83	84	83.5
0648	94	85	84	86	89	85.5	86.5	86
0712	94	88	86	88	93	88	89.5	88.75
0736	93	91	88	90	96	90.5	92	91.25
0800	92	95	90	91	99	93	94.5	93.75
	91	98	92	93	102	95.5	97	96.25
	91	101	94	95	104	98	99	98.5
	91	105	96	97	107	101	101.5	101.25
	91	108	98	98	109	103	103.5	103.25
1000	91	112	101	100	112	106	106.5	106.25
	91	115	103	102	113	108.5	108	108.25
	92	118	105	103	115	110.5	110	110.25
	94	120	108	105	117	112.5	112.5	112.5
	94	122	110	106	118	114	114	114
	95	125	111	108	119	116.5	115	115.75
1200	96	126	114	109	120	117.5	117	117.25
	98	128	117	111	121	119.5	119	119.25
	100	130	119	112	122	121	120.5	120.75
	101	130	120	113	122	121.5	121	121.25
1400	102	131	122	114	122	122.5	122	122.25
	103	131	123	115	121	123	122	122.5
	105	131	124	117	121	124	122.5	123.25
	107	129	125	117	121	123	123	123
	108	129	125	118	120	123.5	122.5	123
1600	109	127	125	117	119	122	122	122
	111	126	125	117	119	121.5	122	121.75
	112	125	125	118	118	121.5	121.5	121.5
	113	124	125	118	117	121	121	121
	114	123	124	117	116	120	120	120



Time (Approximate) Aug. 1, 1972	#3 (°F)	#2 (°F)	#9 (°F)	#11 (°F)	#13 (°F)	Avg. #2 & #11 (°F)	Avg. #9 & #13 (°F)	Avg. all 4 (°F)
1800	115	121	123	117	115	119	119	119
	115	119	121	115	113	117	117	117
	116	117	119	114	112	115.5	115.5	115.5
	117	115	116	112	111	113.5	113.5	113.5
	117	111	111	109	108	110	109.5	109.75
2000	117	107	107	106	106	106.5	106.5	106.5
	117	105	105	104	104	104.5	104.5	104.5
	116	103	103	103	102	103	102.5	102.75
	116	101	101	101	101	101	101	101
	115	100	100	100	100	100	100	100
2200	114	98	98	98	98	98	98	98
	113	97	97	97	97	97	97	97
	112	95	95	96	95	95.5	95	95.25
	111	94	95	95	95	94.5	95	94.75
	110	93	94	94	94	93.5	94	93.75
0000 2 Aug.	109	92	93	93	93	92.5	93	92.75
	107	91	91	92	92	91.5	91.5	91.5
	106	89	90	91	90	90	90	90
	105	88	89	90	89	89	89	89
	104	87	88	89	89	88	88.5	88.25
0200	103	87	87	88	88	87.5	87.5	87.5
	102	86	86	87	87	86.5	86.5	86.5
	101	85	86	87	86	86	86	86
	100	84	85	86	85	85	85	85
	99	83	84	85	85	84	84.5	84.25
0400	97	82	83	84	83	83	83	83
	96	81	82	83	82	82	82	82
	95	80	80	82	81	81	80.5	80.25
	94	79	80	81	80	80	80	80
0600	93	78	79	80	79	79	79	79
	92	77	78	79	78	78	78	78
	91	76	77	79	80	77.5	78.5	78
	90	79	78	80	84	79.5	81	78.25
	89	82	80	82	88	82	84	83

Time (Approximate) Aug. 2, 1972	#3 (°F)	#2 (°F)	#9 (°F)	#11 (°F)	#13 (°F)	Avg. #2 & #11 (°F)	Avg. #9 & #13 (°F)	Avg. all 4 (°F)
	88	87	82	85	92	86	87	86.5
0800	87	90	85	87	96	88.5	90.5	89.5
	86	95	87	89	99	92	93	92.5
	86	98	90	91	102	94.5	96	95.25
	86	102	92	93	105	97.5	98.5	98
1000	86	106	95	95	107	100.5	101	100.75
	87	108	97	96	108	102	102.5	102.25
	87	111	99	98	110	104.5	104.5	104.5
	88	115	102	100	113	107.5	107.5	107.5
	89	118	104	101	114	109.5	109	109.25
	90	120	107	103	115	111.5	111	111.25
1200,	91	122	109	105	116	113.5	112.5	113
	92	123	111	107	117	115	114	114.5
	94	125	114	108	117	116.5	115.5	116
	95	127	116	109	118	118	117	117.5
	97	127	118	110	118	118.5	118	118.25
1400	98	128	120	111	119	119.5	119.5	119.5
	100	128	121	112	118	120	119.5	119.75
	102	128	122	113	118	120.5	120	120.25
	103	129	125	115	118	122	121.5	121.75
1600	105	129	126	116	118	122.5	122	122.25
	106	128	127	116	118	122	122.5	122.25
	107	127	127	117	117	122	122	122
	109	126	127	118	117	122	122	122
	110	126	128	119	117	122.5	122.5	122.5
1800	111	124	127	118	116	121	121.5	121.25
	112	122	125	117	115	119.5	120	119.75
	114	120	123	117	113	118.5	118	118.25
	114	117	120	114	112	115.5	116	115.75
	115	114	116	112	110	113	113	113
	116	110	110	108	107	109	108.5	108.75
2000	116	107	107	106	105	106.5	106	106.25
	116	104	104	103	103	103.5	103.5	103.5
	115	102	102	102	101	102	101.5	101.75

Time (Approximate) Aug. 2, 1972	#3 (°F)	#2 (°F)	#9 (°F)	#11 (°F)	#13 (°F)	Avg. #2 & #11 (°F)	Avg. #9 & #13 (°F)	Avg. all 4 (°F)
	115	100	100	100	100	100	100	100
	114	98	99	99	98	98.5	98.5	98.5
2200	113	96	97	97	96	96.5	96.5	96.5
	112	95	95	96	95	95.5	95	95.25
	111	93	94	94	93	93.5	93.5	93.5
	110	92	93	93	93	92.5	93	92.75
	109	91	91	92	91	91.5	91	91.25
0000 3 Aug.	108	89	90	91	90	90	90	90
	106	88	89	90	89	89	89	89
	105	87	88	89	88	88	88	88
	104	86	87	88	87	87	87	87
	103	85	86	87	86	86	86.5	86.25
.0200	101	85	85	86	86	85.5	85.5	85.5
	100	84	84	85	85	84.5	84.5	84.5
	99	82	83	84	83	83	83	83
	98	81	82	83	82	82	82	82
	97	80	80	81	81	80.5	80.5	80.5
0400	95	78	79	80	79	79	79	79
0424	94	77	78	79	78	78	78	78
0448	93	76	77	78	77	77	77	77
0512	92	75	76	77	76	76	76	76

FIRST DAY'S TEMPERATURE RANGES

HIGH	117	131	125	118	122	124	123	123.25
LOW	91	79	80	81	80	80	80	80
AVG	104	105	102.5	99.5	101	102	101.5	101.63

SECOND DAY'S TEMPERATURE RANGES

HIGH	116	129	128	119	119	122.5	122.5	122.5
LOW	86	75	76	77	76	76	76	76
AVG	101	102	102	98	97.5	99.25	99.25	99.25

## APPENDIX E

### Uncertainty Analysis

An uncertainty analysis was carried out on both the analytical solution and on a one dimensional TRUMP model of the rocket motor storage container system. In both models, the volumetric heat capacity of the sand ( $\rho c$ ), the conductivity of the sand ( $k$ ), and the emissivity of the surfaces were each varied by ten percent to determine the sensitivity of the system temperature response to each variation. Although other factors may also be varied, it was theorized that these three had the greatest effect on the heat transfer of the system. These factors were also known with the least accuracy; the maximum uncertainty of each was estimated to be plus or minus ten percent (odds 20 to 1).

In the analytical solution, varying the volumetric heat capacity changed parameter  $a$ , varying the emissivity changed parameter  $\beta$ , and varying the conductivity changed both parameters  $a$  and  $\beta$ . The effects on each parameter from each variation are given in Table V.

TABLE V

Change in Parameters due to Changes in Thermal Properties

Change in Property	Change in Parameters
Volumetric Heat Capacity + 10%	$a + .12$
Volumetric Heat Capacity - 10%	$a - .12$
Emissivity + 10%	$\beta + .49$
Emissivity - 10%	$\beta - .37$
Conductivity + 10%	$a - .11, \beta - .22$
Conductivity - 10%	$a + .13, \beta + .35$

Each factor was varied holding the other factors constant. The changes in temperature and time delay were computed from the difference between these new values and those previously obtained from the analytical solution. To obtain uncertainty bounds on the analytical curve, the second power equation [Ref. 16] was used, namely

$$\omega_T = \sqrt{\omega_C^2 + \omega_k^2 + \omega_\epsilon^2}$$

where

$\omega_T$  = resulting uncertainty in the calculated temperature due to uncertainties in temperature caused by

$\omega_C$  = estimated uncertainty in volumetric heat capacity

$\omega_k$  = estimated uncertainty in conductivity

$\omega_\epsilon$  = estimated uncertainty in emissivity

An identical calculation was carried out to calculate the uncertainty in time delay. The results of these calculations are shown in Figures 12 and 13 for the surface and center of the rocket motor respectively. The uncertainty in temperature varied with time with a maximum variation of  $\pm 2.75^\circ\text{F}$  at the center of the motor and a maximum variation of  $\pm 1.85^\circ\text{F}$  at the surface of the rocket motor. The time delay varied by  $\pm 31$  minutes at the center of the motor and  $\pm 11$  minutes at the surface. The actual experimental data was also plotted on these Figures for comparison.

The experimental data also had an uncertainty bound. Three primary factors made up this uncertainty bound; the accuracy of the thermocouple wire ( $\pm 1.5^\circ\text{F}$ ), the readability of the recorder ( $\pm 1^\circ\text{F}$ ), and the variation in temperature

caused by inaccuracy in the placement of the thermocouples ( $\pm 1^\circ\text{F}$ , estimated). The overall uncertainty in the experimental data was also calculated from the second power equation as

$$\omega_T = \sqrt{\omega_{\text{WIRE}}^2 + \omega_{\text{READ}}^2 + \omega_{\text{PLACE}}^2} \approx 2^\circ\text{F}$$

These uncertainty bounds are also shown in Figures 12 and 13.

A procedure, similar to that used to find the uncertainties of the analytical solution, was used to analyze the resulting uncertainty in the TRUMP numerical calculation. The results of these calculations are shown in Figures 14 and 15. The uncertainty in temperature varied with time with a maximum variation of  $\pm 2.95^\circ\text{F}$  at the center of the rocket motor and a maximum variation of  $\pm 1.95^\circ\text{F}$  at the surface of the motor. The time delay varied from  $\pm 20$  minutes at the center of the motor to  $\pm 9$  minutes at the surface of the motor.

On the basis of the propagation of uncertainty analysis, it was determined that the solutions were most sensitive, in order of importance, to changes in the volumetric heat capacity, emissivity, and the conductivity.

# LIST OF REFERENCES

1. Arpaci, V. S., Conduction Heat Transfer, p. 324-328, Addison-Wesley, 1966.
2. Lawrence Radiation Laboratory Report No. UCRL-14754, Rev. II, TRUMP: A Computer Program for Transient and Steady-State Temperature Distributions in Multi-dimensional Systems, by A. L. Edwards, 1 July 1969.
3. Erbayrum, C., A Computer Program for Solving Transient Heat Conduction Problems, M.S. Thesis, Naval Postgraduate School, Monterey, California, 1971.
4. Meyer, J. F., MacKenzie, D. K., and Wirzburger, A. H., Thermal Mapping of Surface Temperatures Using Cholesteric Liquid Crystals, laboratory study done at Naval Postgraduate School, Monterey, California, 9 June 1972.
5. Crawford, L. and Lemlich, R., "Natural Convection in Horizontal Concentric Cylindrical Annuli," Industrial and Engineering Chemistry Fundamentals, Vol. 1, No. 4, p. 260-264, November 1962.
6. Baumeister, T., Marks Standard Handbook for Mechanical Engineers, 7th Edition, p. 4-11, 4-95, 4-111, McGraw-Hill, 1967.
7. Liu, C. Y., Mueller, W. K., and Landis, F., Natural Convection Heat Transfer in Long Horizontal Cylindrical Annuli, paper presented at 1961 International Heat Transfer Conference, Boulder, Colorado, 28 August - 1 September 1961.
8. Fergason, J. L., Taylor, T. R., and Harsch, T. B., "Liquid Crystals and their Applications," Electro-Technology, p. 41-50, January 1970.
9. Fergason, J. L., "Liquid Crystals," Scientific American, V. 211, p. 77-85, August 1964.
10. Naval Air Development Center Report No. NADC-MA-6922, Development of a Reusable Strippable Film as a Carrier for Liquid Crystals for Use in NDT, by E. Th. Vadala, p. 1-3, 22 May 1969.
11. Hoehn, R. and Binkert, B., Cholesteric Liquid Crystals: A New Visual Aid to Study Flap Circulation, paper presented at Annual Meeting of the American Society of Plastic and Reconstructive Surgeons, Los Angeles, California, 3 October 1970.

12. Mock, J. A., "Liquid Crystals Track Flaws in a Colorful Way," Materials Engineering, p. 66-67, February 1969.
13. McLachlan, N. W., Bessel Functions for Engineers, 2nd Ed., p. 135-136, Oxford University Press, 1961.
14. Hottel, H. C., and Sarofim, A. F., Radiative Transfer, p. 31-39, McGraw-Hill, 1967.
15. Chapman, A. J., Heat Transfer, 2nd Ed., p. 450-455, Macmillan Co., 1967.
16. Kline, S. J., and McClintock, F. A., "Describing Uncertainties in Single-Sample Experiments," Mechanical Engineering, p. 3-8, January 1953.